QC
879.5
.U47
no.10

NOAA Technical Report NESDIS 10

Atlas of Reflectance Patterns for Uniform Earth and Cloud Surfaces (NIMBUS-7 ERB--61 Days)

Washington, D.C.
July 1984

LIBRARY
NOV 20 1984
N.O.A.A.
U. S. Dept. of Commerce

U. S. DEPARTMENT OF COMMERCE
National Oceanic and Atmospheric Administration
National Environmental Satellite, Data, and Information Service

W QC879.5.U47 SERIES ANALYZED.

NOAA TECHNICAL REPORTS

National Environmental Satellite, Data, and Information Service

The National Environmental Satellite, Data, and Information Service (NESDIS) manages the Nation's civil operational Earth-observing satellite systems, as well as global national data bases for meteorology, oceanography, geophysics, and solar-terrestrial sciences. From these sources, it develops and disseminates environmental data and information products critical to the protection of life and property, national defense, the national economy, energy development and distribution, global food supplies, and the development of natural resources.

Publication in the NOAA Technical Report series does not preclude later publication in scientific journals in expanded or modified form. The NESDIS series of NOAA Technical Reports is a continuation of the former NESS and EDIS series of NOAA Technical Reports and the NESC and EDS series of Environmental Science Services Administration (ESSA) Technical Reports.

These reports are available from the National Technical Information Service (NTIS), U.S. Department of Commerce, Sills Bldg., 5285 Port Royal Road, Springfield, VA 22161. Prices on request for paper copies or microfiche.

A more complete listing of these reports, by title and NTIS accession number, is available from the Assessment and Information Services Center, National Oceanic and Atmospheric Administration, Code E/AI13, Page Bldg. 2, 3300 Whitehaven Street, N.W., Washington, DC 20235. A partial listing of more recent reports appears below:

NESS Series

NESS 89 A Statistical Approach to Rainfall Estimation Using Satellite and Conventional Data. Linwood F. Whitney, Jr. April 1982. (PB82 215435)

NESS 90 Total Precipitable Water and Rainfall Determinations From the SEASAT Scanning Multichannel Microwave Radiometer (SMMR). John C. Alishouse, May 1982. (PB83 138263)

NESS 91 Numerical Smoothing and Differentiation by Finite Differences. Henry E. Fleming and Lawrence J. Crone, May 1982. (PB82-258385)

NESS 92 Satellite Infrared Observations of Oceanic Long Waves in the Eastern Equatorial Pacific 1975 to 1981. Richard Legeckis, November 1982. (PB83 161133)

NESS 93 A Method for Improving the Estimation of Conditional Instability from Satellite Retrievals. W.E. Togstad, J.M. Lewis, and H.M. Woolf, November 1982. (PB83 169938)

EDIS Series

EDS 29 GATE Convection Subprogram Data Center: Final Report on Rawinsonde Data Validation. Robert W. Reeves, March 1978. (PB-281-861)

EDS 30 Gamma Distribution Bias and Confidence Limits. Harold L. Crutcher and Raymond L. Joiner, September 1978. (PB-289-721)

EDIS 31 Calibration and Intercomparison of the GATE C-Band Radars. M. Hudlow, R. Arkell, V. Patterson, P. Pytlowany, F. Richards, and S. Geotis (MIT), November 1979. (PB81 120305)

EDIS 32 Distribution of Radiosonde Errors. Harold L. Crutcher, May 1979. (PB-297-383)

EDIS 33 Accurate Least-Squares Techniques Using the Orthogonal Function Approach. Jerry Sullivan, March 1980. (PB80 223241)

EDIS 34 An Application of Stochastic Forecasting to Monthly Averaged 700 mb Heights. Albert Koscielny, June 1982. (PB82 244625)

NESDIS Series

NESDIS 1 Satellite Observations on Variations in Southern Hemisphere Snow Cover. Kenneth F. Dewey and Richard Heim, Jr., June 1983. (PB83 252908)

NESDIS 2 NODC 1 An Environmental Guide to Ocean Thermal Energy Conversion (OTEC) Operations in the Gulf of Mexico. National Oceanographic Data Center (DOC/NOAA Interagency Agreement Number EX-76-A-29-1041), June 1983. (PB84 115146)

NESDIS 3 Determination of the Planetary Radiation Budget From TIROS-N Satellites. Arnold Gruber, Irwin Ruff, and Charles Earnest, August 1983. (PB84 100916)

NESDIS 4 Some Applications of Satellite Radiation Observations to Climate Studies. T. S. Chen, George Ohring, and Haim Ganot, September 1983. (PB84 108109)

NESDIS 5 A Statistical Technique for Forecasting Severe Weather From Vertical Soundings by Satellite and Radiosonde. David L. Keller and William L. Smith, June 1983. (PB84 114099)

(Continued on inside back cover)

W
QC
879.5
U47
no.10

NOAA Technical Report NESDIS 10

Atlas of Reflectance Patterns for Uniform Earth and Cloud Surfaces (NIMBUS-7 ERB--61 Days)

V. R. Taylor and
L. L. Stowe

Washington, D.C.
July 1984

U. S. DEPARTMENT OF COMMERCE
Malcolm Baldrige, Secretary
National Oceanic and Atmospheric Administration
John V. Byrne, Administrator
National Environmental Satellite, Data, and Information Service
John H. Mc Elroy, Assistant Administrator

TABLE OF CONTENTS

Section			page(s)
I. Acknowledgements			iii
II. Introduction			1
III. Angular Bin Array and Numbering Scheme	Fig.	1.0	4
IV. Angular Reflectance Diagrams:			
Clear Ocean	Figs.	1.1 - 1.5	5 - 9
Clear Land		2.1 - 2.4	10 - 13
Clear Snow		3.1 - 3.4	14 - 17
Clear Ice		4.1 - 4.4	18 - 21
Low Cloud		5.1 - 5.5	22 - 26
Middle Cloud		6.1 - 6.5	27 - 31
High Water Cloud		7.1 - 7.5	32 - 36
High Ice Cloud		8.1 - 8.5	37 - 41
IV. Tables of Anisotropic Factor(.1), Relative Dispersion(.2) and Population(.3) for Individual Angular Bins:			
Clear Ocean	Tables	1.1 - 1.3	43 - 45
Clear Land		2.1 - 2.3	46 - 48
Clear Snow		3.1 - 3.3	49 - 51
Clear Ice		4.1 - 4.3	52 - 54
Low Cloud		5.1 - 5.3	55 - 57
Middle Cloud		6.1 - 6.3	58 - 60
High Water Cloud		7.1 - 7.3	61 - 63
High Ice Cloud		8.1 - 8.3	64 - 66
V. Appendix A: 'Reflectance Characteristics of Earth and Cloud Surfaces Derived from Nimbus-7 ERB' - Published in Journal of Geophysical Research, Vol. 89 No. D4, June, 1984			A1 - A21
VI. Appendix B: Tape specification for Nimbus-7 ERB 61-day uniform surface data.			B1

Acknowledgements

The efforts of the following individuals were especially appreciated: G. Dunlap for generous photographic support; M. Varnadore for initial use of her graphics programs; H. Jacobowitz for encouragement and valuable technical consultations; and A. Gruber for his general support of the project and incisive critical review of the JGR paper.

DATE DUE

I/3408

INTRODUCTION

Scanning channel data of the Nimbus-7 ERB instrument have been combined with auxiliary information to describe the radiative characteristics of surfaces as observed through the atmosphere. This information has been recorded on the ERB 'Sub-Target Radiance Tapes' (STRT). A description of that data base and procedures for obtaining the data may be found in Stowe and Fromm (1983). Selected data from the STRTs have been sorted into eight uniform earth and cloud surface types. Diagrams illustrating the bi-directional reflectivity of these surfaces have been constructed.

Several of these diagrams have already been published in a paper by Taylor and Stowe (1984). That paper is included as appendix A of this report to provide a complete discussion of: 1) how these diagrams can be interpreted; 2) why they are important and useful; 3) how they compare with other empirical and theoretical results and 4) the methods of diagram construction. The paper also discusses the observed dependence of albedo on solar zenith angle (SZA) and includes figures illustrating this dependence. An extensive list of references is also given.

This report contains a complete set of reflectance diagrams (patterns) and tables listing the values that were used in their construction and interpretation. Fig. 1.0 shows the sequential numbering system and the layout of the polar coordinate bin array into which the data were sorted. Satellite zenith angles and azimuths relative to the sun (zero degrees azimuth) are given for bin boundaries and centers. The entire hemisphere above any viewed point is represented by this array, since symmetry is assumed about the 'principal' solar plane (the plane containing the sun, viewed point and zenith). Data from symmetrical points about the principal plane are combined into the same bin.

The reflectance diagrams (Figs. 1.1 - 8.5) comprise the first main section of the report and show contours of anisotropic factor. The anisotropic factor is a ratio between the radiance (radiant intensity) in a given direction and the radiance that would have resulted if the surface reflected isotropically. This can be stated mathematically as,

$$f(\theta', \phi') = \pi \bar{R}(\theta', \phi') \Big/ \int_0^{2\pi} \int_0^{\pi/2} \bar{R}(\theta, \phi) \cos\theta \sin\theta \, d\theta \, d\phi \qquad (1)$$

where, $R(\theta', \phi')$ is the average of all normalized radiance observations in an angular bin centered at θ' and ϕ'. Radiances are normalized to a solar zenith angle (SZA) of 0° when divided by cosine(SZA) at the time of observation. The contour labeled '1.0' represents the angles at which the isotropic assumption gives the correct radiant exitance (flux density) for that surface and solar zenith angle range. Any departure from 1.0 represents the fractional error that would be made if isotropy were used to estimate the radiant exitance. Areas are clear or stippled (lined or crosshatched) when the anisotropic factor is greater (less) than one. To conserve space, each diagram consists of a pair of matched 'half' patterns from two consecutive SZA ranges, differing by 0.1 in cosine(SZA). The values of albedo, total population, integral (denominater in eq. 1, in watts/m^2) and integral/pi (isotropic mean radiance, in w/m^2str.) are given below each half pattern. The albedo is simply the ratio of the integral (already normalized to SZA = 0°) and the solar constant (assumed to be 1376 W/m^2). The mean normalized radiance in any

direction is obtained by multiplying the isotropic mean radiance by the anisotropic factor for that direction.

Prior to the application of an objective analysis technique, anisotropic factors for empty bins were estimated by interpolation. This was accomplished by a simple population and inverse distance weighted average of nearest neighbors. The interpolated values are included in the tables. Some analyses were tried which required mimimum bin populations and a corresponding increase in the need for interpolation. These, however, were not significantly smoother and were abandoned. Patterns with low populations (approx. 600 or less) are quite noisy and probably not representative as far as small-scale details are concerned. Such patterns, nevertheless, adequately represent larger-scale features and are included.

The second major section of the report contains tabulated listings (Tables 1.1 - 8.3) for anisotropic factor, relative dispersion and bin population. These are ordered by sequential bin number (see Fig. 1.0) and by solar zenith angle range. Relative dispersion is defined as the standard deviation divided by the mean radiance in each bin. It represents both the uncertainty of measurement (scene identification, instrument noise) and the natural variability of the surface type. To get standard deviation about the mean normalized radiance, one may calculate the triple product of the integral/pi value at the bottom of each figure and the corresponding table values of relative dispersion and anisotropic factor. Empty bins in the relative dispersion tables (represented by zeros in population tables and interpolated values in anisotropic factor tables) are filled by designator values of -9.99 .

Slight discrepancies may be noticed between a few of the anisotropic factors in the tables and values represented by the contours in the figures. Also, some small differences may be noted between the example figures in appendix A and the corresponding figures of the atlas. These differences are due to grid transformations and an adjustment of variable parameters made in connection with the objective analysis technique. The anisotropic factors in the tables are the source for both analysis versions and should be used if a discrepancy is noted.

Appendix B describes the format of a tape which contains the diagrams and other relevant data in digital form. The tape may be obtained for a nominal fee from NOAA-NESDIS, Satellite Data Services Division, World Weather Bldg. Rm. 100, Washington D. C., 20233.

In the time elapsed since the appendix article was accepted for publication, the data base has been considerably enlarged (from 61 to 272 days). A preliminary report based upon the larger data base has been made by Taylor et al. (1983) and further studies are in progress. In those cases for which the same surface type definitions were used, the patterns presented here are very similar to those from the larger data base.

REFERENCES

1. Stowe, L. L. and M. D. Fromm, 1983: Nimbus-7 ERB Sub-Target Radiance Tape (STRT) Data Base, NOAA Tech. Memo. NESDIS-3, U. S. Dept. of Commerce, Wash. D. C., 84 pp.

2. Taylor, V. R. and L. L. Stowe, 1984: Reflectance Characteristics of Uniform Earth and Cloud Surfaces Derived from Nimbus-7 ERB, Journal of Geophysical Research, Vol. 89 No. D4, June.

3. Taylor, V. R., J. M. Vilardo and L. L. Stowe, 1983: Nimbus-7 ERB Reflectance Patterns for ERBE, Proceedings of Fifth AMS Conference on Atmospheric Radiation, Baltimore, Md., November, pp. 452-455.

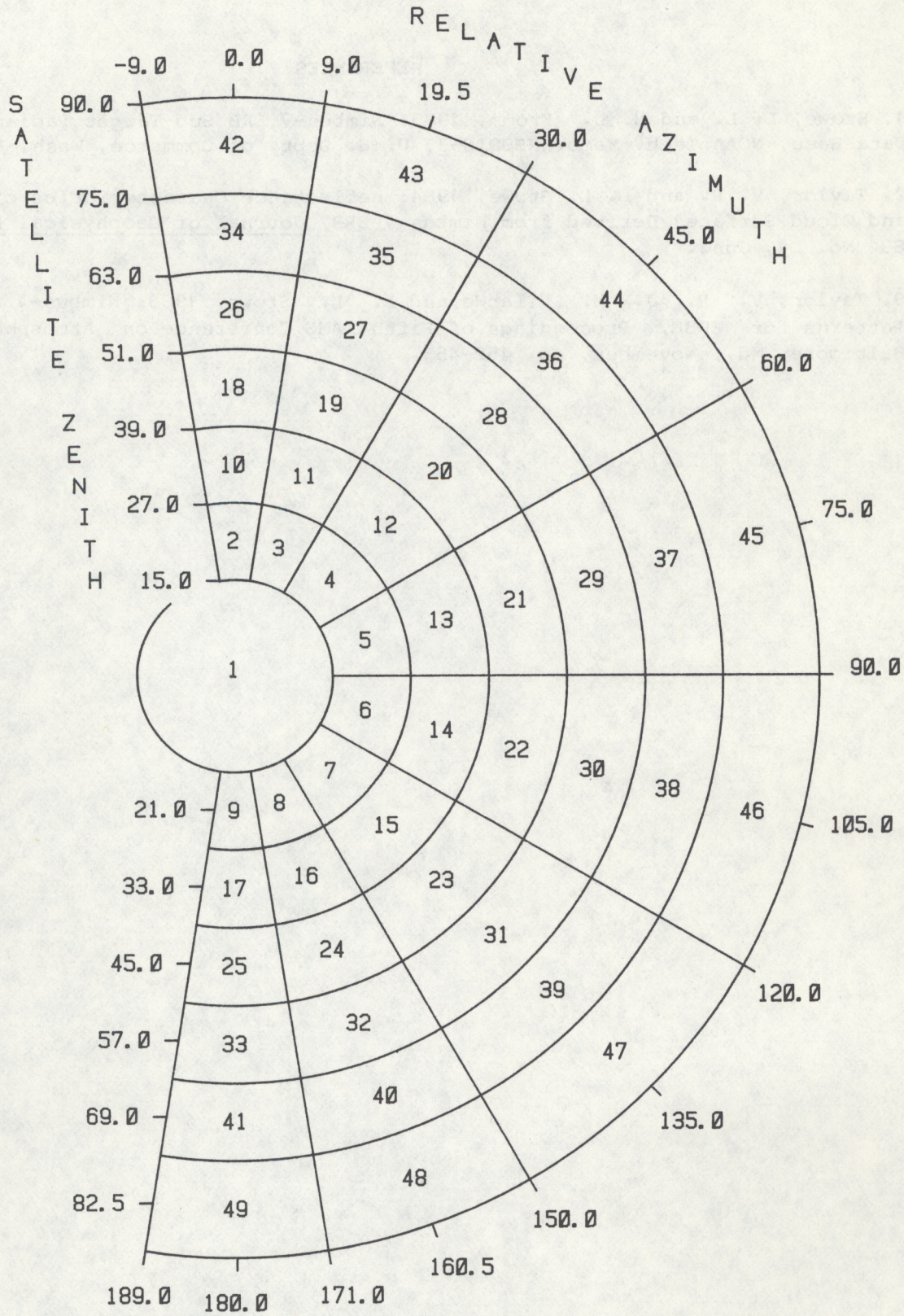

FIG. 1.0 COORDINATES AND NUMBERING SCHEME FOR ANGULAR BIN ARRAY

NIMBUS-7 ERB BI-DIRECTIONAL REFLECTANCE

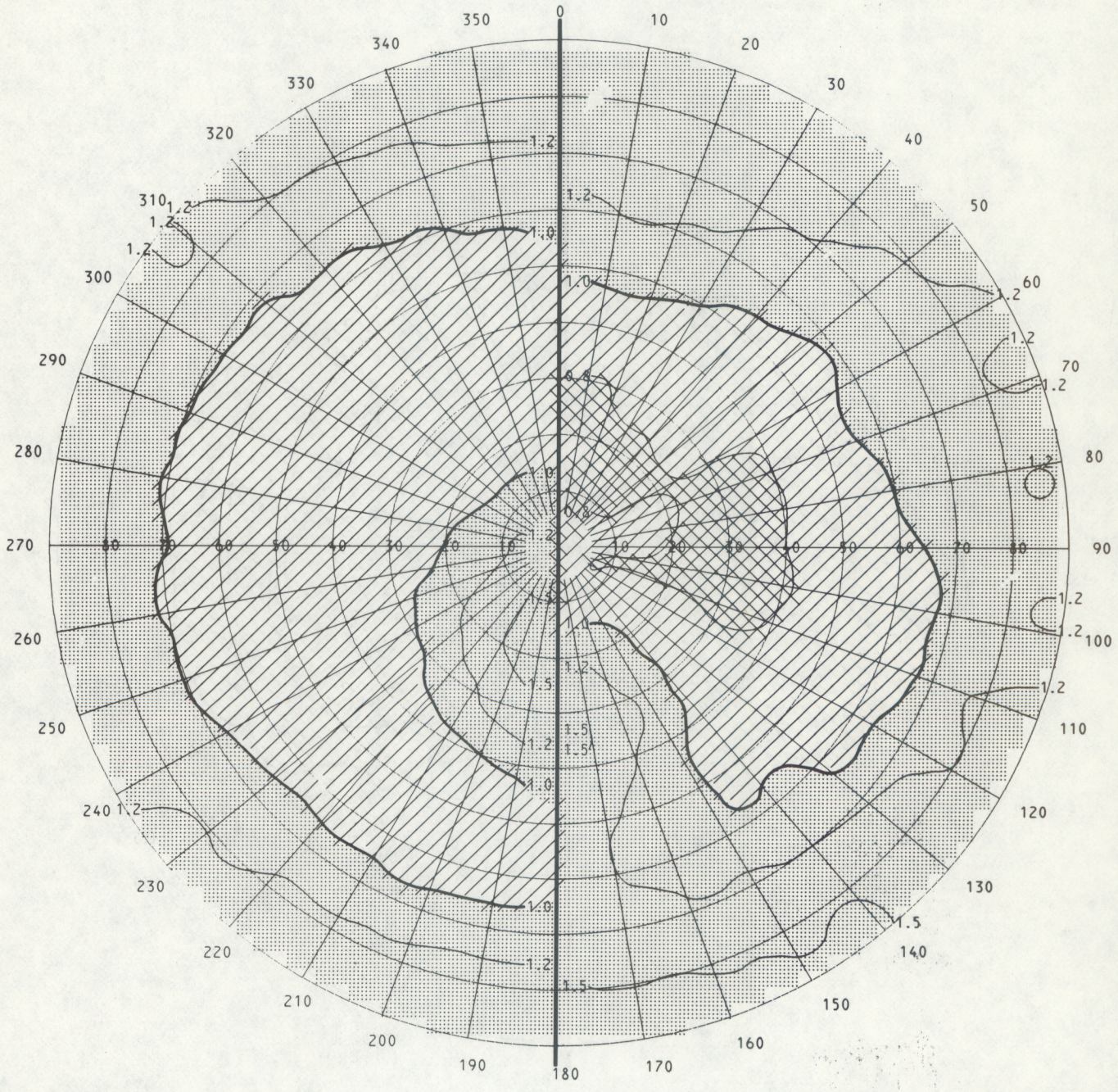

ALBEDO=.09
POPULATION= 27065
SOLAR ZENITH ANG (0.0-25.8)
INTEGRAL= 119.5 INTEGRAL/PI= 38.0

ALBEDO=.10
POPULATION= 12345
SOLAR ZENITH ANG (25.8-36.9)
INTEGRAL= 139.6 INTEGRAL/PI= 44.4

CLEAR OCEAN

Fig. 1.1

NIMBUS-7 ERB BI-DIRECTIONAL REFLECTANCE

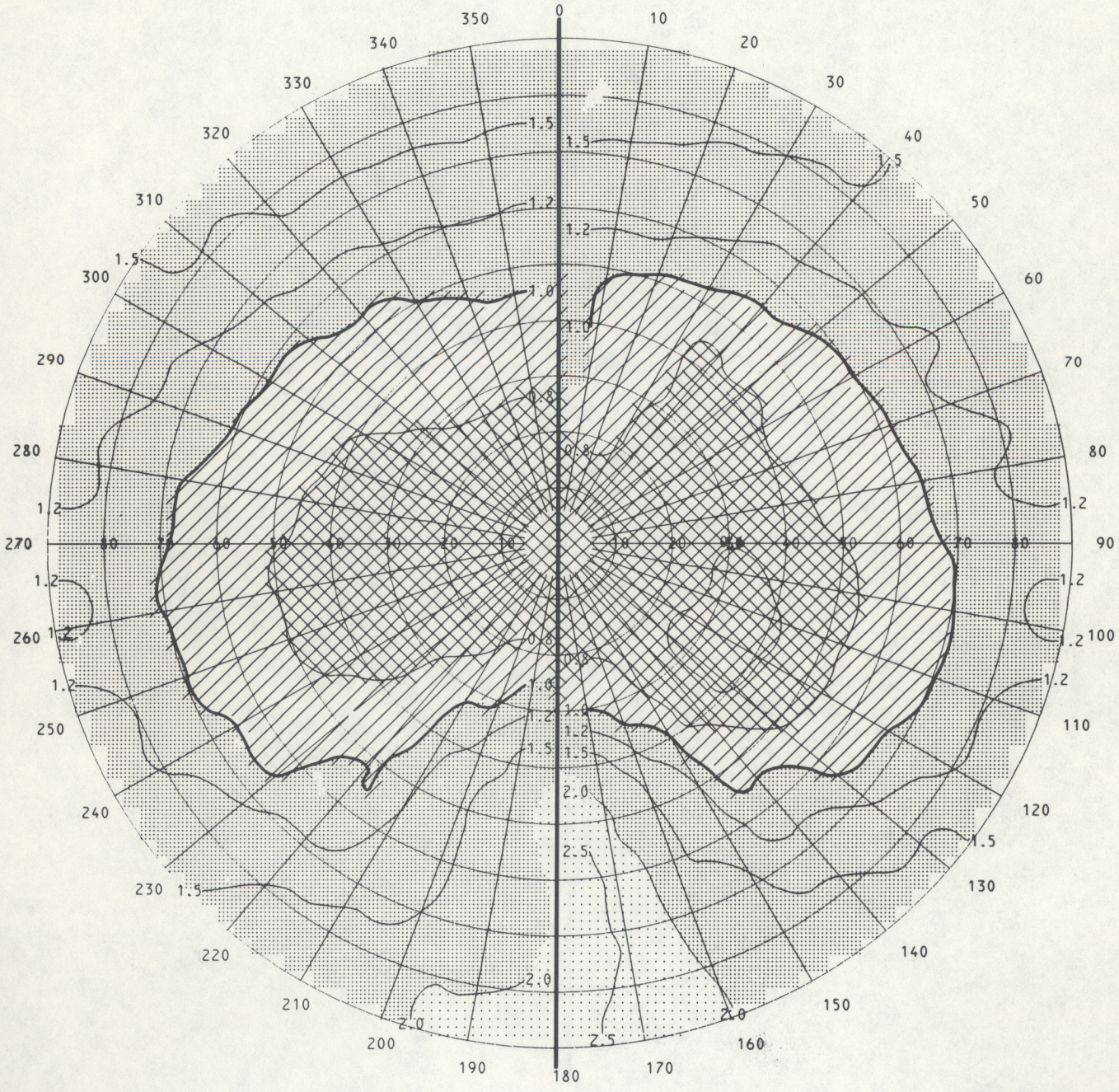

ALBEDO=.11
POPULATION= 9923
SOLAR ZENITH ANG (36.9-45.6)
INTEGRAL= 153.2 INTEGRAL/PI= 48.8

ALBEDO=.13
POPULATION= 4858
SOLAR ZENITH ANG (45.6-53.1)
INTEGRAL= 175.6 INTEGRAL/PI= 55.9

CLEAR OCEAN

Fig. 1.2

NIMBUS-7 ERB BI-DIRECTIONAL REFLECTANCE

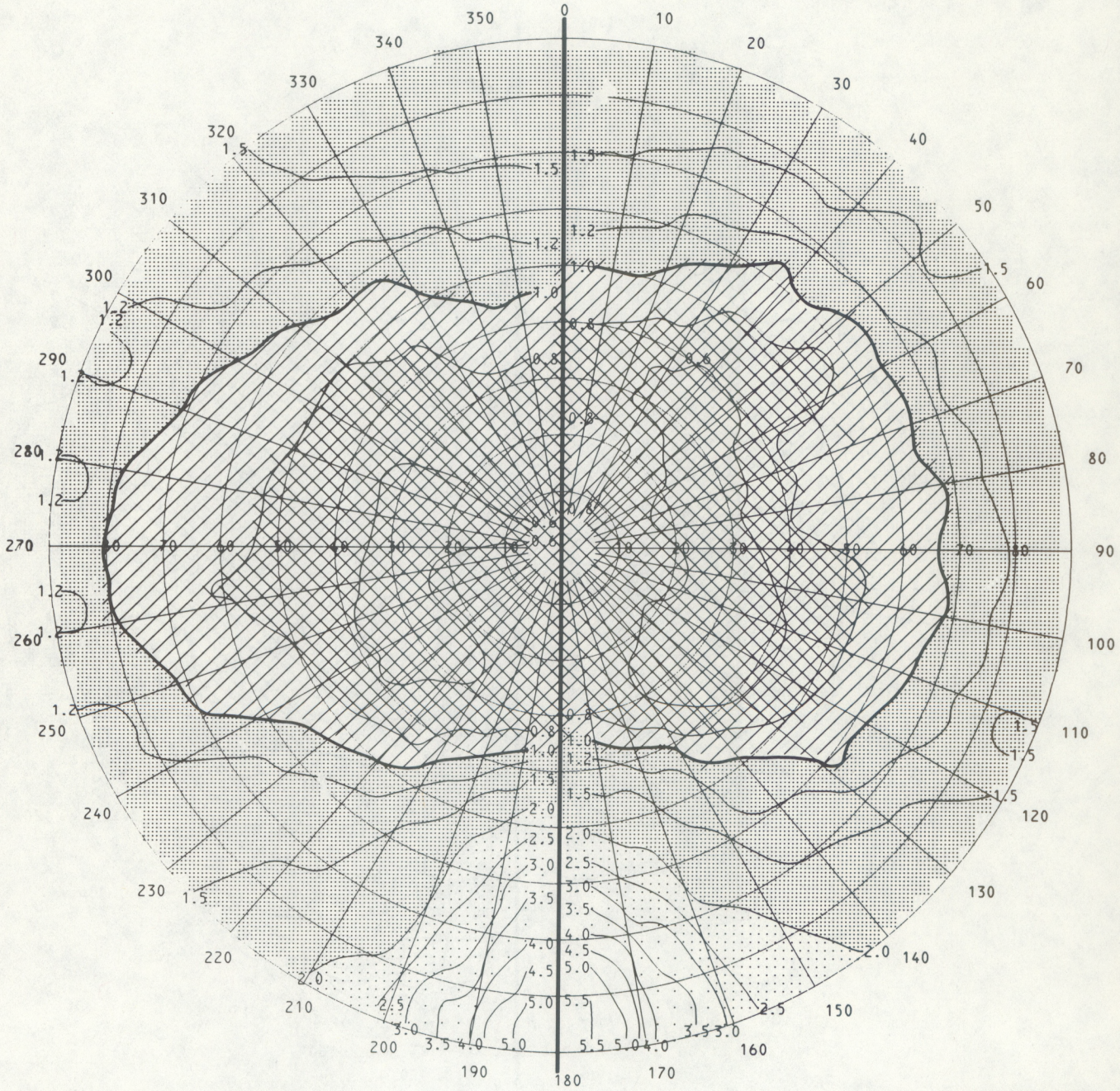

ALBEDO=.14
POPULATION= 2642
SOLAR ZENITH ANG (53.1-60.0)
INTEGRAL= 199.4 INTEGRAL/PI= 63.4

ALBEDO=.18
POPULATION= 1680
SOLAR ZENITH ANG (60.0-66.4)
INTEGRAL= 252.0 INTEGRAL/PI= 80.1

CLEAR OCEAN

Fig. 1.3

NIMBUS-7 ERB BI-DIRECTIONAL REFLECTANCE

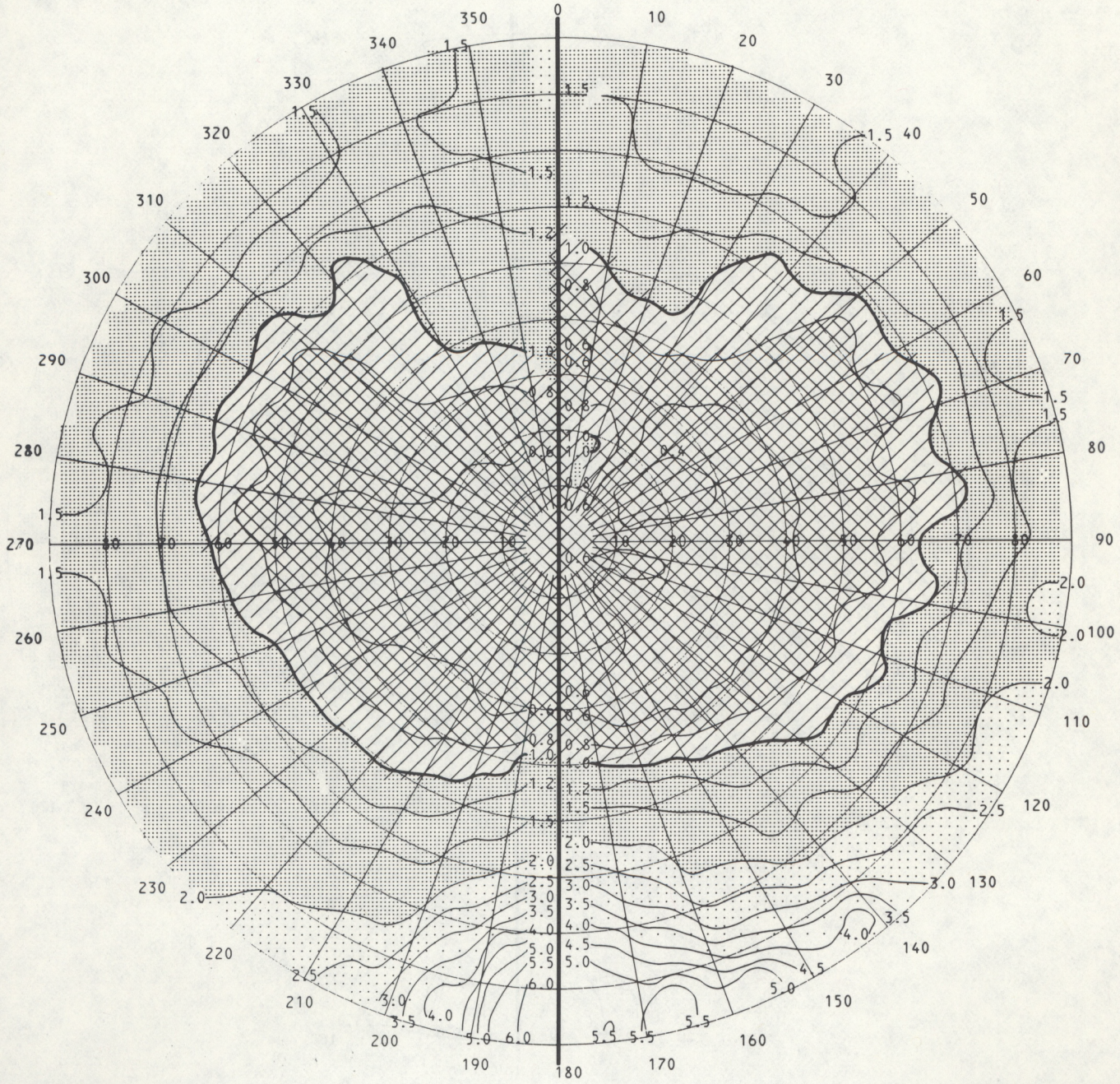

ALBEDO=.26
POPULATION= 774
SOLAR ZENITH ANG (66.4-72.5)
INTEGRAL= 355.1 INTEGRAL/PI= 113.0

ALBEDO=.32
POPULATION= 482
SOLAR ZENITH ANG (72.5-78.5)
INTEGRAL= 444.2 INTEGRAL/PI= 141.4

CLEAR OCEAN

Fig. 1.4

NIMBUS-7 ERB BI-DIRECTIONAL REFLECTANCE

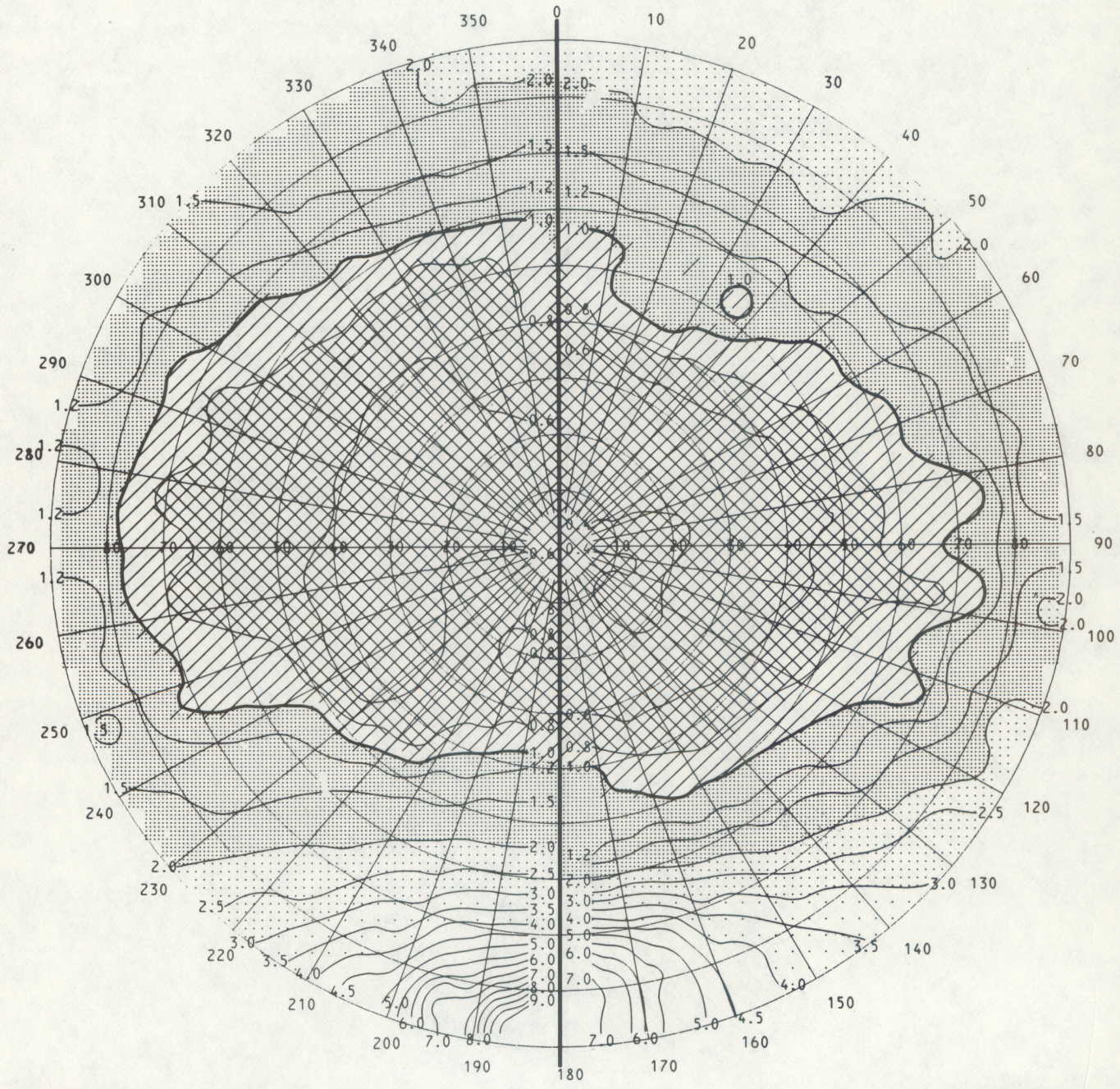

ALBEDO=.39
POPULATION= 536
SOLAR ZENITH ANG (78.5-84.3)
INTEGRAL= 537.3 INTEGRAL/PI= 171.0

ALBEDO=.43
POPULATION= 284
SOLAR ZENITH ANG (84.3-90.0)
INTEGRAL= 599.3 INTEGRAL/PI= 190.7

CLEAR OCEAN

Fig. 1.5

NIMBUS-7 ERB BI-DIRECTIONAL REFLECTANCE

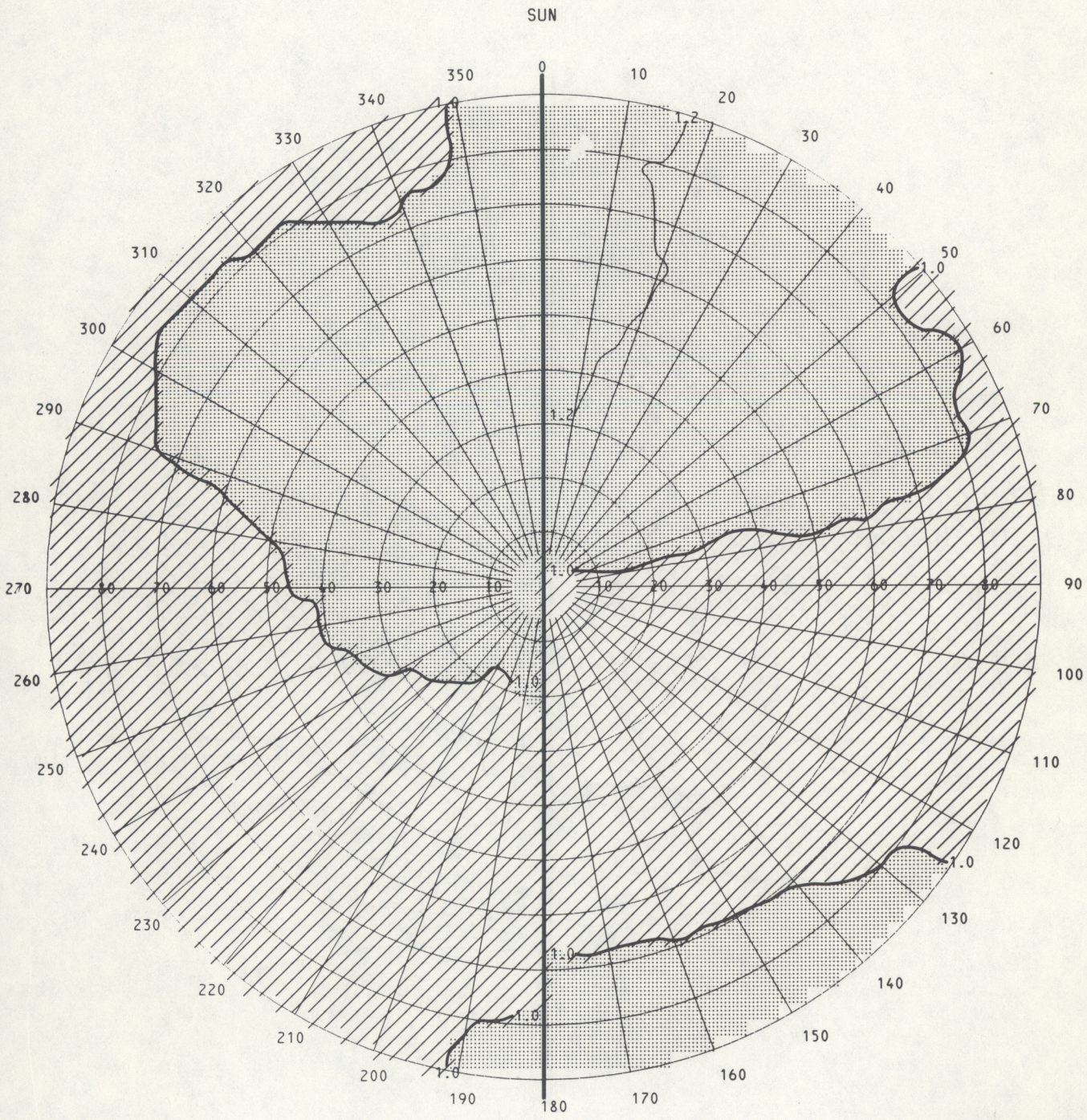

ALBEDO=.22

POPULATION= 38658

SOLAR ZENITH ANG (0.0-25.8)

INTEGRAL= 298.0 INTEGRAL/PI= 94.8

ALBEDO=.18

POPULATION= 20731

SOLAR ZENITH ANG (25.8-36.9)

INTEGRAL= 252.3 INTEGRAL/PI= 80.3

CLEAR LAND

Fig. 2.1

NIMBUS-7 ERB BI-DIRECTIONAL REFLECTANCE

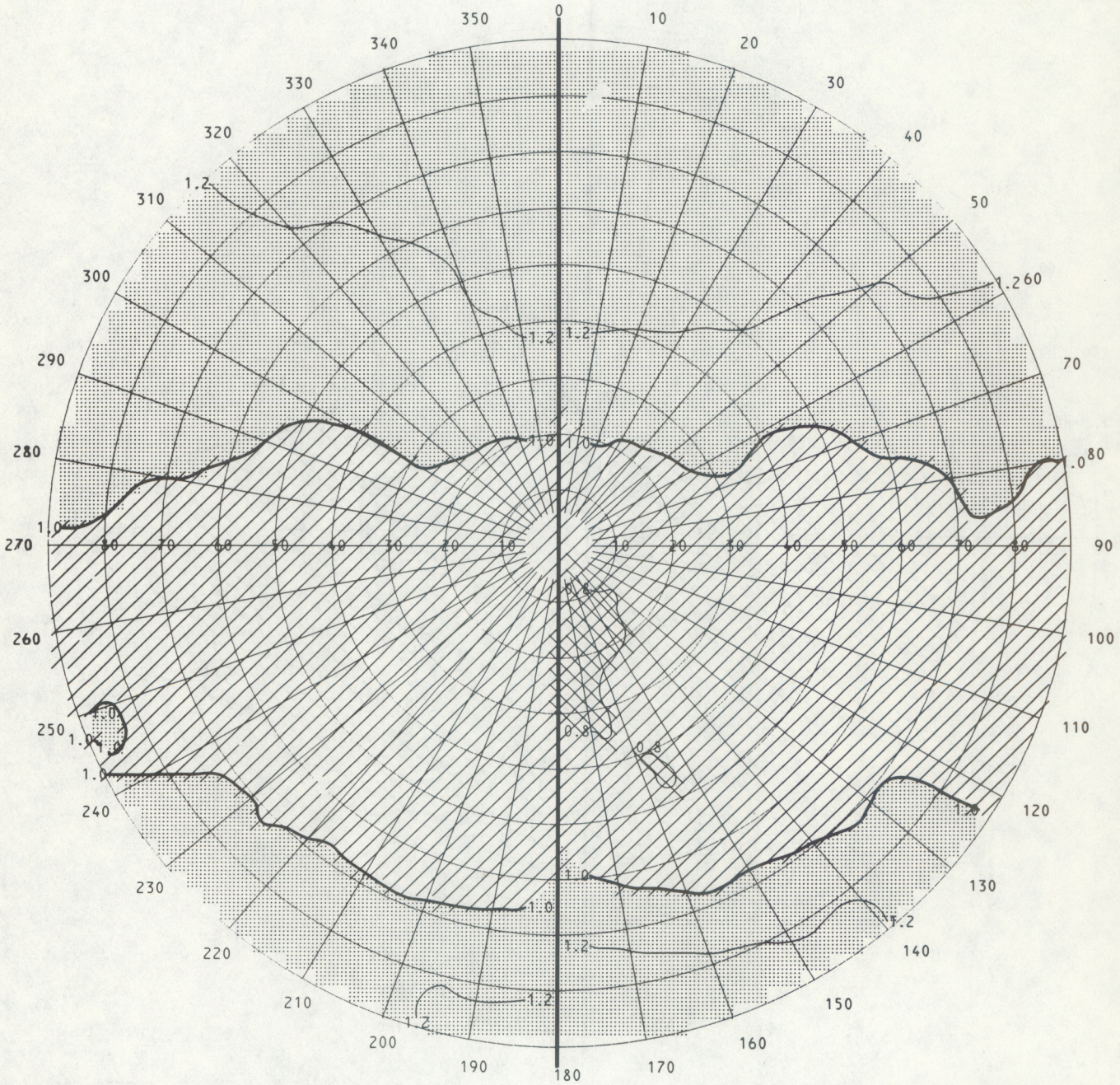

ALBEDO=.22
POPULATION= 16049
SOLAR ZENITH ANG (36.9-45.6)
INTEGRAL= 302.4 INTEGRAL/PI= 96.1

ALBEDO=.23
POPULATION= 10023
SOLAR ZENITH ANG (45.6-53.1)
INTEGRAL= 314.8 INTEGRAL/PI= 100.1

CLEAR LAND

Fig. 2.2

NIMBUS-7 ERB BI-DIRECTIONAL REFLECTANCE

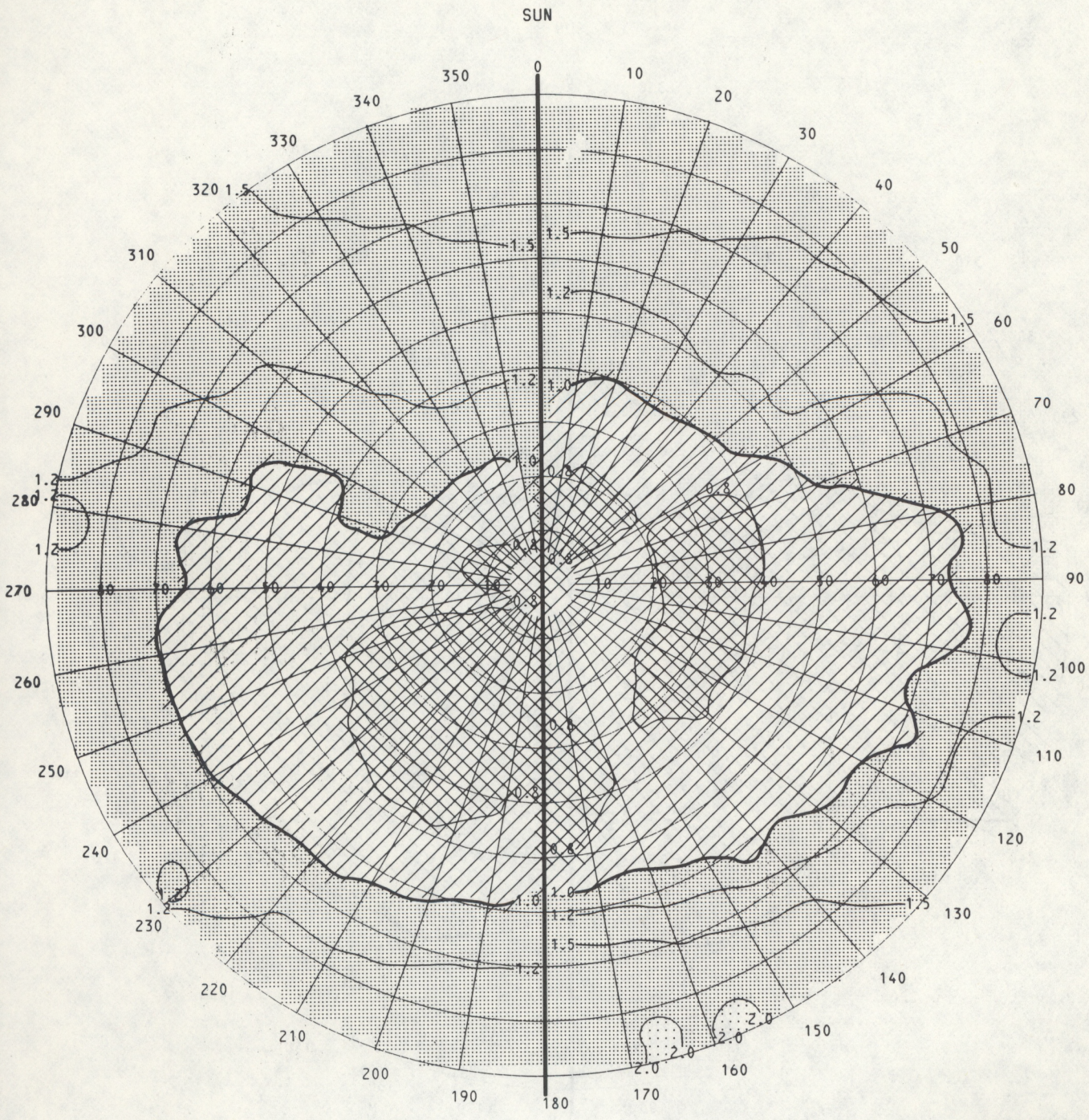

ALBEDO=.23

POPULATION= 3360

SOLAR ZENITH ANG (53.1-60.0)

INTEGRAL= 316.1 INTEGRAL/PI= 100.5

ALBEDO=.26

POPULATION= 1041

SOLAR ZENITH ANG (60.0-66.4)

INTEGRAL= 358.3 INTEGRAL/PI= 114.0

CLEAR LAND

Fig. 2.3

NIMBUS-7 ERB BI-DIRECTIONAL REFLECTANCE

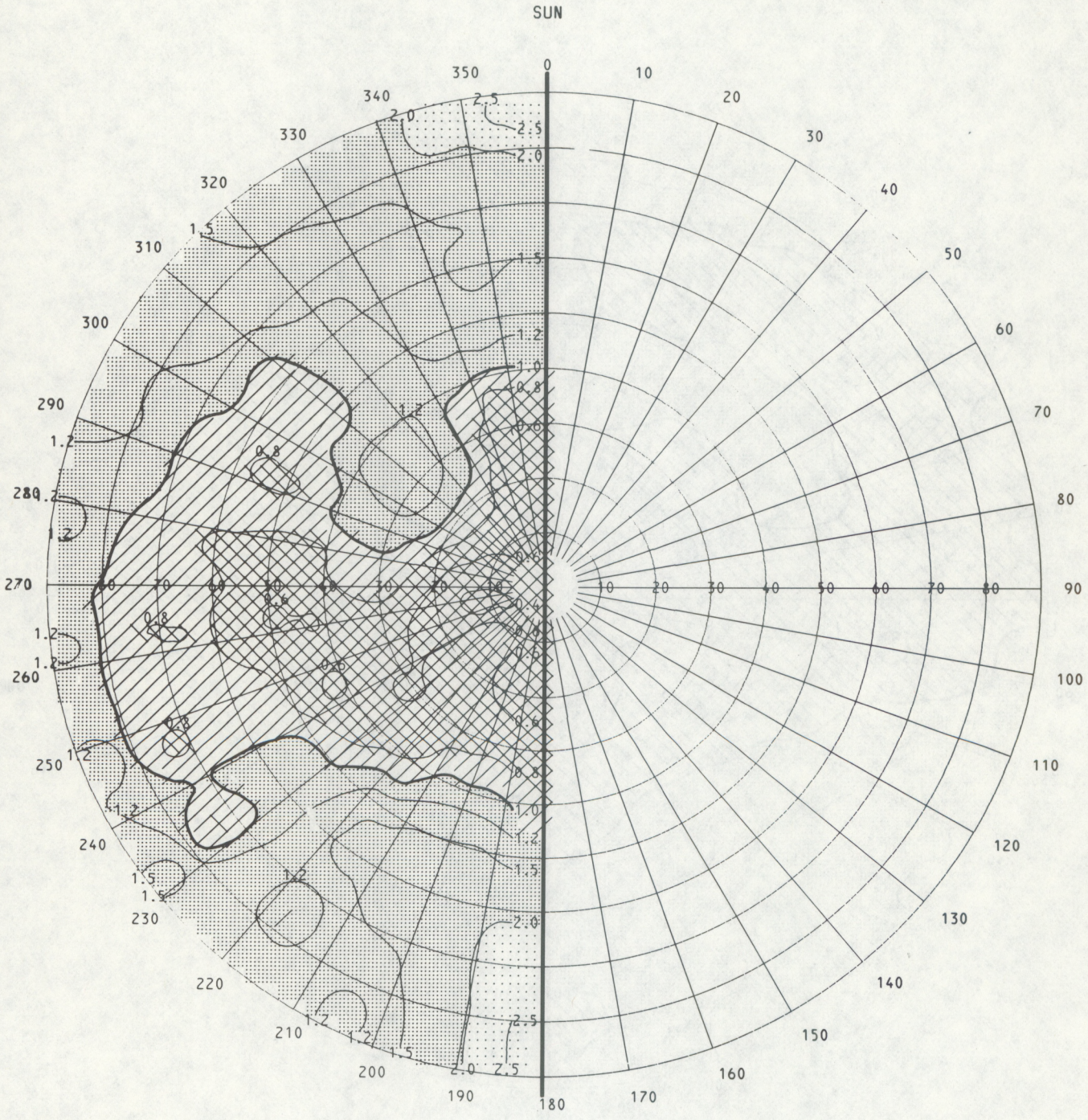

ALBEDO=.30

POPULATION= 381

SOLAR ZENITH ANG (66.4-72.5)

INTEGRAL= 409.5 INTEGRAL/PI= 130.2

CLEAR LAND

Fig. 2.4

NIMBUS-7 ERB BI-DIRECTIONAL REFLECTANCE

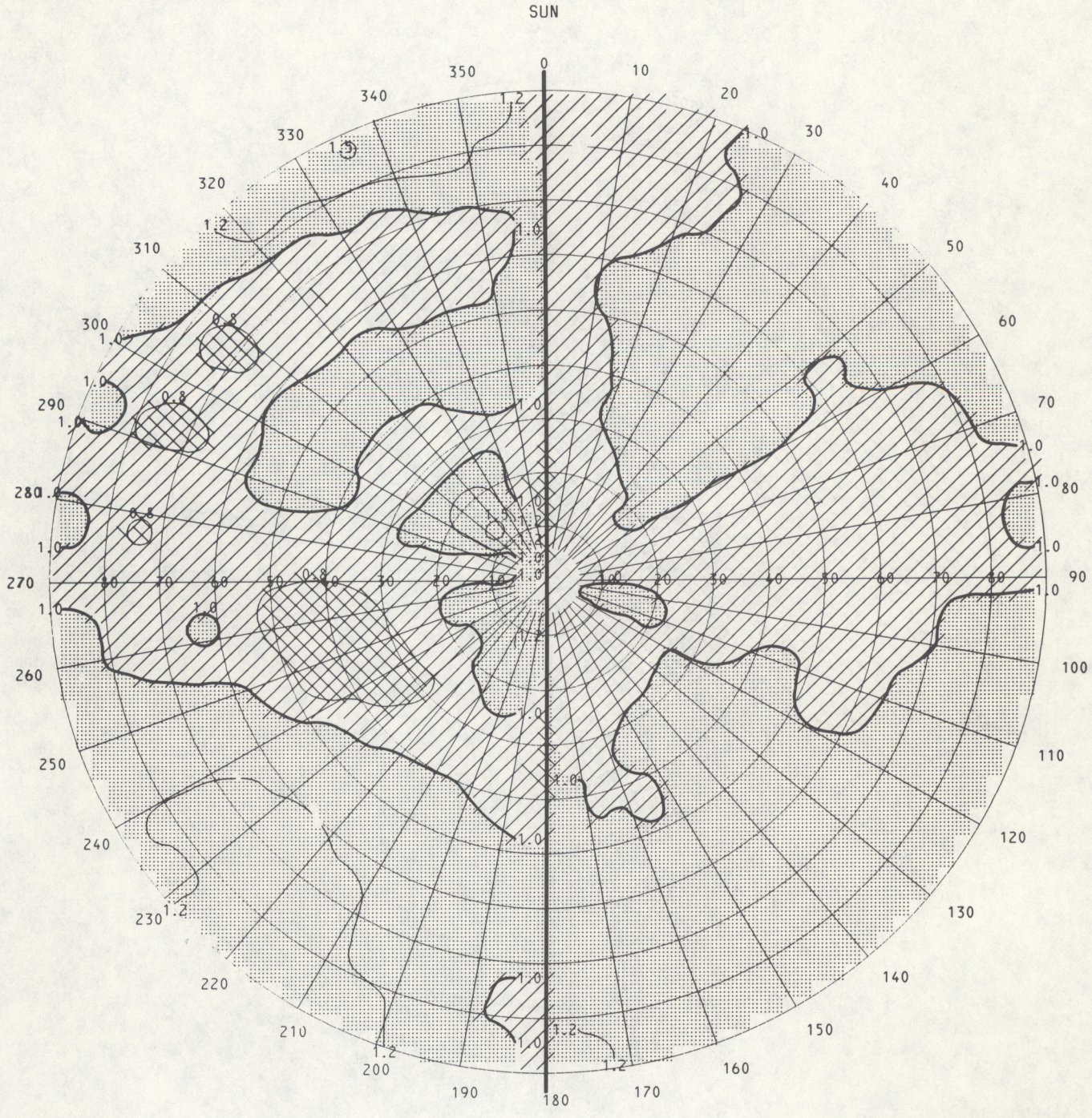

ALBEDO=.33
POPULATION= 214
SOLAR ZENITH ANG (36.9-45.6)
INTEGRAL= 460.8 INTEGRAL/PI= 146.6

ALBEDO=.65
POPULATION= 2021
SOLAR ZENITH ANG (45.6-53.1)
INTEGRAL= 899.0 INTEGRAL/PI= 286.1

CLEAR SNOW

Fig. 3.1

NIMBUS-7 ERB BI-DIRECTIONAL REFLECTANCE

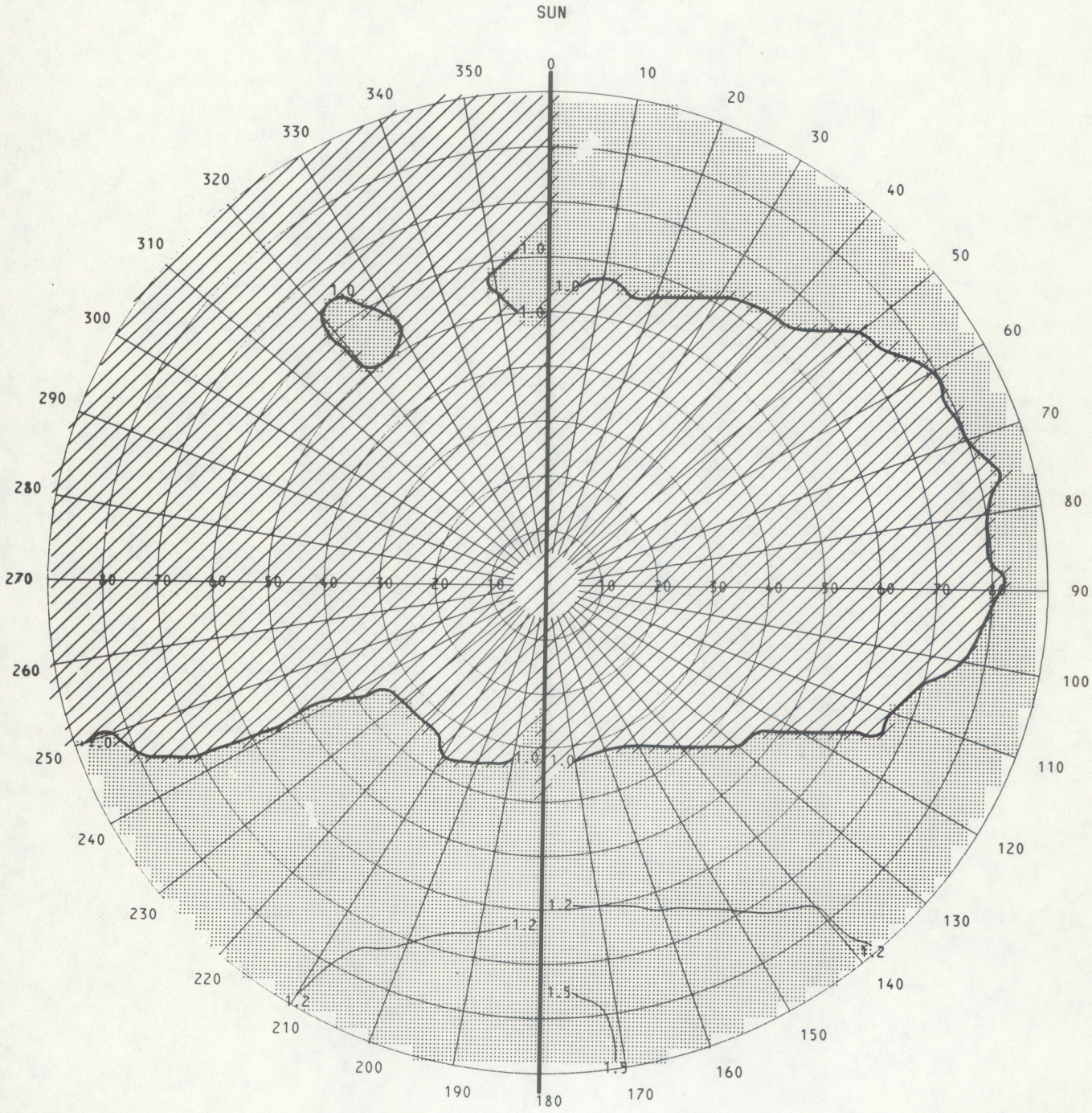

ALBEDO=.72
POPULATION= 8914
SOLAR ZENITH ANG (53.1-60.0)
INTEGRAL= 992.7 INTEGRAL/PI= 315.9

ALBEDO=.73
POPULATION= 12484
SOLAR ZENITH ANG (60.0-66.4)
INTEGRAL=1005.4 INTEGRAL/PI= 320.0

CLEAR SNOW

Fig. 3.2

NIMBUS-7 ERB BI-DIRECTIONAL REFLECTANCE

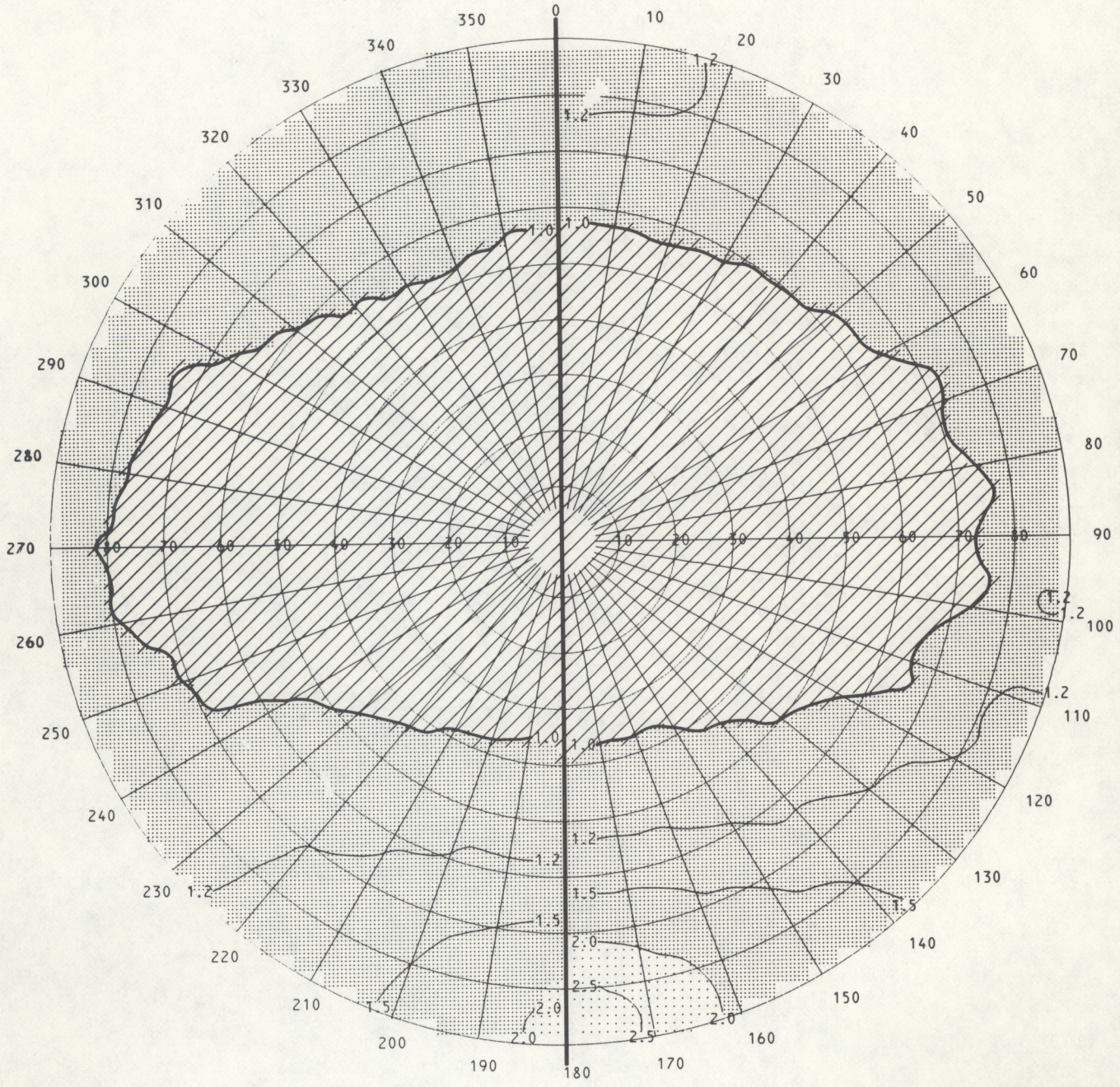

ALBEDO=.72

POPULATION= 12618

SOLAR ZENITH ANG (66.4-72.5)

INTEGRAL= 997.5 INTEGRAL/PI= 317.5

ALBEDO=.72

POPULATION= 9573

SOLAR ZENITH ANG (72.5-78.5)

INTEGRAL= 988.9 INTEGRAL/PI= 314.7

CLEAR SNOW

Fig. 3.3

NIMBUS-7 ERB BI-DIRECTIONAL REFLECTANCE

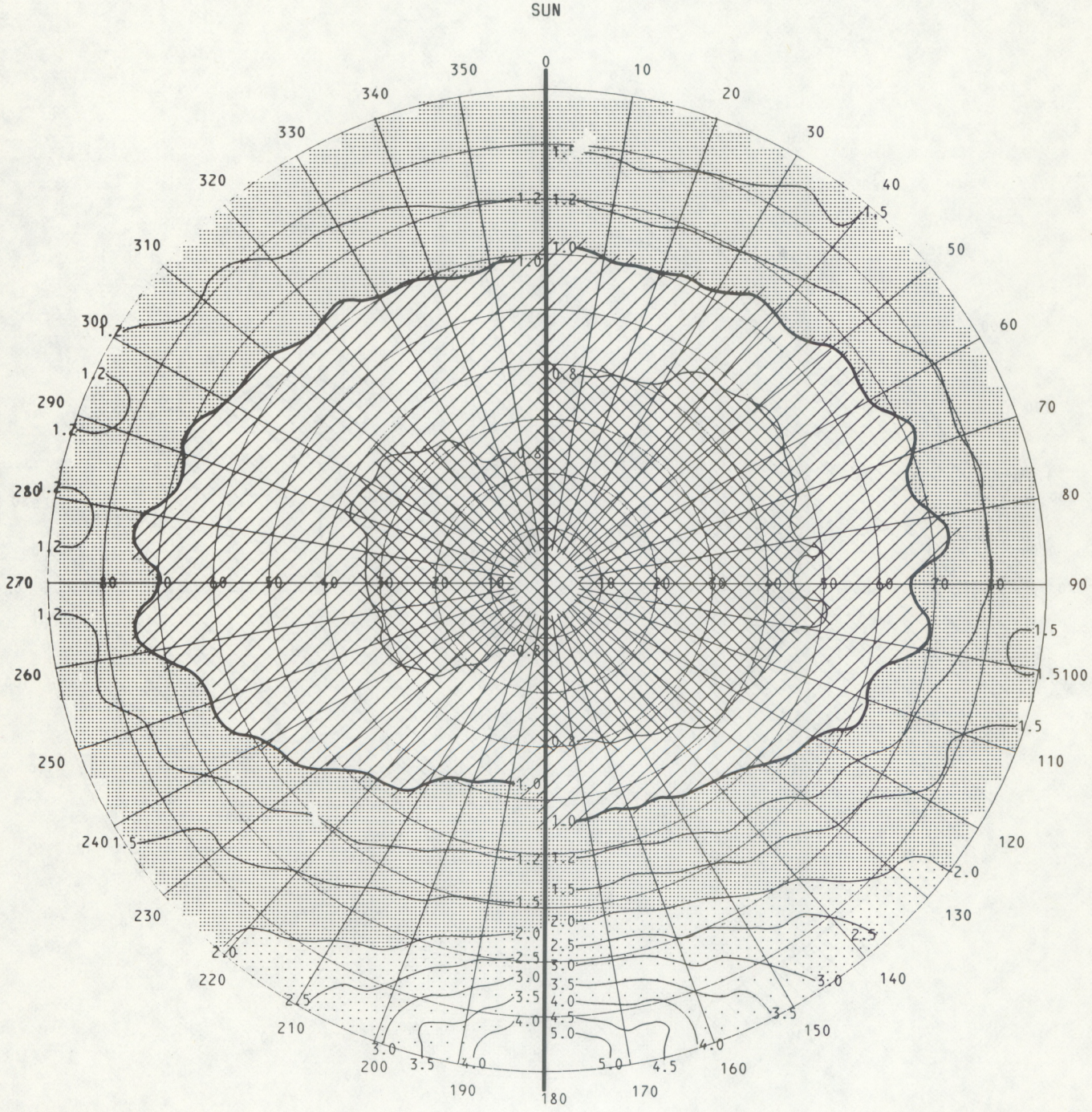

ALBEDO=.70
POPULATION= 7000
SOLAR ZENITH ANG (78.5-84.3)
INTEGRAL= 968.4 INTEGRAL/PI= 308.2

ALBEDO=.74
POPULATION= 3580
SOLAR ZENITH ANG (84.3-90.0)
INTEGRAL=1019.5 INTEGRAL/PI= 324.5

CLEAR SNOW

Fig. 3.4

NIMBUS-7 ERB BI-DIRECTIONAL REFLECTANCE

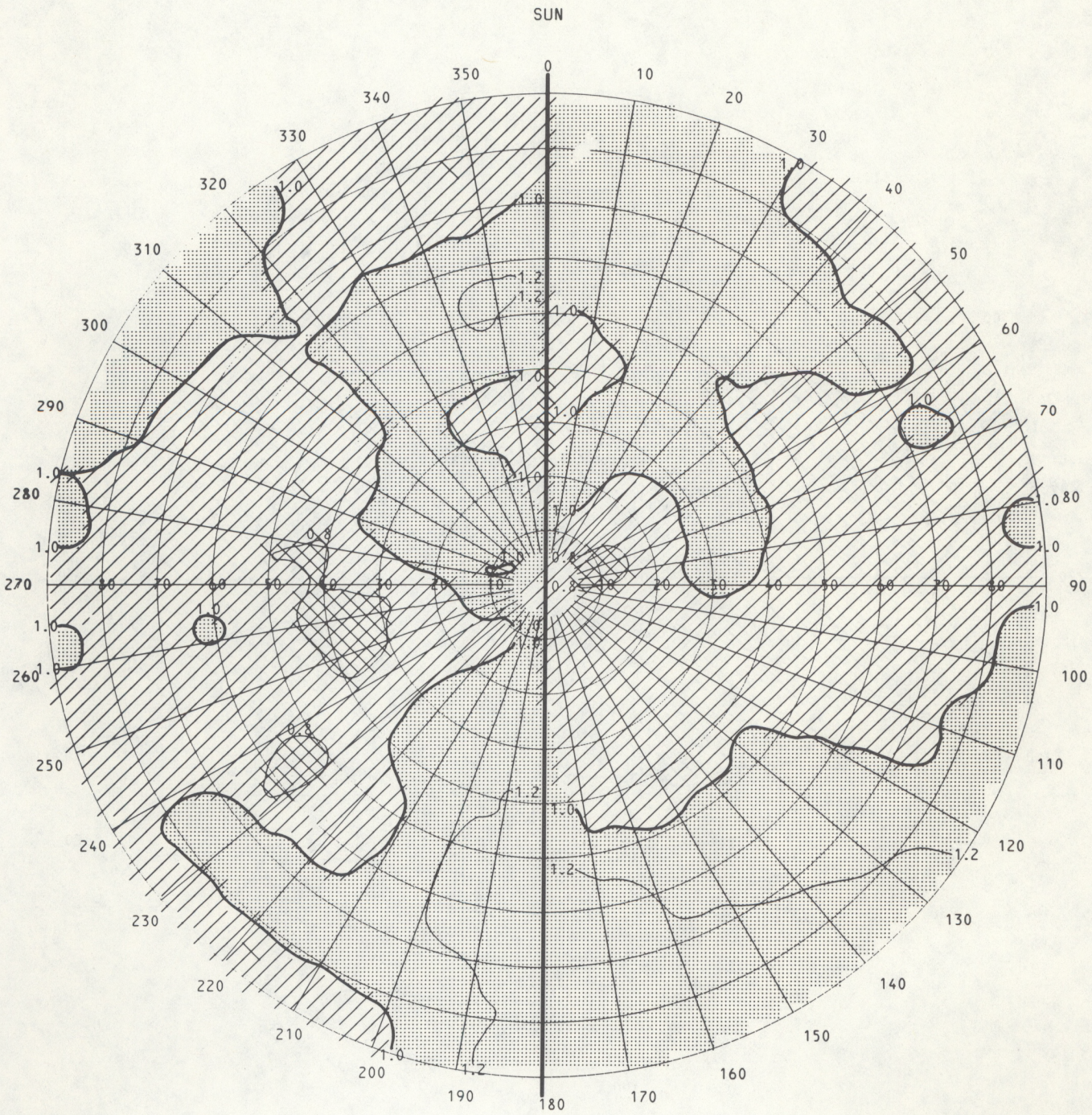

ALBEDO=.51
POPULATION= 368
SOLAR ZENITH ANG (45.6-53.1)
INTEGRAL= 709.0 INTEGRAL/PI= 225.6

ALBEDO=.52
POPULATION= 1134
SOLAR ZENITH ANG (53.1-60.0)
INTEGRAL= 720.5 INTEGRAL/PI= 229.2

CLEAR ICE

Fig. 4.1

NIMBUS-7 ERB BI-DIRECTIONAL REFLECTANCE

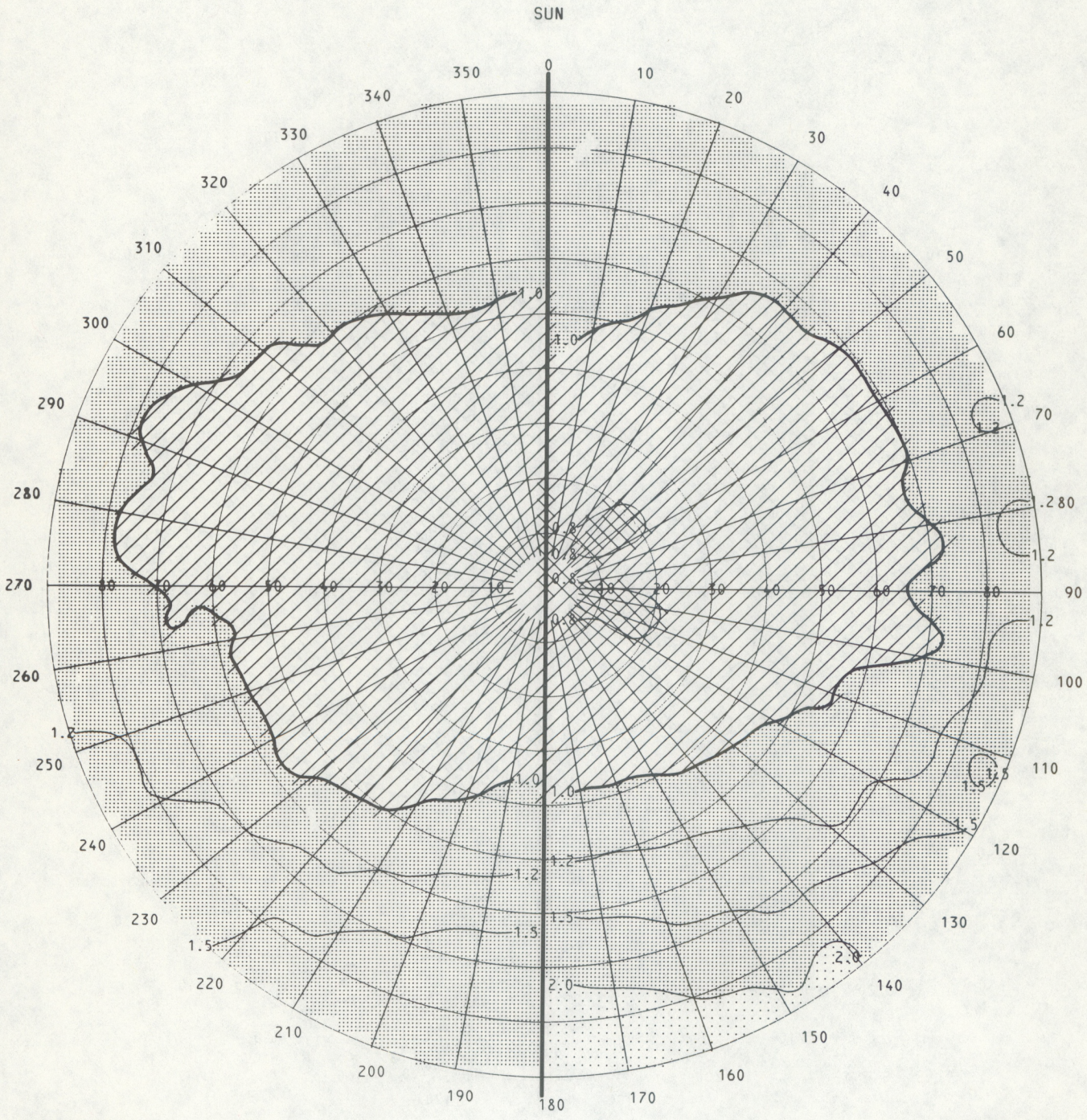

ALBEDO=.56
POPULATION= 2027
SOLAR ZENITH ANG (60.0-66.4)
INTEGRAL= 773.4 INTEGRAL/PI= 246.1

ALBEDO=.59
POPULATION= 2155
SOLAR ZENITH ANG (66.4-72.5)
INTEGRAL= 815.4 INTEGRAL/PI= 259.5

CLEAR ICE

Fig. 4.2

NIMBUS-7 ERB BI-DIRECTIONAL REFLECTANCE

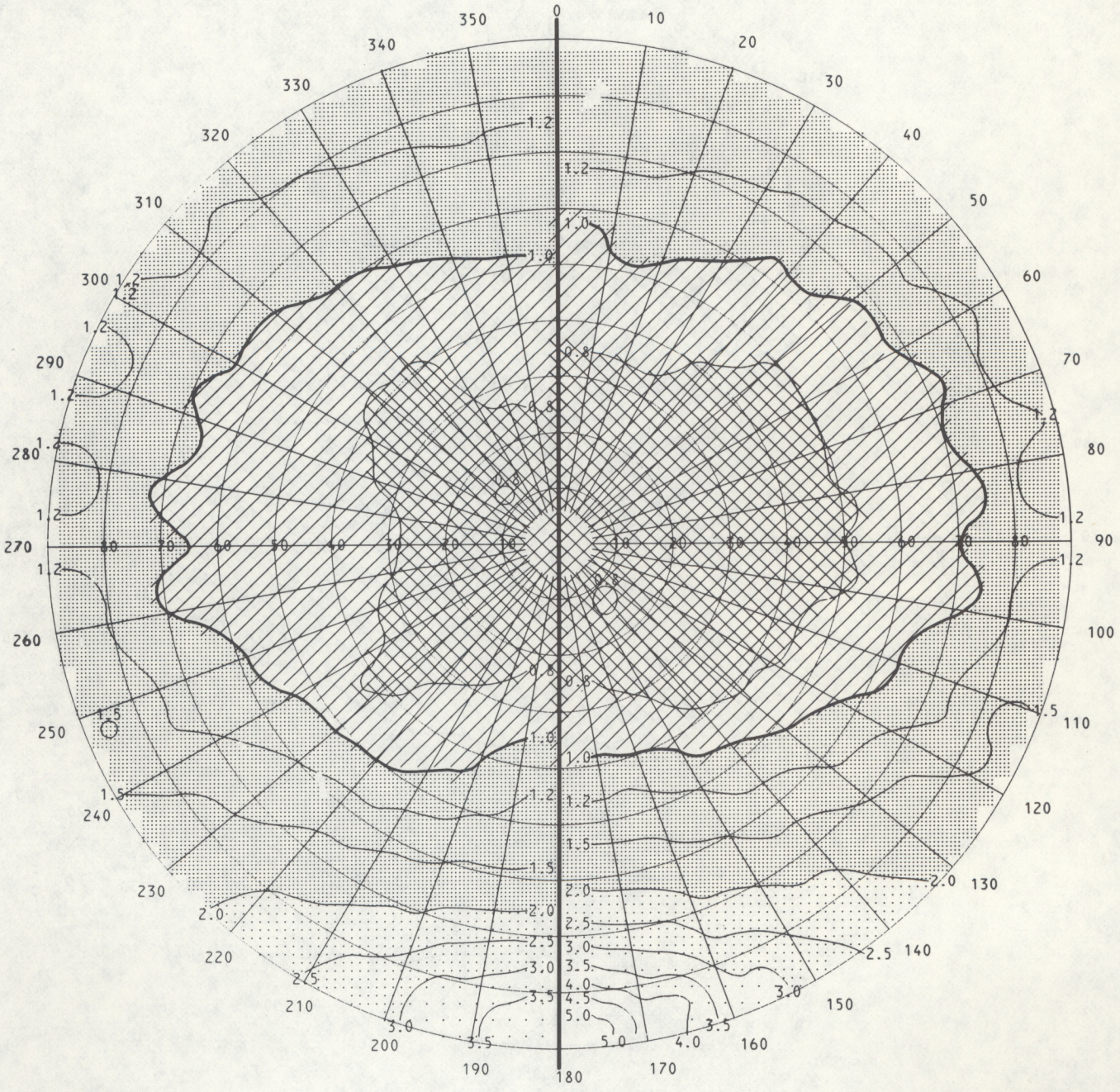

ALBEDO=.58

POPULATION= 1748

SOLAR ZENITH ANG (72.5-78.5)

INTEGRAL= 792.8 INTEGRAL/PI= 252.2

ALBEDO=.60

POPULATION= 1732

SOLAR ZENITH ANG (78.5-84.3)

INTEGRAL= 820.0 INTEGRAL/PI= 261.0

CLEAR ICE

Fig. 4.3

NIMBUS-7 ERB BI-DIRECTIONAL REFLECTANCE

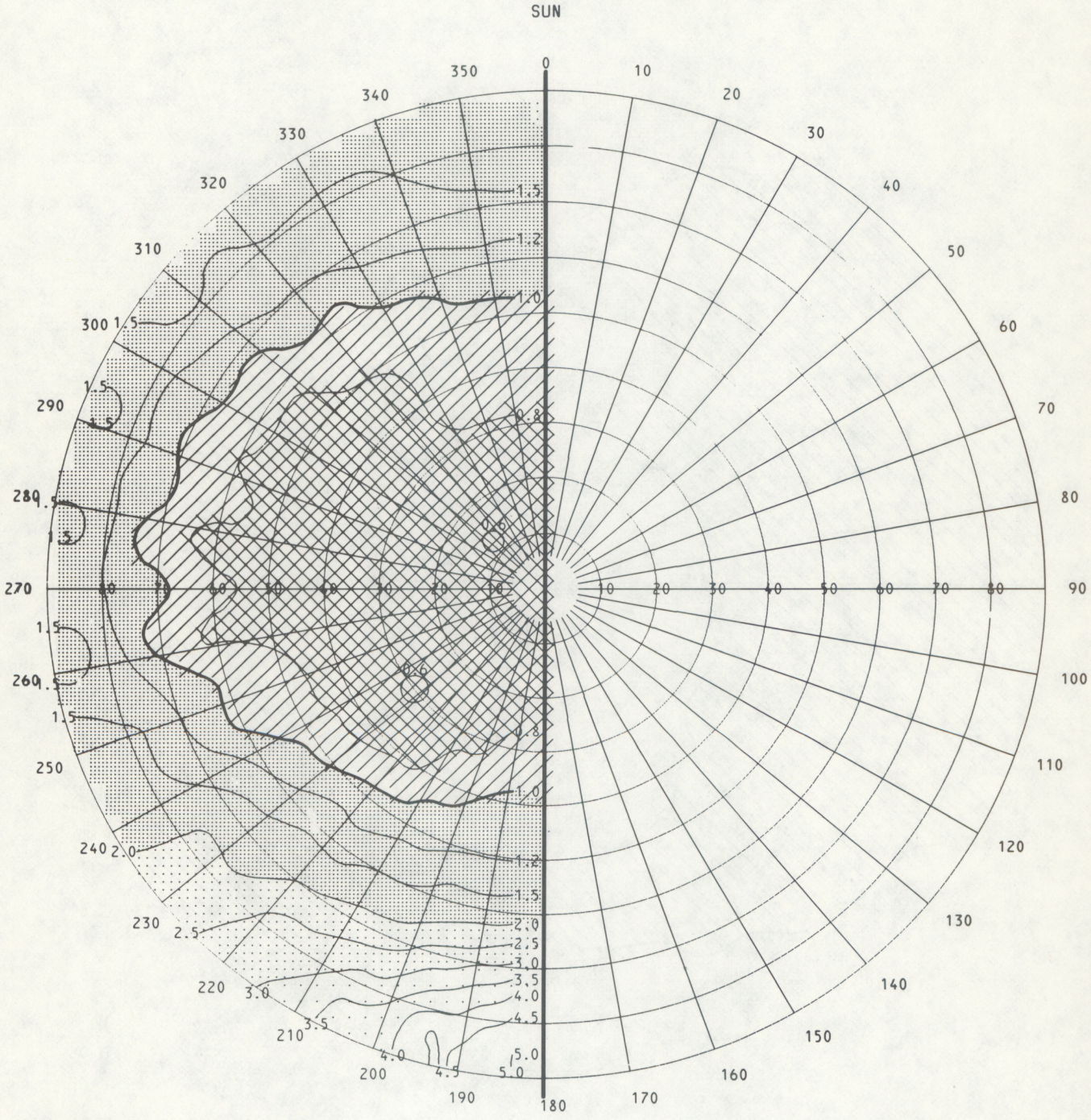

ALBEDO=.65

POPULATION= 961

SOLAR ZENITH ANG (84.3-90.0)

INTEGRAL= 897.1 INTEGRAL/PI= 285.5

CLEAR ICE

Fig. 4.4

NIMBUS-7 ERB BI-DIRECTIONAL REFLECTANCE

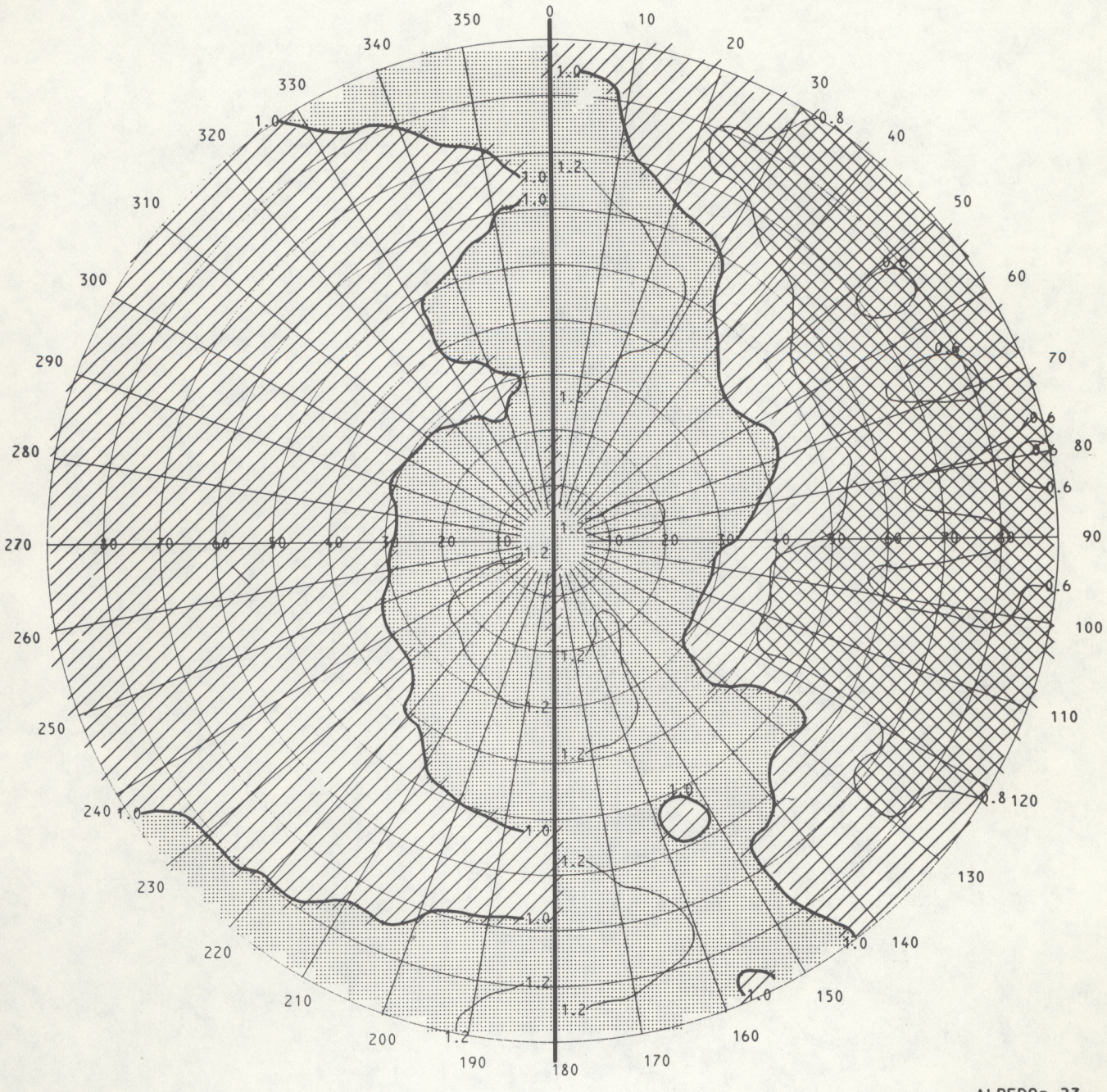

ALBEDO=.14

POPULATION= 16129

SOLAR ZENITH ANG (0.0-25.8)

INTEGRAL= 190.9 INTEGRAL/PI= 60.8

ALBEDO=.23

POPULATION= 4343

SOLAR ZENITH ANG (25.8-36.9)

INTEGRAL= 323.7 INTEGRAL/PI= 103.0

LOW CLOUD

Fig. 5.1

NIMBUS-7 ERB BI-DIRECTIONAL REFLECTANCE

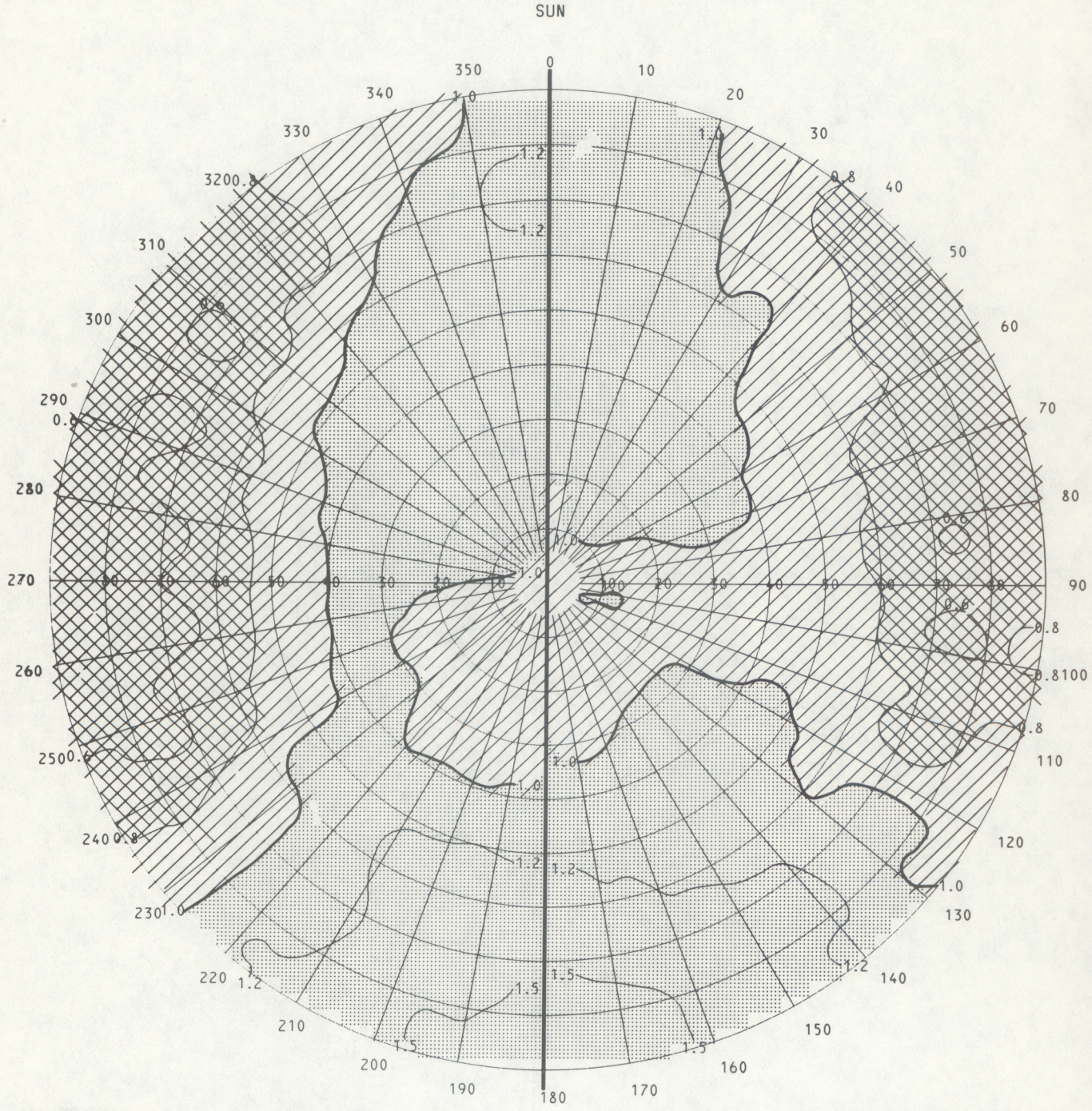

ALBEDO=.36
POPULATION= 2546
SOLAR ZENITH ANG (36.9-45.6)
INTEGRAL= 502.0 INTEGRAL/PI= 159.7

ALBEDO=.47
POPULATION= 1657
SOLAR ZENITH ANG (45.6-53.1)
INTEGRAL= 649.5 INTEGRAL/PI= 206.6

LOW CLOUD

Fig. 5.2

NIMBUS-7 ERB BI-DIRECTIONAL REFLECTANCE

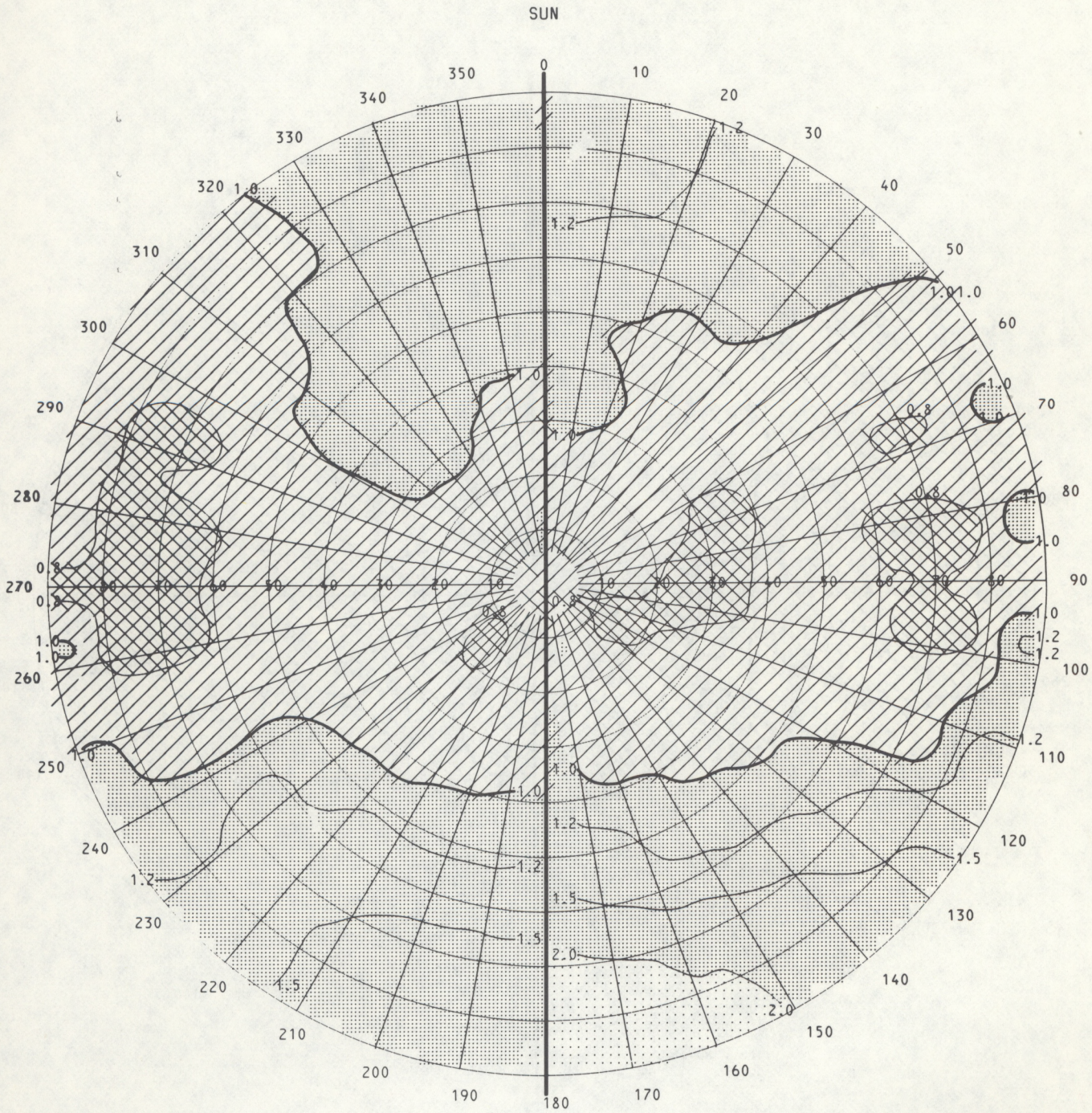

ALBEDO=.49
POPULATION= 1756
SOLAR ZENITH ANG (53.1-60.0)
INTEGRAL= 671.3 INTEGRAL/PI= 213.6

ALBEDO=.48
POPULATION= 1624
SOLAR ZENITH ANG (60.0-66.4)
INTEGRAL= 657.8 INTEGRAL/PI= 209.4

LOW CLOUD

Fig. 5.3

NIMBUS-7 ERB BI-DIRECTIONAL REFLECTANCE

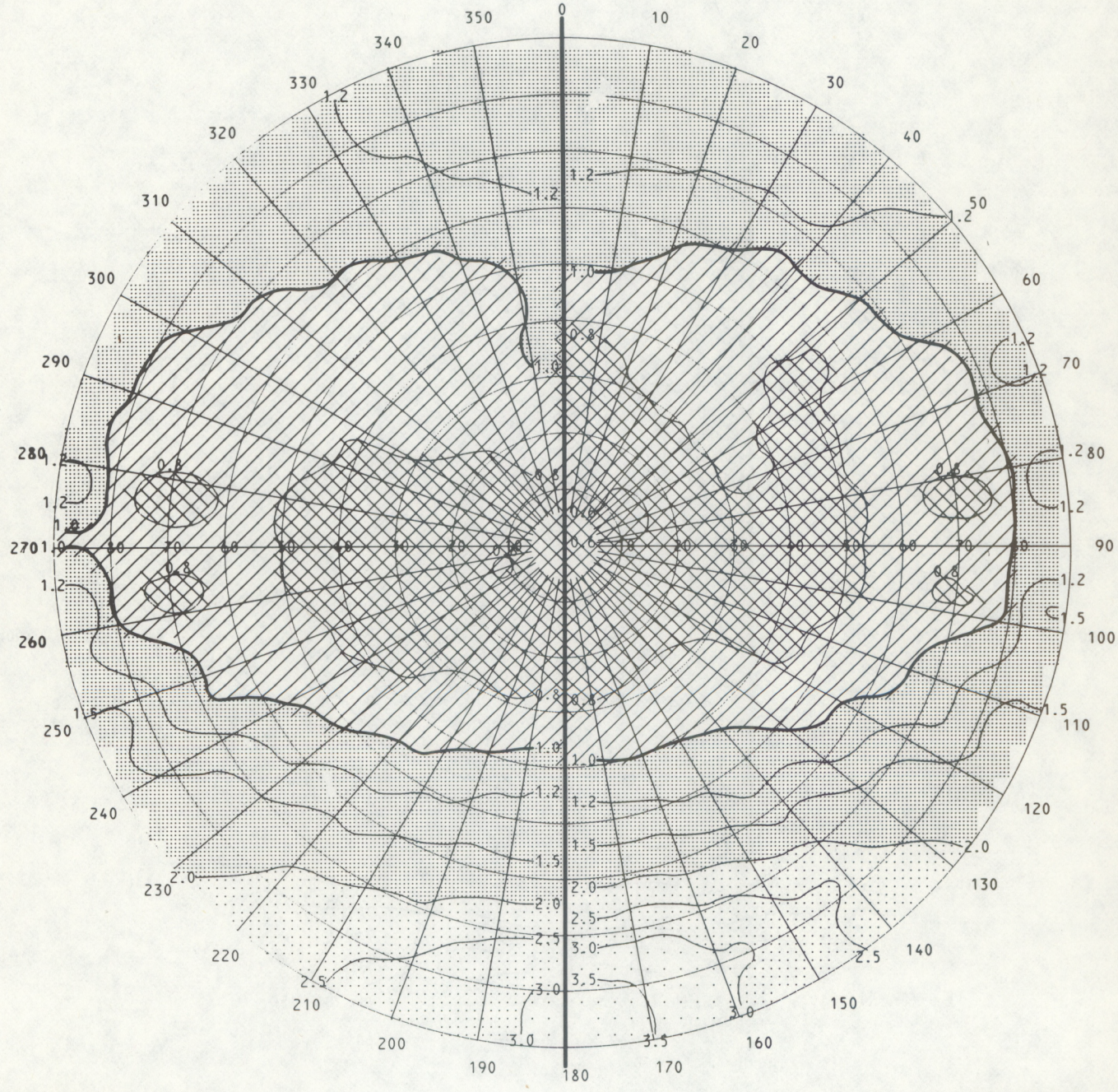

ALBEDO=.50
POPULATION= 1570
SOLAR ZENITH ANG (66.4-72.5)
INTEGRAL= 687.4 INTEGRAL/PI= 218.7

ALBEDO=.53
POPULATION= 1083
SOLAR ZENITH ANG (72.5-78.5)
INTEGRAL= 733.4 INTEGRAL/PI= 233.4

LOW CLOUD

Fig. 5.4

NIMBUS-7 ERB BI-DIRECTIONAL REFLECTANCE

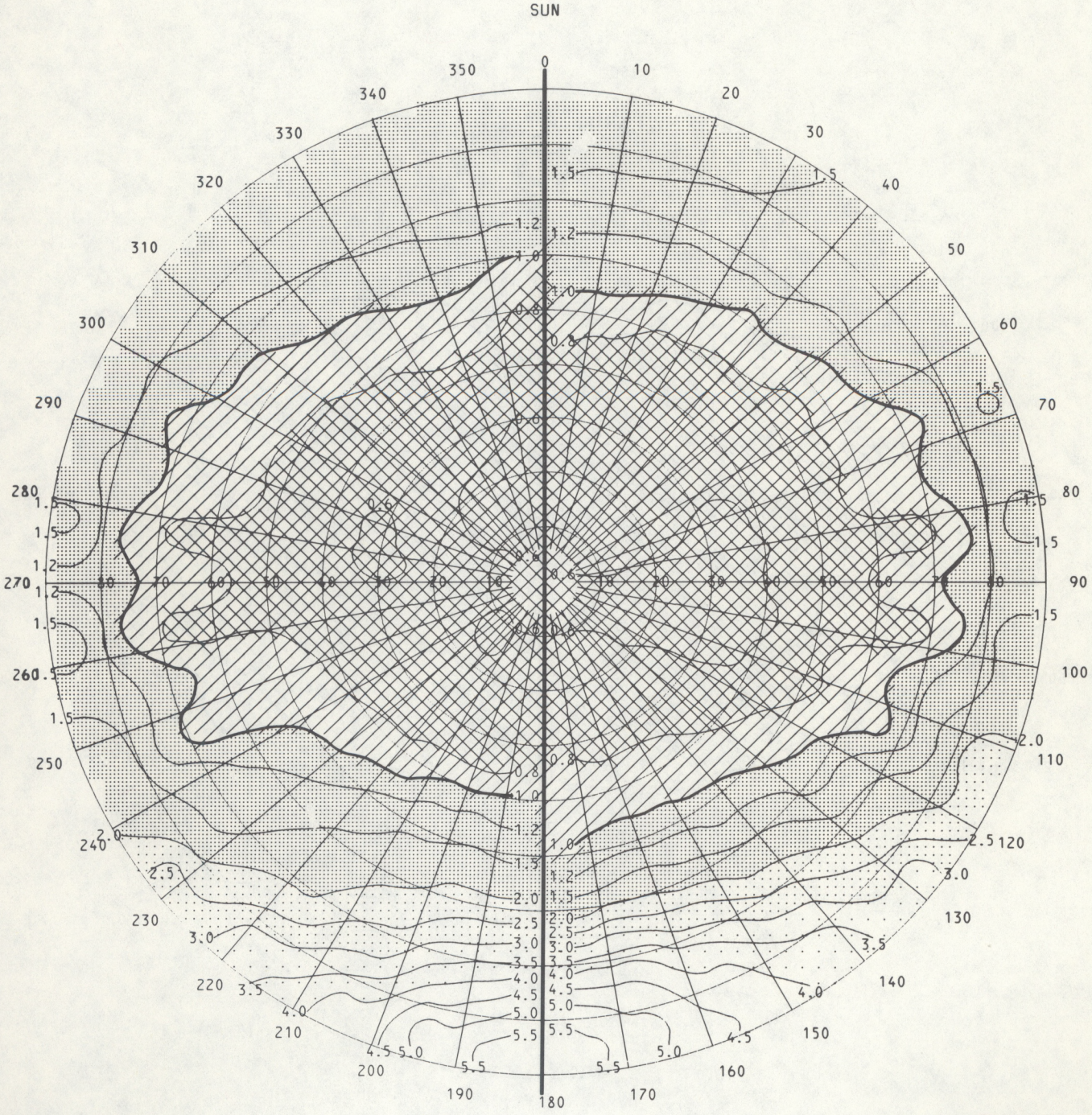

ALBEDO=.54
POPULATION= 946
SOLAR ZENITH ANG (78.5-84.3)
INTEGRAL= 739.1 INTEGRAL/PI= 235.2

ALBEDO=.59
POPULATION= 747
SOLAR ZENITH ANG (84.3-90.0)
INTEGRAL= 812.7 INTEGRAL/PI= 258.6

LOW CLOUD

Fig. 5.5

NIMBUS-7 ERB BI-DIRECTIONAL REFLECTANCE

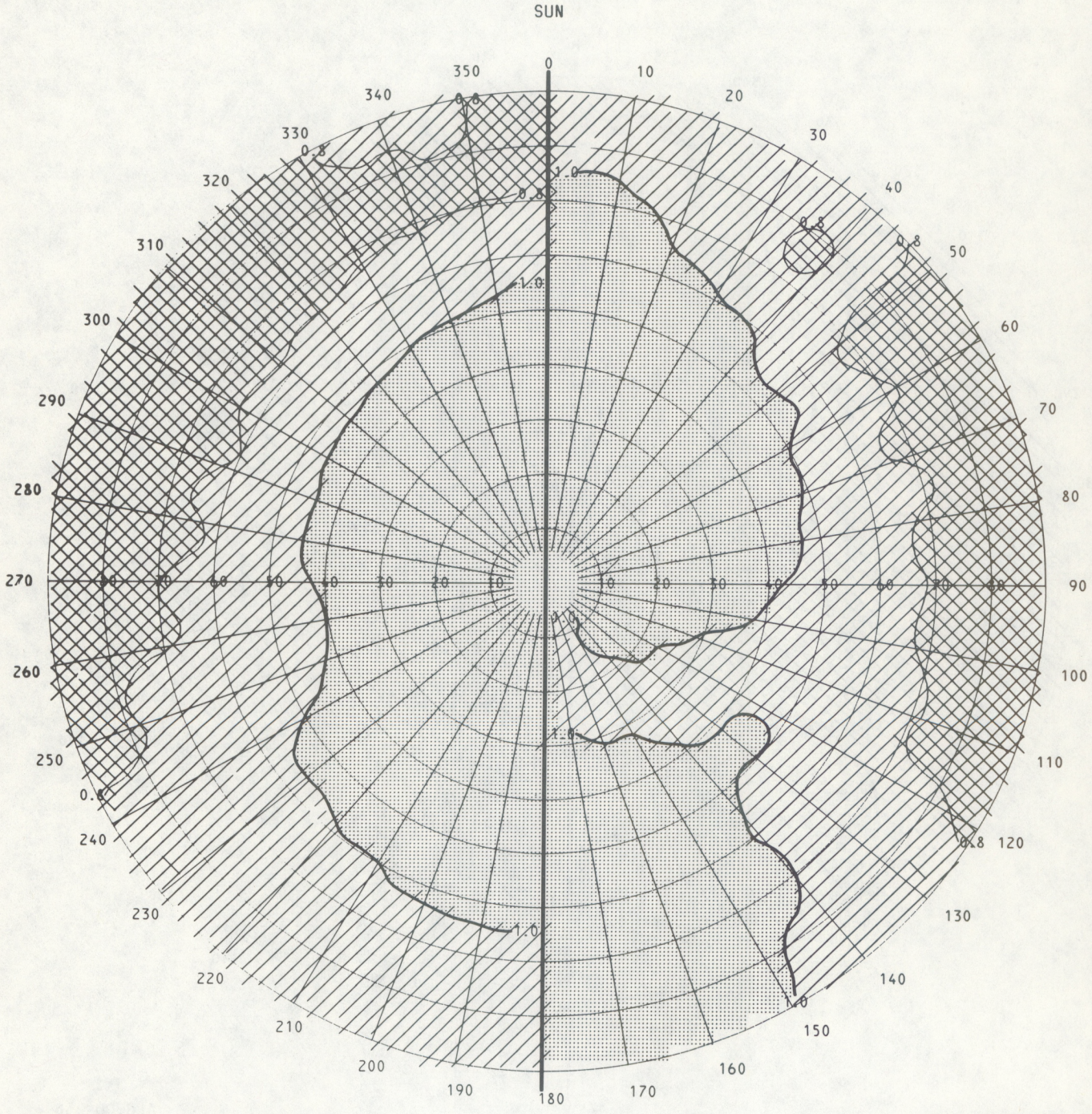

ALBEDO=.36
POPULATION= 9153
SOLAR ZENITH ANG (0.0-25.8)
INTEGRAL= 491.7 INTEGRAL/PI= 156.5

ALBEDO=.45
POPULATION= 7878
SOLAR ZENITH ANG (25.8-36.9)
INTEGRAL= 620.8 INTEGRAL/PI= 197.5

MIDDLE CLOUD

Fig. 6.1

NIMBUS-7 ERB BI-DIRECTIONAL REFLECTANCE

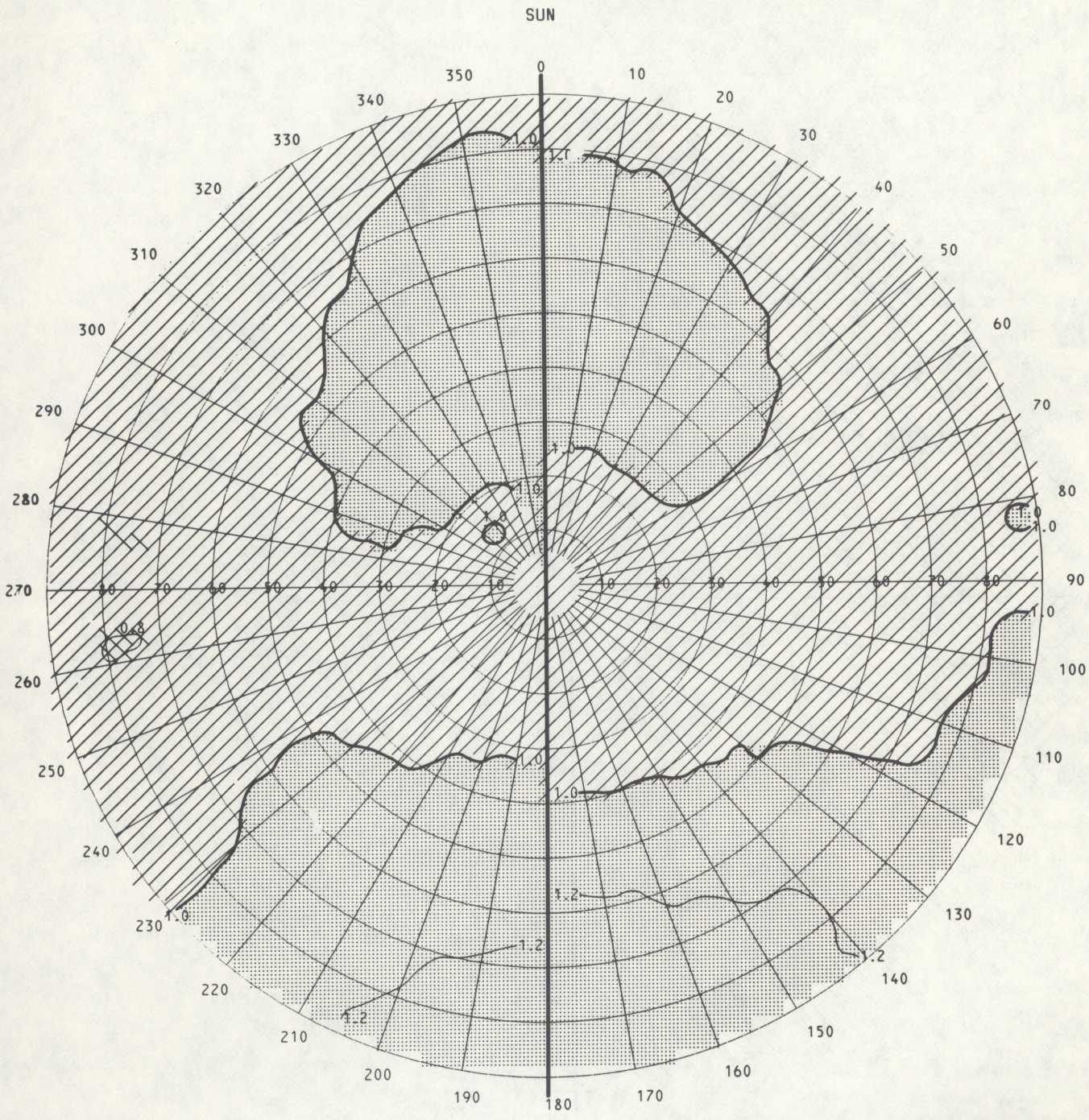

ALBEDO=.50
POPULATION= 6990
SOLAR ZENITH ANG (36.9-45.6)
INTEGRAL= 684.1 INTEGRAL/PI= 217.7

ALBEDO=.56
POPULATION= 5304
SOLAR ZENITH ANG (45.6-53.1)
INTEGRAL= 769.5 INTEGRAL/PI= 244.9

MIDDLE CLOUD

Fig. 6.2

NIMBUS-7 ERB BI-DIRECTIONAL REFLECTANCE

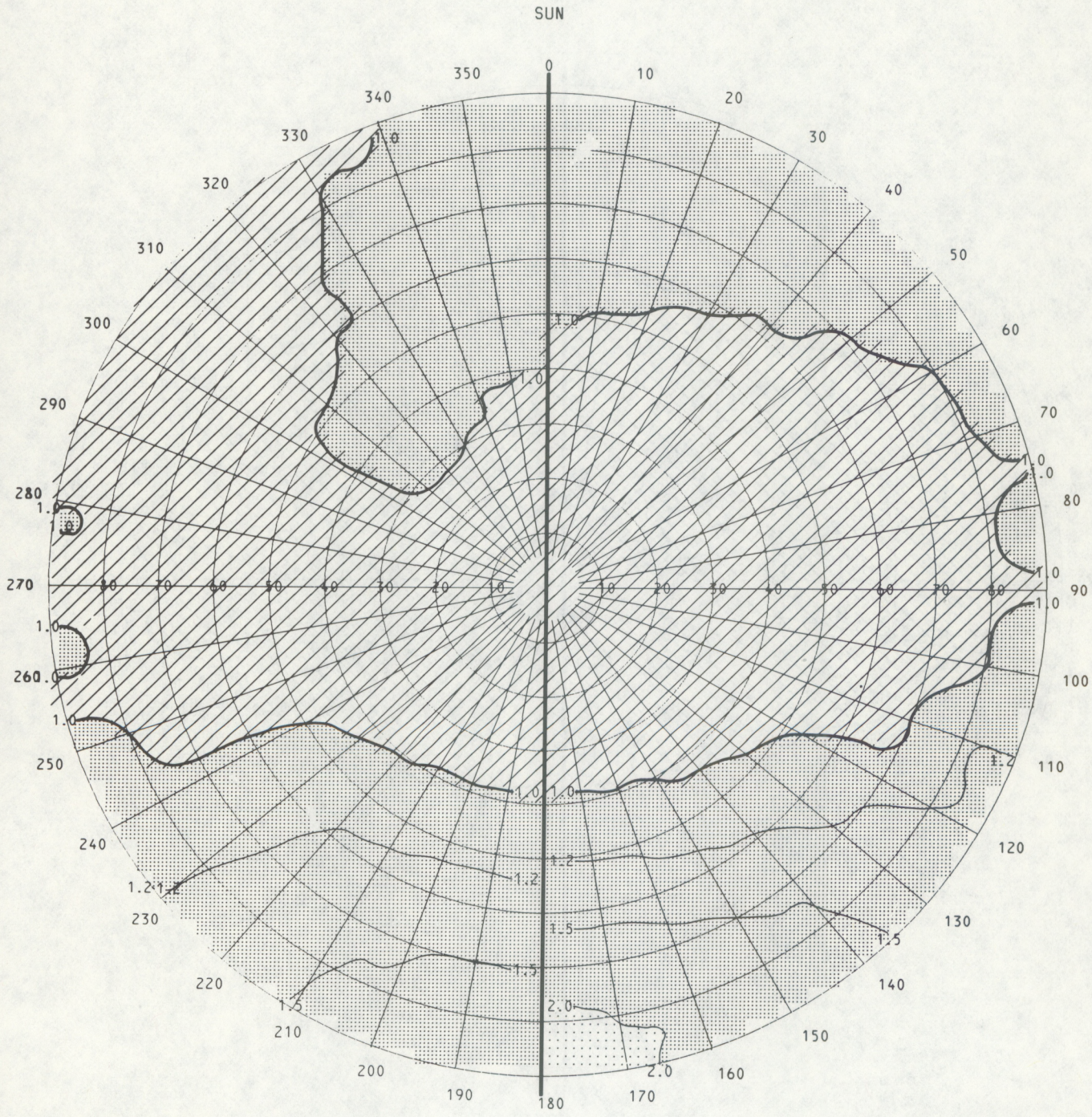

ALBEDO=.59

POPULATION= 4971

SOLAR ZENITH ANG (53.1-60.0)

INTEGRAL= 818.4 INTEGRAL/PI= 260.5

ALBEDO=.60

POPULATION= 7151

SOLAR ZENITH ANG (60.0-66.4)

INTEGRAL= 827.3 INTEGRAL/PI= 263.2

MIDDLE CLOUD

Fig. 6.3

NIMBUS-7 ERB BI-DIRECTIONAL REFLECTANCE

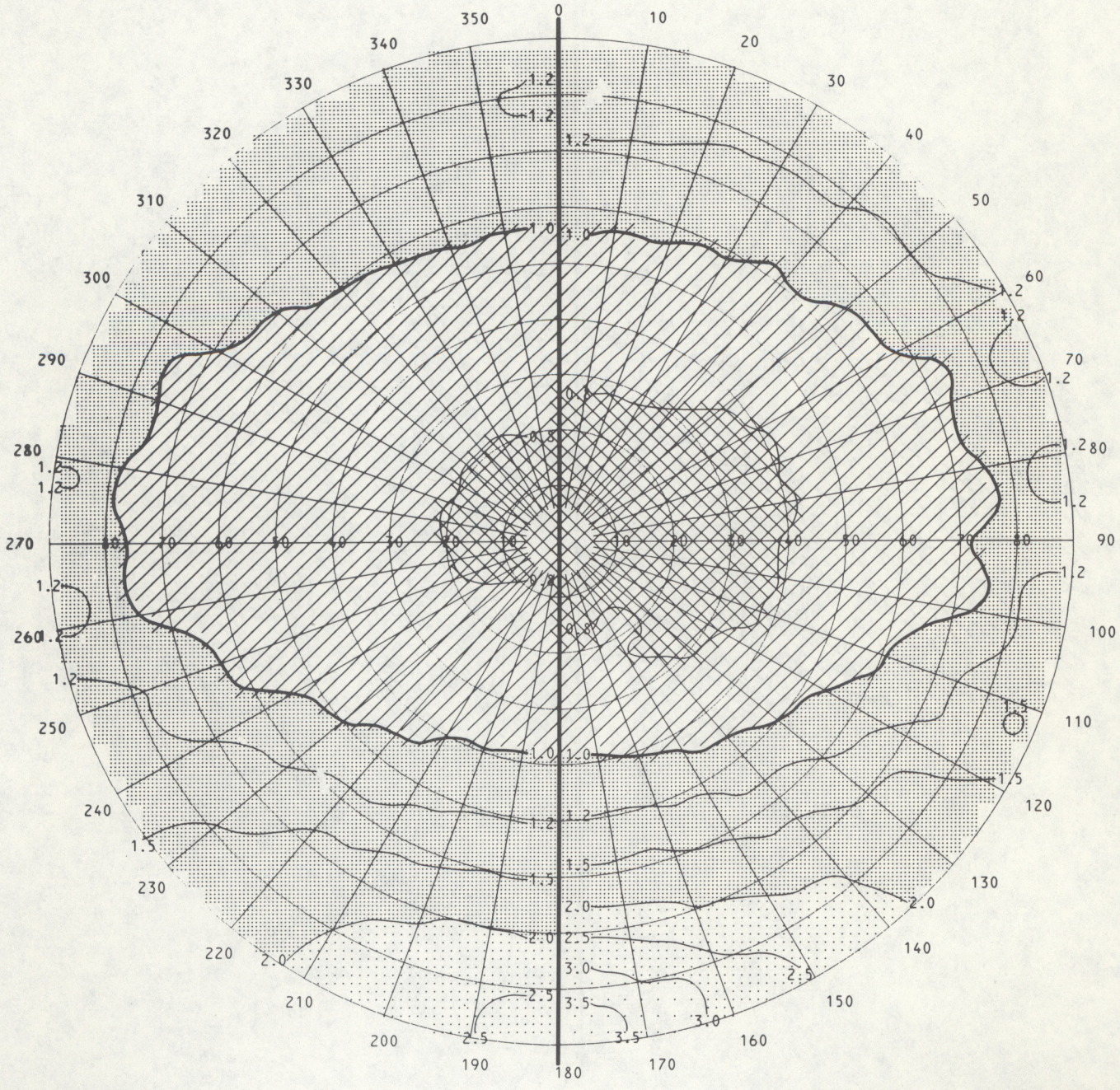

ALBEDO=.59
POPULATION= 9486
SOLAR ZENITH ANG (66.4-72.5)
INTEGRAL= 816.9 INTEGRAL/PI= 260.0

ALBEDO=.59
POPULATION= 10651
SOLAR ZENITH ANG (72.5-78.5)
INTEGRAL= 817.0 INTEGRAL/PI= 260.0

MIDDLE CLOUD

Fig. 6.4

NIMBUS-7 ERB BI-DIRECTIONAL REFLECTANCE

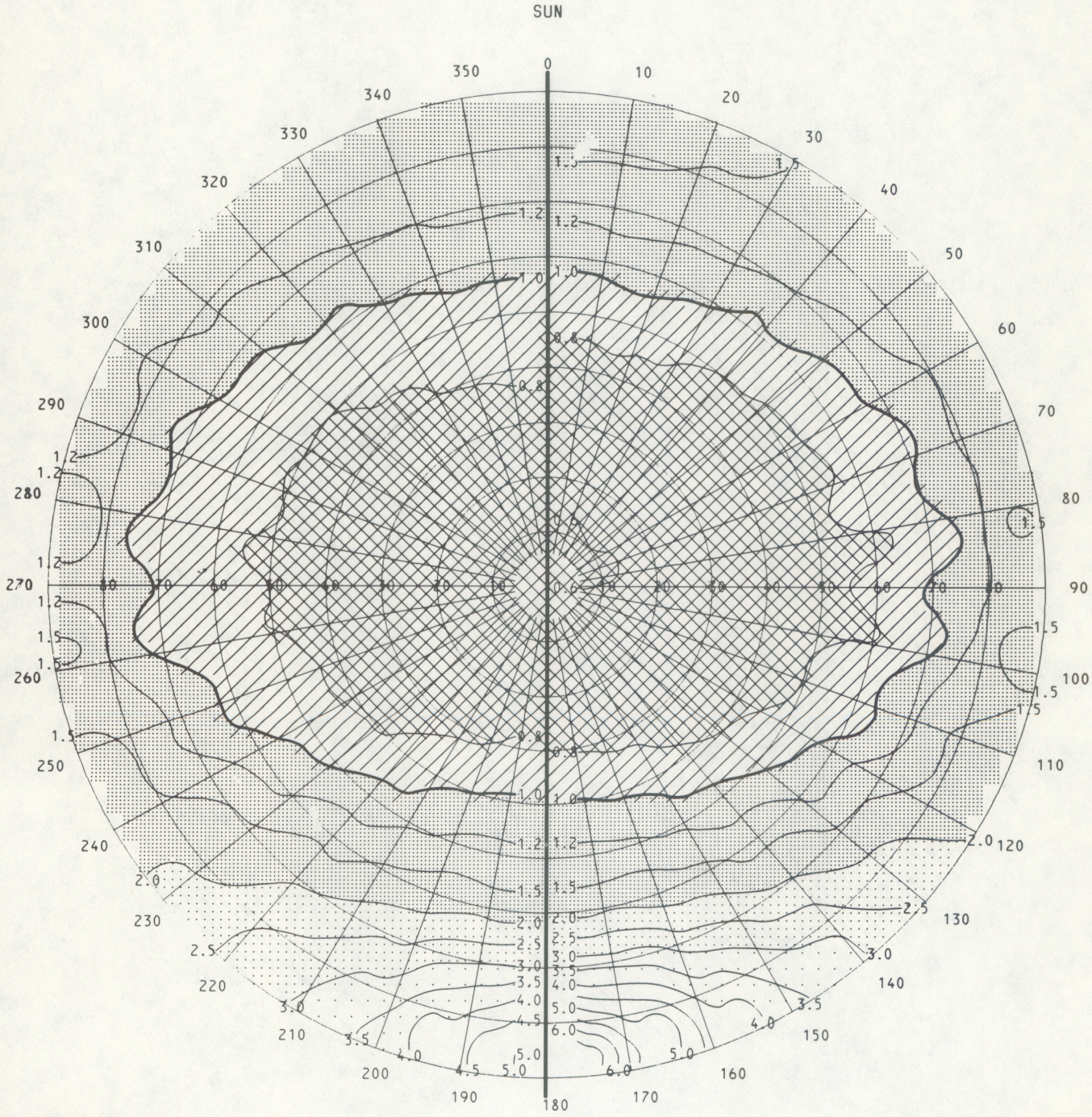

ALBEDO=.60
POPULATION= 9517
SOLAR ZENITH ANG (78.5-84.3)
INTEGRAL= 828.0 INTEGRAL/PI= 263.5

ALBEDO=.66
POPULATION= 4118
SOLAR ZENITH ANG (84.3-90.0)
INTEGRAL= 907.3 INTEGRAL/PI= 288.7

MIDDLE CLOUD

Fig. 6.5

NIMBUS-7 ERB BI-DIRECTIONAL REFLECTANCE

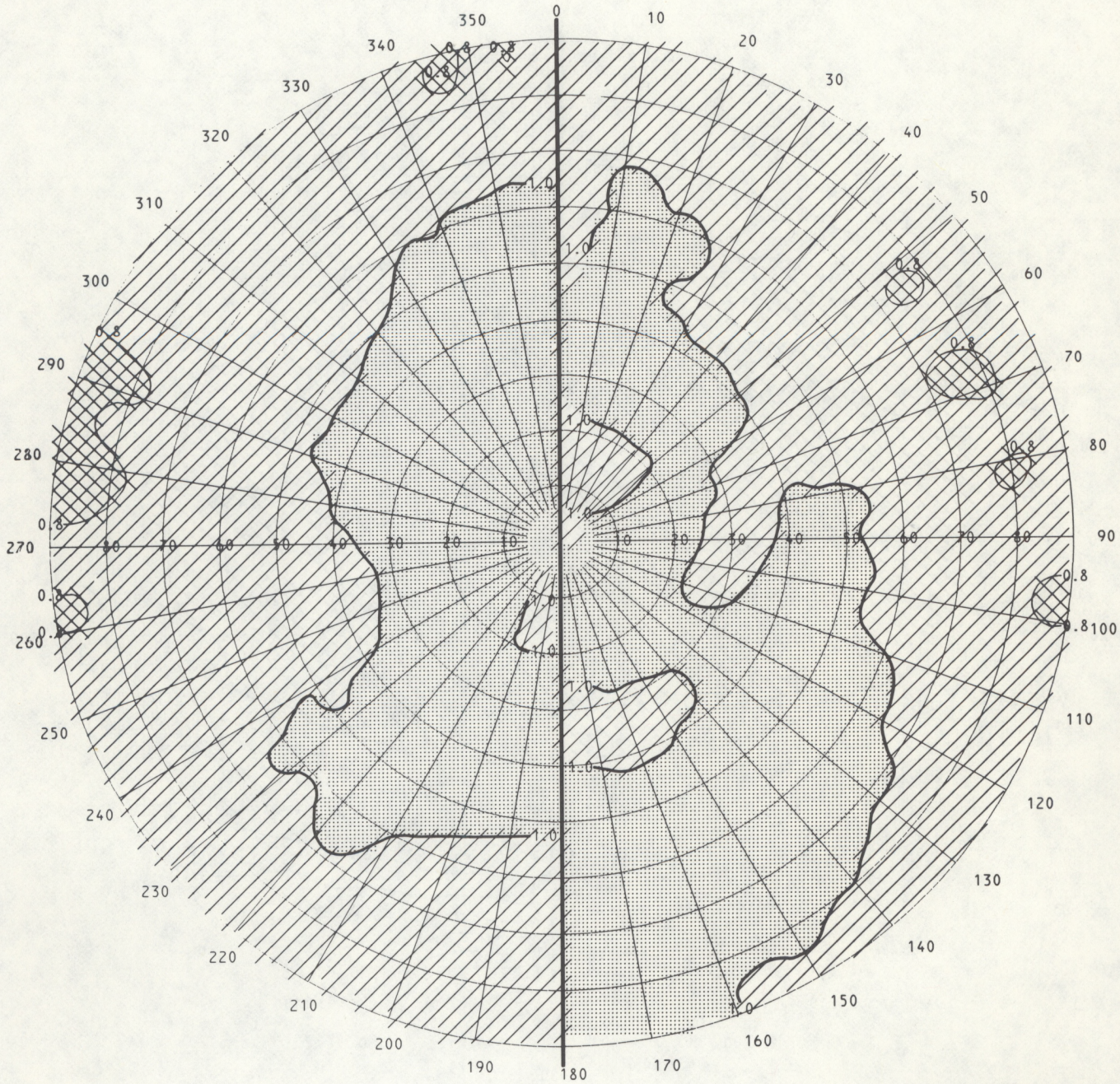

ALBEDO=.50
POPULATION= 2333
SOLAR ZENITH ANG (0.0-25.8)
INTEGRAL= 686.0 INTEGRAL/PI= 218.2

ALBEDO=.54
POPULATION= 981
SOLAR ZENITH ANG (25.8-36.9)
INTEGRAL= 744.3 INTEGRAL/PI= 236.9

HI WTR CLD

Fig. 7.1

NIMBUS-7 ERB BI-DIRECTIONAL REFLECTANCE

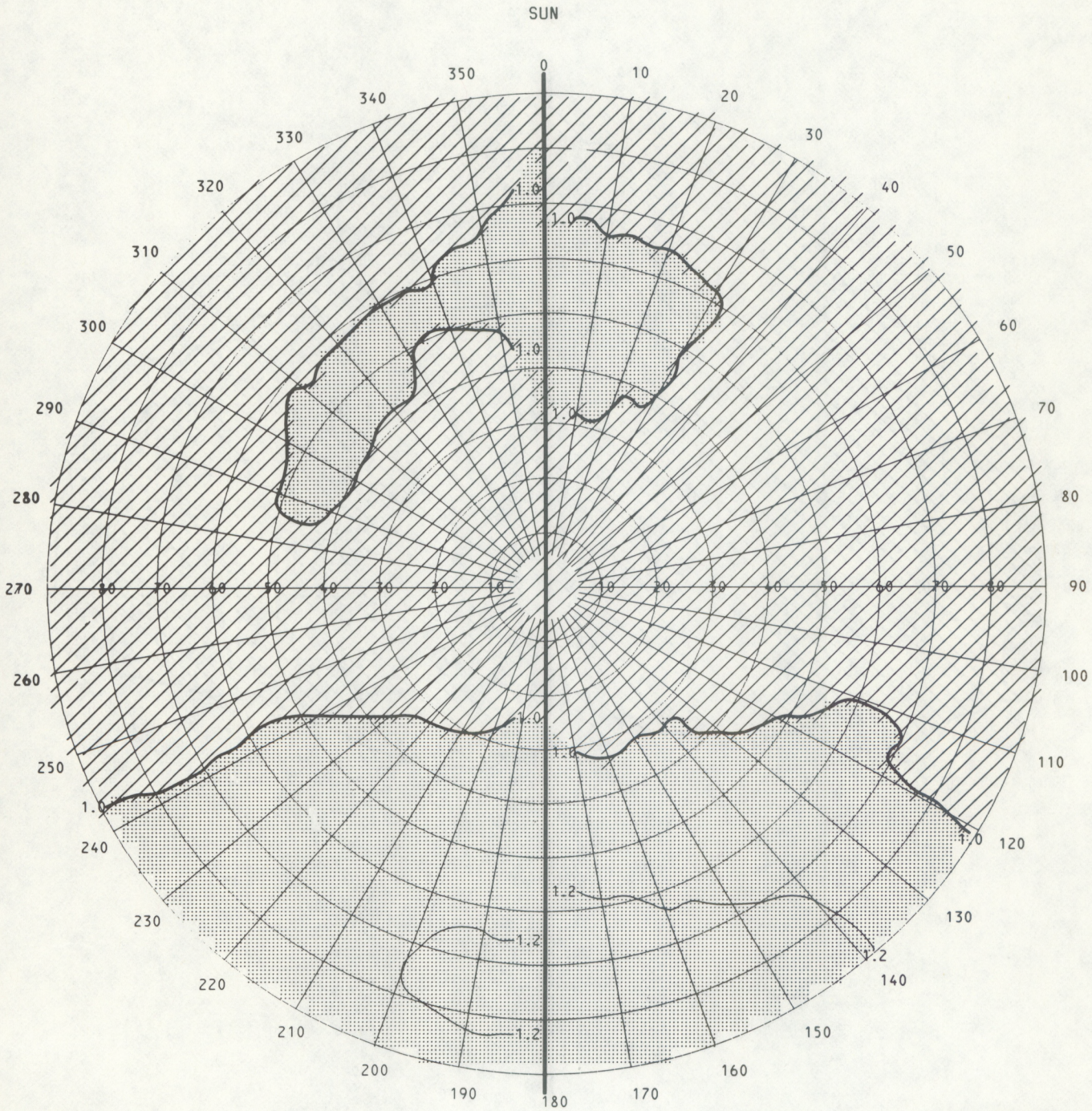

ALBEDO=.56
POPULATION= 1299
SOLAR ZENITH ANG (36.9-45.6)
INTEGRAL= 770.9 INTEGRAL/PI= 245.2

ALBEDO=.59
POPULATION= 1558
SOLAR ZENITH ANG (45.6-53.1)
INTEGRAL= 806.7 INTEGRAL/PI= 256.7

HI WTR CLD

Fig. 7.2

NIMBUS-7 ERB BI-DIRECTIONAL REFLECTANCE

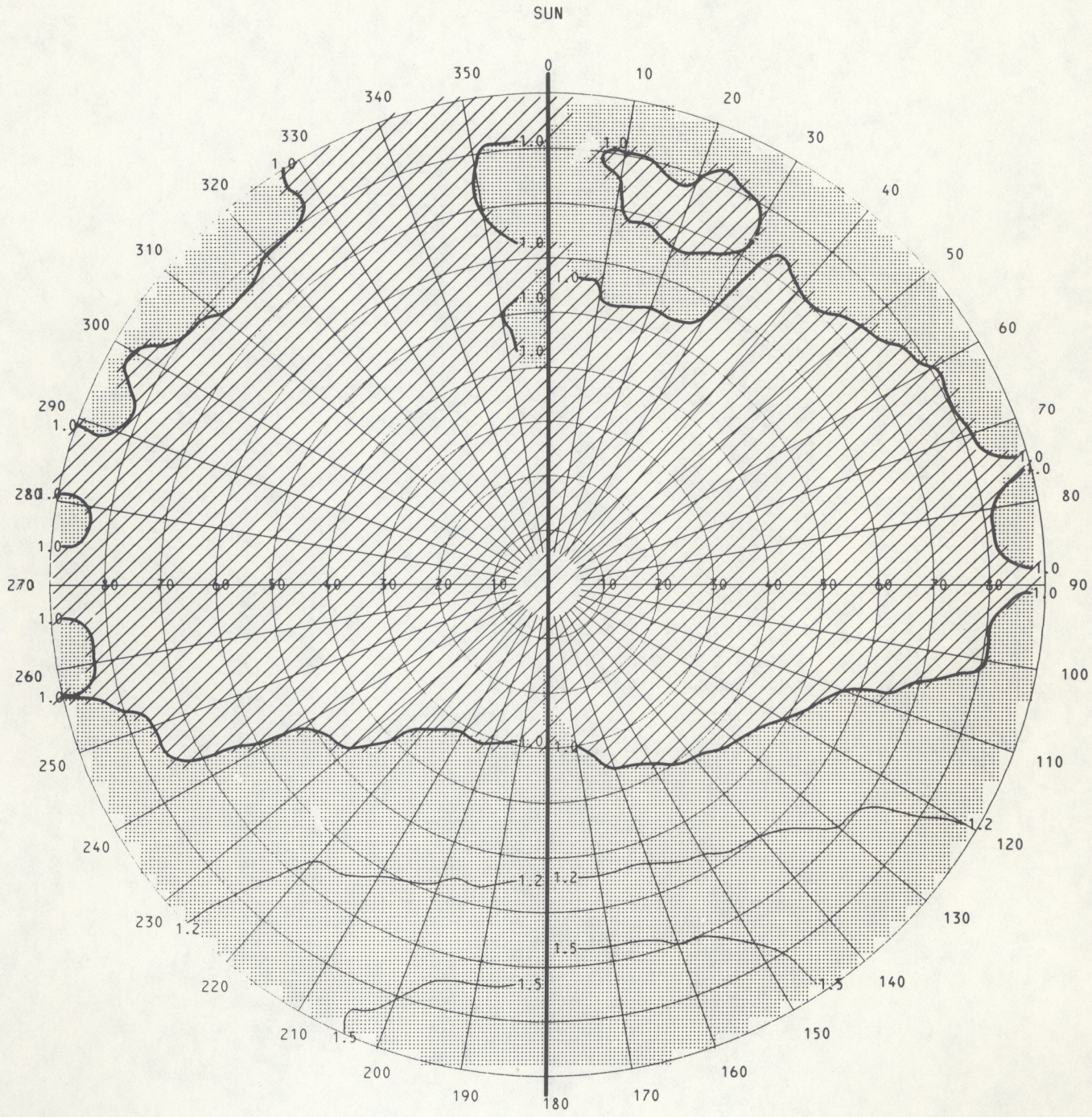

ALBEDO=.63
POPULATION= 1696
SOLAR ZENITH ANG (53.1-60.0)
INTEGRAL= 861.3 INTEGRAL/PI= 274.1

ALBEDO=.64
POPULATION= 1209
SOLAR ZENITH ANG (60.0-66.4)
INTEGRAL= 879.8 INTEGRAL/PI= 280.0

HI WTR CLD

Fig. 7.3

NIMBUS-7 ERB BI-DIRECTIONAL REFLECTANCE

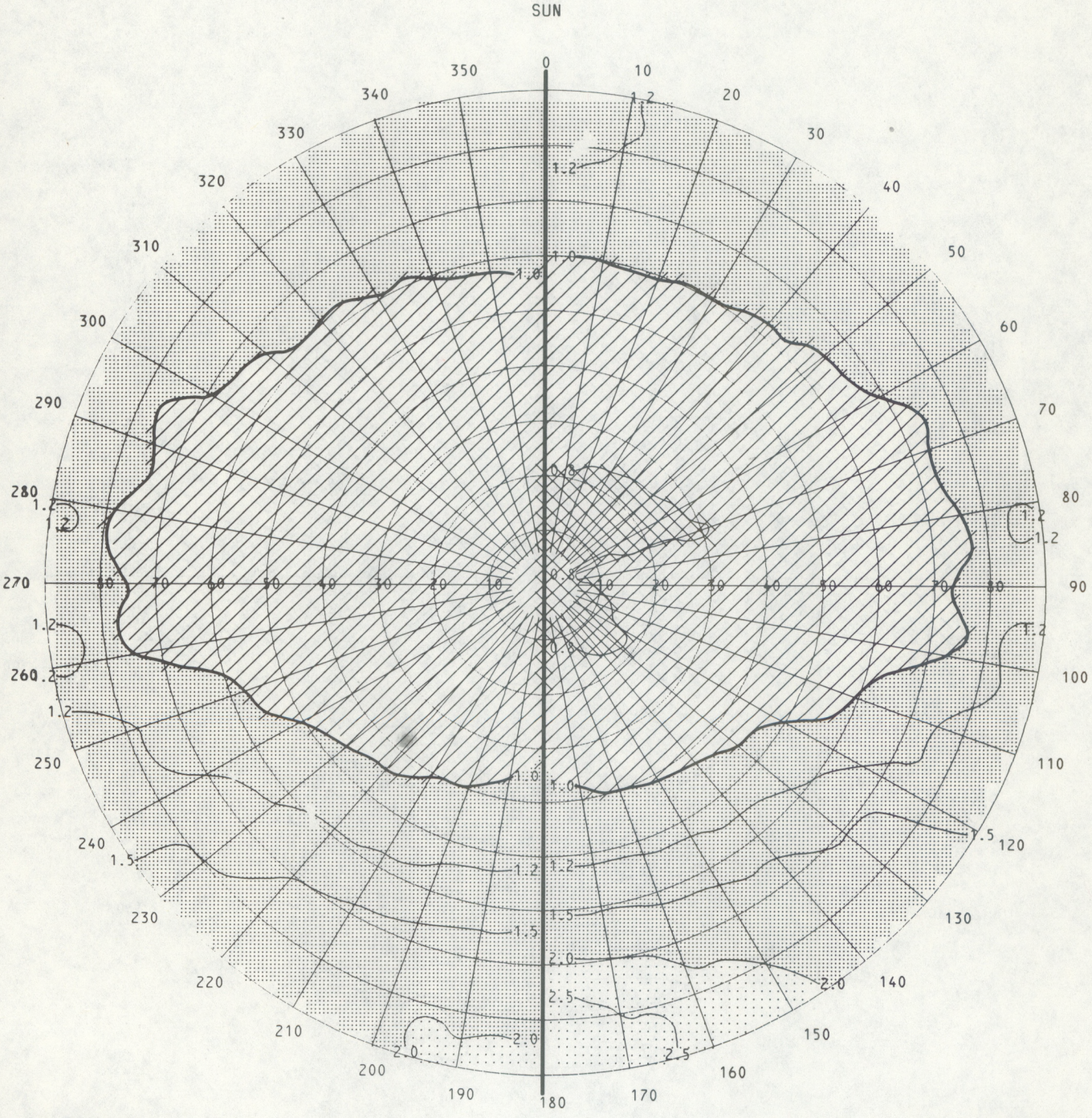

ALBEDO=.66
POPULATION= 1480
SOLAR ZENITH ANG (66.4-72.5)
INTEGRAL= 907.9 INTEGRAL/PI= 288.9

ALBEDO=.66
POPULATION= 2624
SOLAR ZENITH ANG (72.5-78.5)
INTEGRAL= 913.1 INTEGRAL/PI= 290.6

HI WTR CLD

Fig. 7.4

NIMBUS-7 ERB BI-DIRECTIONAL REFLECTANCE

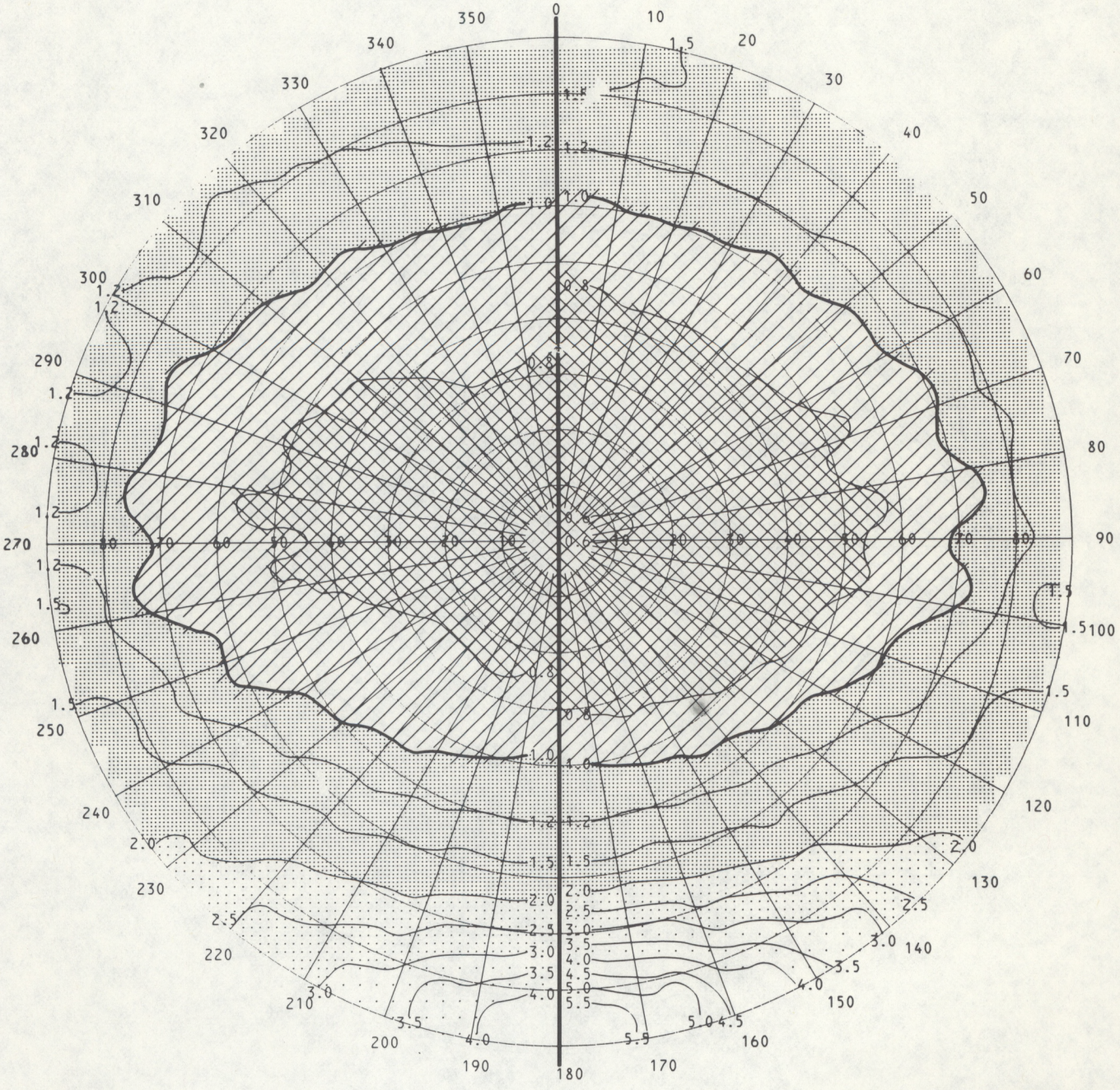

ALBEDO=.67

POPULATION= 3335

SOLAR ZENITH ANG (78.5-84.3)

INTEGRAL= 922.8 INTEGRAL/PI= 293.6

ALBEDO=.69

POPULATION= 2303

SOLAR ZENITH ANG (84.3-90.0)

INTEGRAL= 953.0 INTEGRAL/PI= 303.2

HI WTR CLD

Fig. 7.5

NIMBUS-7 ERB BI-DIRECTIONAL REFLECTANCE

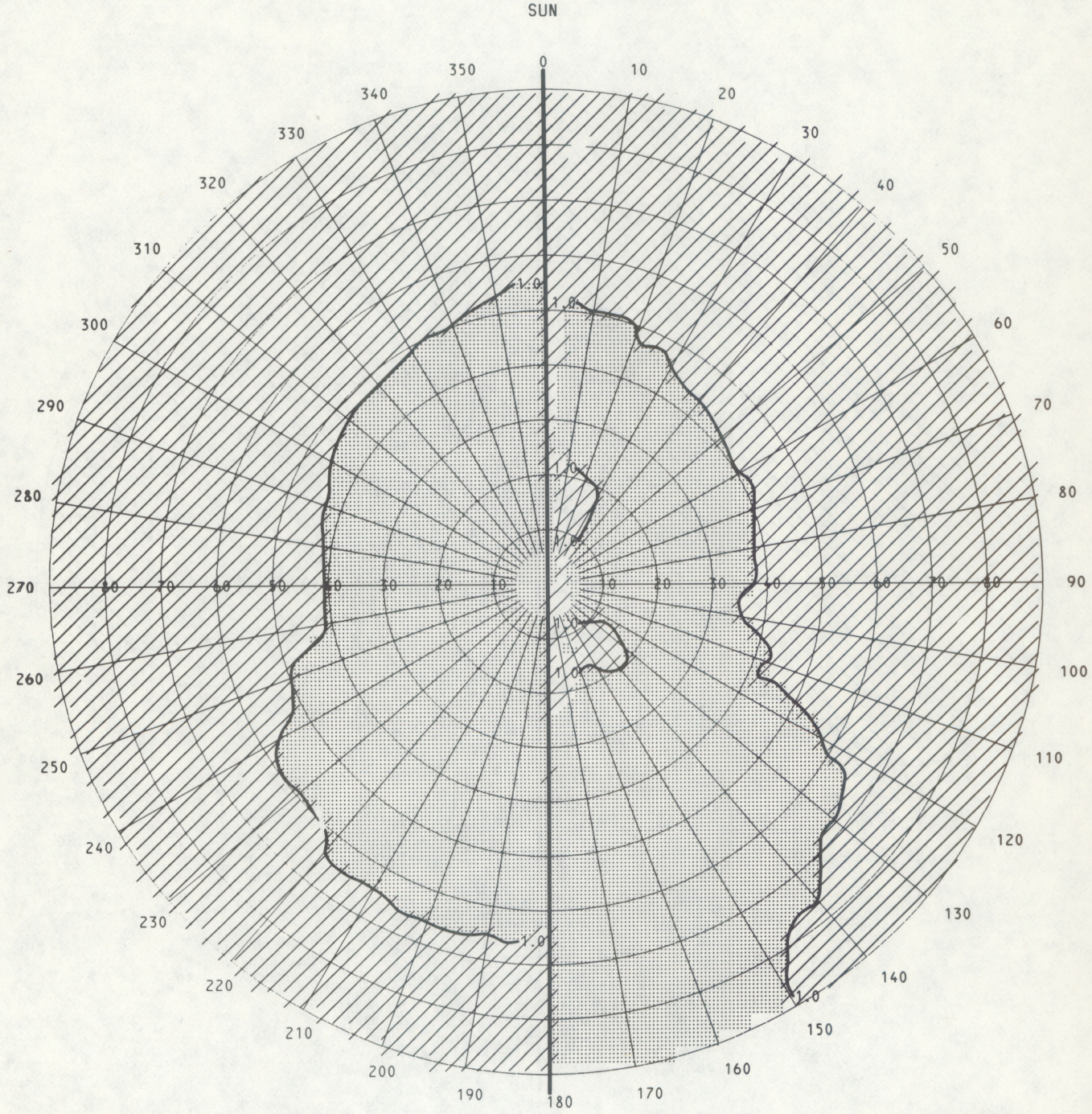

ALBEDO=.58

POPULATION= 16388

SOLAR ZENITH ANG (0.0-25.8)

INTEGRAL= 801.6 INTEGRAL/PI= 255.1

ALBEDO=.60

POPULATION= 4498

SOLAR ZENITH ANG (25.8-36.9)

INTEGRAL= 829.0 INTEGRAL/PI= 263.9

HI ICE CLD

Fig. 8.1

NIMBUS-7 ERB BI-DIRECTIONAL REFLECTANCE

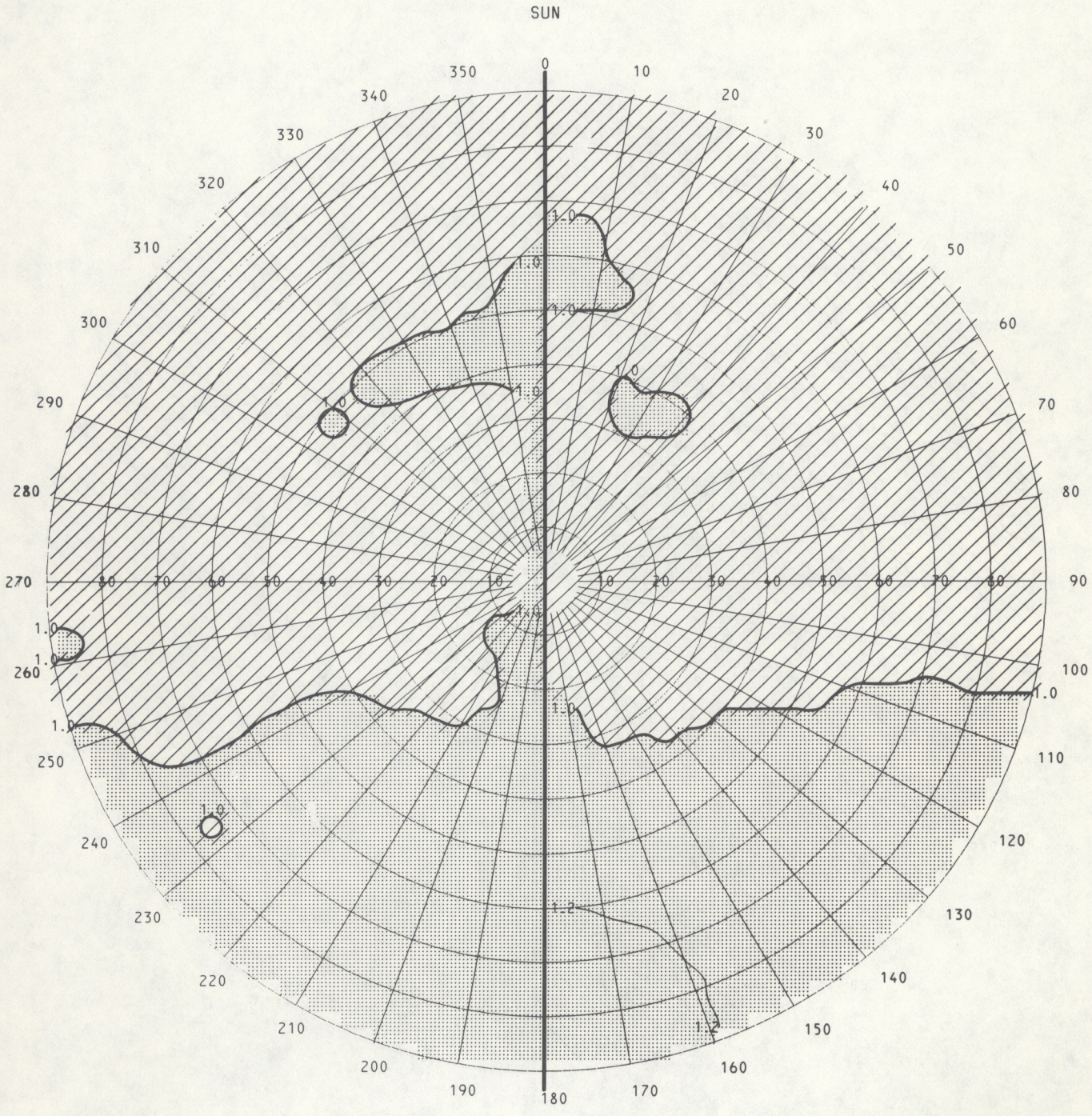

ALBEDO=.62

POPULATION= 2695

SOLAR ZENITH ANG (36.9-45.6)

INTEGRAL= 849.3 INTEGRAL/PI= 270.2

ALBEDO=.64

POPULATION= 2637

SOLAR ZENITH ANG (45.6-53.1)

INTEGRAL= 875.8 INTEGRAL/PI= 278.7

HI ICE CLD

Fig. 8.2

NIMBUS-7 ERB BI-DIRECTIONAL REFLECTANCE

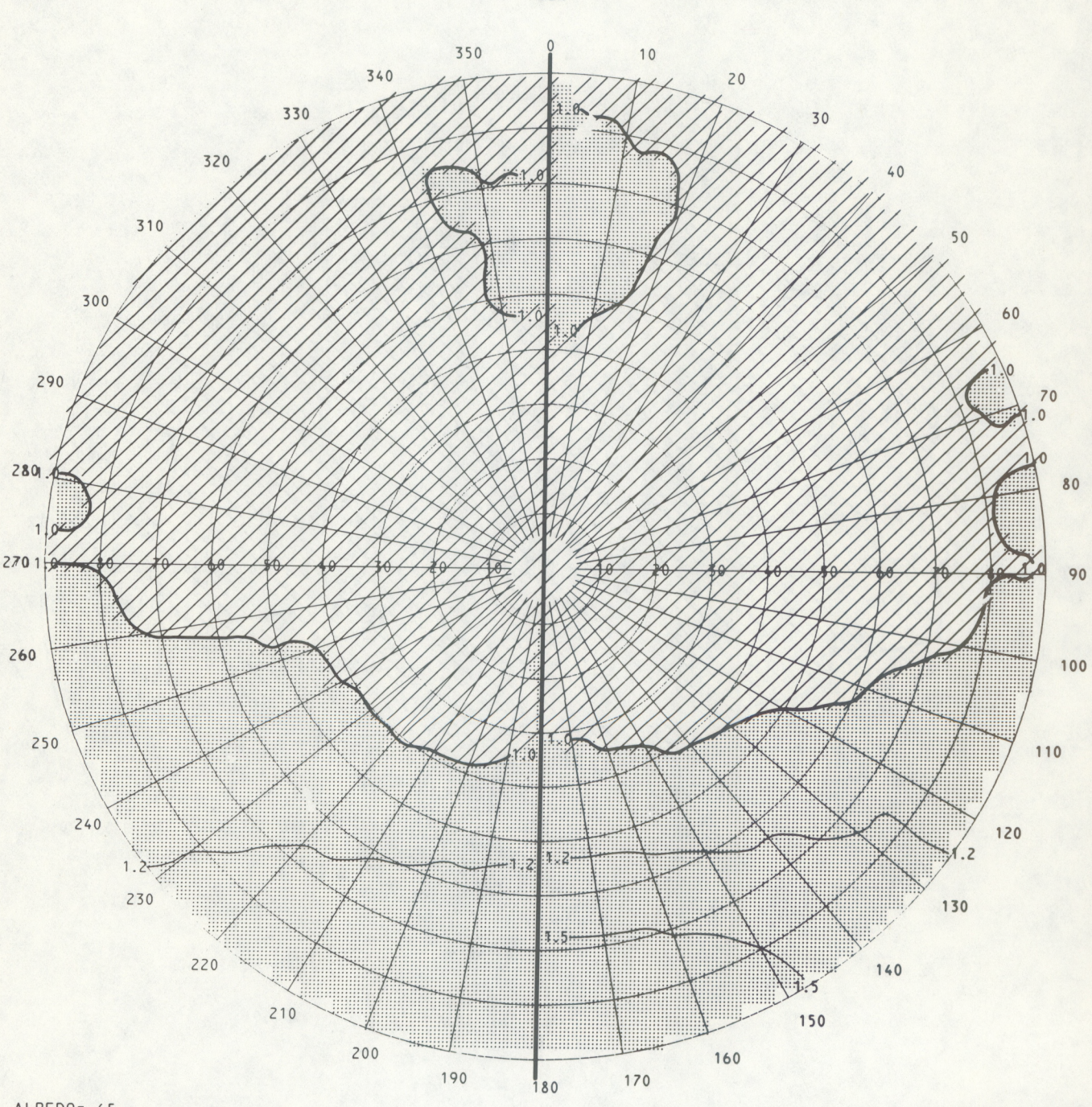

ALBEDO=.65
POPULATION= 2530
SOLAR ZENITH ANG (53.1-60.0)
INTEGRAL= 893.1 INTEGRAL/PI= 284.2

ALBEDO=.67
POPULATION= 2548
SOLAR ZENITH ANG (60.0-66.4)
INTEGRAL= 925.7 INTEGRAL/PI= 294.6

HI ICE CLD

Fig. 8.3

NIMBUS-7 ERB BI-DIRECTIONAL REFLECTANCE

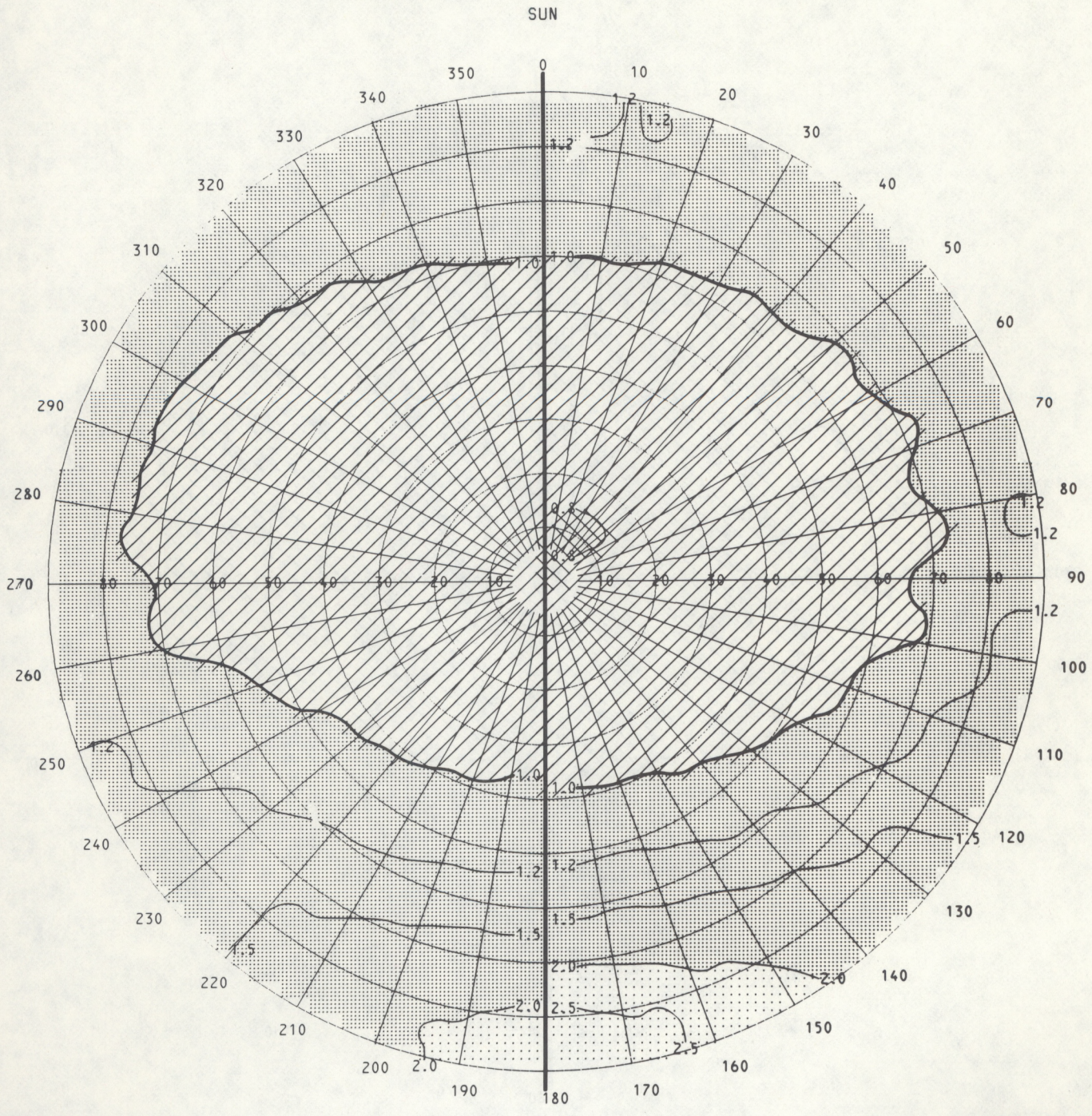

ALBEDO=.70
POPULATION= 3292
SOLAR ZENITH ANG (66.4-72.5)
INTEGRAL= 967.7 INTEGRAL/PI= 308.0

ALBEDO=.70
POPULATION= 5502
SOLAR ZENITH ANG (72.5-78.5)
INTEGRAL= 957.9 INTEGRAL/PI= 304.9

HI ICE CLD

Fig. 8.4

NIMBUS-7 ERB BI-DIRECTIONAL REFLECTANCE

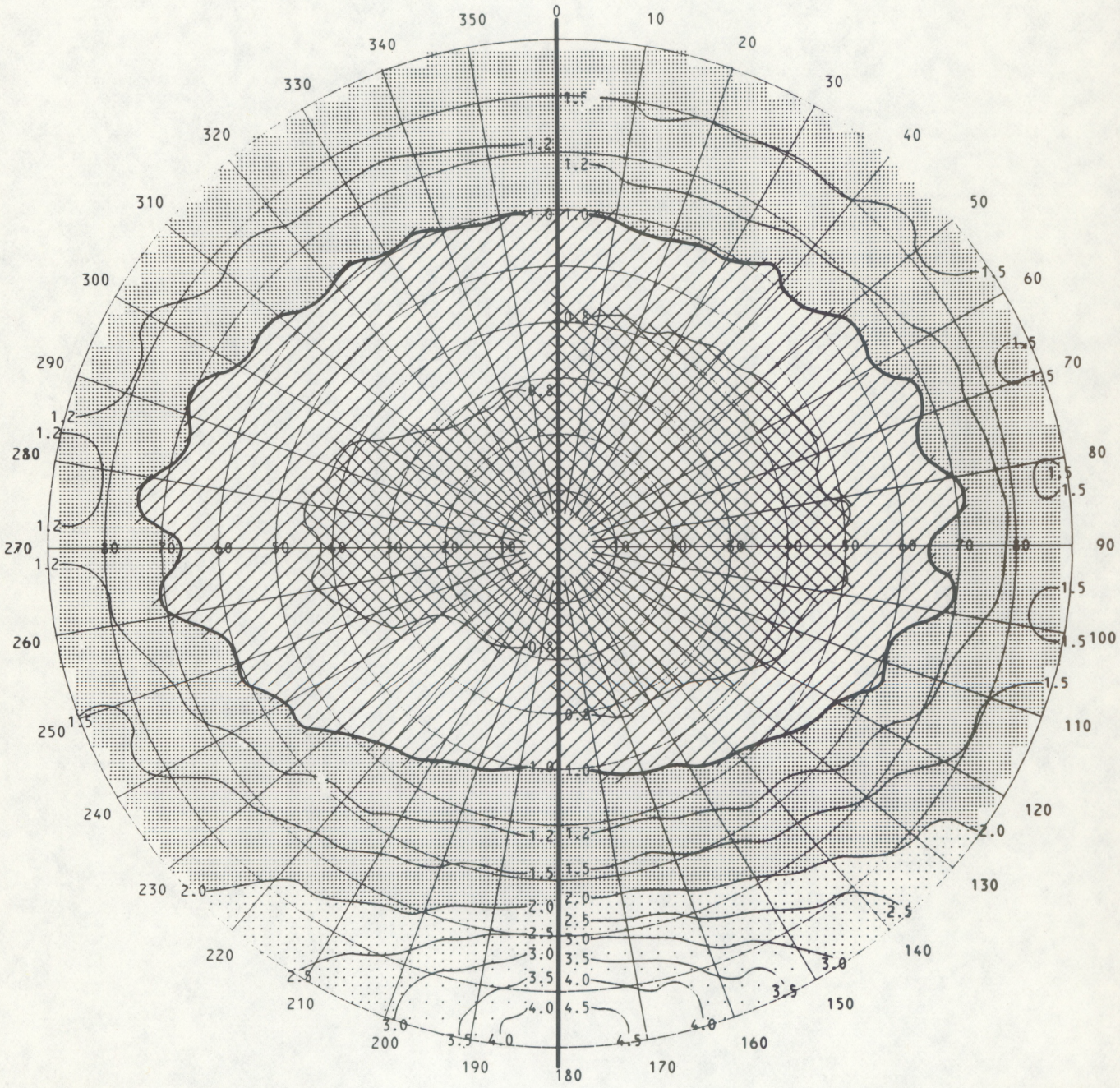

ALBEDO=.69
POPULATION= 9568
SOLAR ZENITH ANG (78.5-84.3)
INTEGRAL= 956.2 INTEGRAL/PI= 304.4

ALBEDO=.72
POPULATION= 9086
SOLAR ZENITH ANG (84.3-90.0)
INTEGRAL= 993.4 INTEGRAL/PI= 316.1

HI ICE CLD

Fig. 8.5

TABLE 1.1 ANISOTROPIC FACTORS FOR CLEAR OCEAN

	SOLAR ZENITH ANGLE RANGE (DEG.)									
	0.0	25.8	36.8	45.5	53.1	59.9	66.4	72.5	78.4	84.3
	25.8	36.8	45.5	53.1	59.9	66.4	72.5	78.4	84.3	90.0
BIN										
1	1.31	0.80	0.73	0.62	0.60	0.55	0.54	0.42	0.47	0.42
2	0.89	0.81	0.77	0.74	0.66	0.76	0.48	0.68	0.62	0.45
3	0.90	0.78	0.75	0.87	0.78	0.85	0.67	0.96	0.54	0.47
4	0.90	0.78	0.74	0.70	0.65	0.64	0.60	0.43	0.53	0.54
5	0.96	0.82	0.73	0.63	0.51	0.56	0.56	0.37	0.48	0.37
6	1.03	0.77	0.64	0.69	0.64	0.64	0.38	0.63	0.61	0.42
7	1.24	0.94	0.71	0.63	0.57	0.53	0.47	0.48	0.64	0.38
8	1.54	1.15	0.86	0.82	0.62	0.71	0.55	0.69	0.83	0.49
9	1.69	1.24	0.85	0.59	0.53	0.74	0.34	0.67	0.48	0.47
10	0.82	0.81	0.83	1.13	0.70	0.75	1.19	0.30	0.71	0.48
11	0.82	0.82	0.86	0.94	0.77	0.58	0.82	0.65	0.73	0.47
12	0.84	0.91	0.83	0.75	0.63	0.51	0.80	0.55	0.43	0.52
13	0.84	0.70	0.69	0.68	0.60	0.58	0.63	0.43	0.54	0.49
14	0.89	0.79	0.65	0.53	0.53	0.50	0.39	0.52	0.43	0.47
15	0.97	0.90	0.83	0.55	0.56	0.44	0.69	0.53	0.60	0.56
16	1.20	1.34	1.11	0.99	0.70	0.74	0.56	0.50	0.76	0.59
17	1.40	1.75	1.42	1.10	0.70	1.05	0.82	0.81	0.71	0.70
18	0.93	0.99	1.00	1.10	0.96	0.86	0.90	0.57	0.96	0.71
19	0.89	0.97	0.98	0.83	1.00	0.88	1.16	1.04	0.67	1.12
20	0.84	0.91	0.87	0.81	0.75	0.67	0.77	0.82	0.68	0.96
21	0.83	0.87	0.81	0.86	0.71	0.96	0.56	0.67	0.66	0.52
22	0.84	0.82	0.72	0.66	0.75	0.65	0.71	0.65	0.59	0.65
23	0.83	0.88	0.91	0.76	0.77	0.82	0.82	0.87	0.65	0.85
24	0.88	1.13	1.37	1.43	1.25	1.39	0.99	1.19	1.28	0.94
25	0.98	1.53	2.21	2.60	2.15	1.74	1.53	1.40	1.53	1.46
26	1.04	1.05	1.12	1.26	1.38	1.35	1.33	1.11	1.06	1.01
27	0.97	1.15	1.12	1.20	1.13	1.09	1.02	1.16	0.85	0.98
28	0.93	0.99	1.00	1.00	0.93	0.81	0.79	0.63	0.85	0.93
29	0.89	1.03	0.95	0.90	0.89	0.80	0.76	0.74	0.63	0.89
30	0.86	0.82	0.89	0.89	0.80	0.88	1.05	0.85	0.75	0.78
31	0.94	0.94	0.89	0.91	1.22	1.00	1.19	1.11	1.53	1.16
32	0.86	1.12	1.40	1.65	1.84	1.78	1.36	1.89	2.05	1.35
33	0.93	1.25	2.06	3.11	4.00	3.19	2.35	2.84	2.49	0.00
34	1.19	1.31	1.38	1.50	1.57	1.58	1.71	1.01	1.37	1.43
35	1.10	1.37	1.41	1.36	1.45	1.39	1.33	1.59	1.51	1.69
36	1.02	1.11	1.31	1.25	1.23	1.22	1.21	1.20	1.12	1.64
37	1.00	1.16	1.05	1.16	0.91	1.10	1.15	0.87	0.78	0.93
38	0.97	1.04	0.98	0.97	0.85	1.04	1.23	1.25	0.87	0.87
39	1.05	1.18	1.16	1.18	1.48	1.40	1.79	1.67	1.59	1.77
40	1.06	1.24	1.49	1.79	2.03	2.35	2.00	2.67	3.34	3.51
41	1.11	1.42	2.03	3.09	5.02	5.40	5.62	5.28	4.85	5.62
42	1.35	1.46	1.64	1.76	1.60	1.63	2.22	1.61	1.95	1.98
43	1.32	1.48	1.57	1.76	1.79	1.65	1.37	1.65	2.00	2.13
44	1.21	1.26	1.60	1.41	1.33	1.60	1.87	1.46	1.48	0.00
45	1.14	0.00	0.00	0.00	0.00	0.00	0.00	0.00	0.00	0.00
46	1.15	1.23	1.24	1.25	0.00	0.00	0.00	0.00	0.00	0.00
47	1.28	1.49	1.51	1.59	1.54	1.89	2.09	0.00	2.13	3.13
48	1.34	1.59	1.93	2.01	2.59	2.84	3.04	5.35	5.40	4.55
49	1.30	1.51	2.16	2.79	6.14	6.94	7.57	5.13	11.22	8.62

TABLE 1.2 RELATIVE DISPERSIONS FOR CLEAR OCEAN

	SOLAR ZENITH ANGLE RANGE (DEG.)									
	0.0	25.8	36.8	45.5	53.1	59.9	66.4	72.5	78.4	84.3
	25.8	36.8	45.5	53.1	59.9	66.4	72.5	78.4	84.3	90.0
BIN										
1	0.48	0.65	0.86	1.01	0.93	1.00	0.96	0.97	0.49	0.53
2	0.45	0.68	0.67	0.81	0.58	0.62	0.64	0.61	0.21	0.11
3	0.45	0.67	0.68	1.06	0.83	0.89	0.90	0.66	0.49	0.35
4	0.38	0.67	0.66	0.83	0.77	0.90	0.72	0.47	0.43	0.45
5	0.45	0.85	0.79	0.93	0.49	0.61	0.81	0.33	0.53	0.44
6	0.36	0.75	0.67	1.18	0.68	0.93	0.45	0.61	0.52	0.63
7	0.25	0.62	0.60	0.90	0.94	0.70	0.91	0.65	0.44	0.31
8	0.34	0.37	0.60	0.94	0.64	0.89	0.59	0.70	0.49	0.57
9	0.49	0.41	0.55	0.27	0.39	1.07	0.50	0.39	0.54	0.80
10	0.36	0.45	0.50	0.96	0.41	0.55	0.27	0.00	0.37	0.00
11	0.36	0.64	0.59	0.86	0.65	0.41	0.62	0.57	0.49	0.26
12	0.43	0.82	0.57	0.53	0.40	0.32	0.94	0.46	0.18	0.39
13	0.41	0.59	0.64	0.82	0.54	0.64	0.85	0.49	0.51	0.56
14	0.56	0.79	0.71	0.71	0.72	0.57	0.32	0.78	0.45	0.43
15	0.35	0.69	0.75	0.36	0.48	0.43	0.69	0.70	0.32	0.34
16	0.30	0.40	0.37	0.70	0.39	0.45	0.58	0.36	0.44	0.17
17	0.36	0.31	0.35	0.40	0.31	0.74	0.58	0.40	0.34	0.45
18	0.54	0.63	0.58	0.66	0.54	0.67	0.58	0.19	0.31	0.00
19	0.46	0.66	0.59	0.38	0.57	0.56	0.70	0.37	0.39	0.60
20	0.36	0.71	0.63	0.48	0.36	0.39	0.70	0.36	0.21	0.47
21	0.56	0.70	0.75	0.95	0.93	0.95	0.61	0.48	0.38	0.51
22	0.66	0.83	0.72	0.58	0.62	0.72	0.74	0.68	0.53	0.27
23	0.48	0.71	0.70	0.77	0.79	0.83	0.67	0.34	0.35	0.16
24	0.39	0.37	0.40	0.53	0.38	0.52	0.44	0.35	0.34	0.43
25	0.36	0.35	0.35	0.35	0.30	0.30	0.35	0.59	0.17	0.14
26	0.58	0.40	0.56	0.69	0.52	0.71	0.44	0.38	0.45	0.28
27	0.49	0.66	0.43	0.71	0.58	0.38	0.41	0.39	0.18	0.47
28	0.56	0.63	0.54	0.74	0.43	0.39	0.38	0.20	0.18	0.34
29	0.50	0.72	0.65	0.76	0.64	0.67	0.60	0.41	0.36	0.17
30	0.61	0.69	0.77	0.87	0.62	0.55	0.56	0.55	0.40	0.25
31	0.69	0.63	0.65	0.75	0.69	0.49	0.50	0.53	0.44	0.13
32	0.38	0.63	0.43	0.59	0.43	0.41	0.49	0.40	0.13	0.04
33	0.44	0.38	0.28	0.29	0.38	0.24	0.17	0.27	0.21	-9.99
34	0.44	0.46	0.41	0.53	0.43	0.47	0.45	0.27	0.22	0.13
35	0.35	0.54	0.47	0.39	0.36	0.35	0.36	0.31	0.28	0.31
36	0.35	0.50	0.58	0.50	0.31	0.40	0.41	0.36	0.29	0.22
37	0.33	0.67	0.65	0.80	0.45	0.66	0.60	0.57	0.34	0.33
38	0.30	0.61	0.59	0.65	0.39	0.65	0.68	0.36	0.31	0.14
39	0.40	0.58	0.44	0.41	0.51	0.45	0.48	0.39	0.27	0.28
40	0.43	0.44	0.38	0.46	0.53	0.50	0.31	0.32	0.32	0.33
41	0.35	0.47	0.32	0.33	0.27	0.24	0.35	0.42	0.33	0.34
42	0.38	0.31	0.34	0.46	0.21	0.24	0.22	0.17	0.08	0.07
43	0.31	0.39	0.34	0.36	0.25	0.26	0.25	0.19	0.17	0.10
44	0.26	0.16	0.46	0.17	0.16	0.24	0.24	0.12	0.25	-9.99
45	0.21	-9.99	-9.99	-9.99	-9.99	-9.99	-9.99	-9.99	-9.99	-9.99
46	0.29	0.49	0.36	0.36	-9.99	-9.99	-9.99	-9.99	-9.99	-9.99
47	0.40	0.43	0.37	0.41	0.27	0.34	0.25	-9.99	0.00	0.14
48	0.35	0.38	0.39	0.45	0.36	0.32	0.43	0.21	0.31	0.29
49	0.27	0.36	0.33	0.24	0.36	0.25	0.05	0.03	0.21	0.20

TABLE 1.3 BIN POPULATIONS FOR CLEAR OCEAN

	SOLAR ZENITH ANGLE RANGE (DEG.)									
	0.0	25.8	36.8	45.5	53.1	59.9	66.4	72.5	78.4	84.3
	25.8	36.8	45.5	53.1	59.9	66.4	72.5	78.4	84.3	90.0
BIN										
1	2922	1241	898	474	259	177	69	34	77	42
2	380	137	156	56	42	17	14	7	7	4
3	873	334	240	113	80	39	13	6	15	14
4	1102	415	308	158	76	48	24	19	17	10
5	1013	350	338	140	102	32	18	15	9	7
6	930	408	326	143	93	47	23	25	15	12
7	873	369	313	150	78	38	20	22	26	17
8	645	268	171	92	67	37	12	10	7	8
9	225	124	120	51	26	24	7	6	14	4
10	217	102	64	37	20	10	2	1	8	1
11	455	172	128	79	44	18	9	11	6	5
12	600	182	141	72	25	22	9	7	3	5
13	481	190	160	59	34	25	12	9	2	8
14	414	162	121	66	34	25	11	7	9	4
15	355	153	145	63	38	26	12	8	7	6
16	315	179	152	81	44	26	12	10	7	3
17	172	81	66	28	16	12	5	4	3	4
18	434	180	154	65	44	28	6	7	11	1
19	935	346	242	123	58	41	16	21	8	3
20	1029	368	254	127	61	48	16	13	10	10
21	878	485	354	186	96	89	21	12	14	5
22	573	334	253	135	69	43	24	15	8	13
23	528	272	208	101	36	36	35	8	16	3
24	541	297	237	102	74	37	24	13	16	4
25	266	148	104	65	34	11	18	3	8	3
26	290	170	113	69	28	13	6	8	3	3
27	744	287	179	76	45	22	14	10	4	3
28	662	274	198	89	46	43	14	5	4	8
29	447	314	257	136	83	49	18	9	16	3
30	288	194	196	96	59	33	21	6	12	5
31	384	198	127	89	31	31	10	8	3	2
32	360	181	124	81	40	29	17	11	4	2
33	134	84	73	31	31	14	5	3	9	0
34	522	466	288	118	65	44	11	4	12	4
35	1367	553	441	195	108	56	30	26	32	9
36	618	208	240	133	82	34	37	12	10	4
37	367	190	272	148	63	51	31	10	14	3
38	427	148	157	65	54	42	18	4	12	6
39	749	392	310	142	73	47	18	17	21	7
40	571	341	285	159	70	45	24	23	12	5
41	239	154	149	65	35	26	5	4	6	8
42	179	240	179	75	27	25	2	7	6	2
43	506	211	226	134	49	43	20	10	12	7
44	167	8	34	28	22	16	5	4	13	0
45	152	0	0	0	0	0	0	0	0	0
46	187	40	24	4	0	0	0	0	0	0
47	263	178	203	72	42	21	11	0	1	2
48	201	153	112	54	24	24	20	6	4	3
49	85	64	83	33	15	16	5	2	3	2

TABLE 2.1 ANISOTROPIC FACTORS FOR CLEAR LAND

	SOLAR ZENITH ANGLE RANGE (DEG.)									
	0.0	25.8	36.8	45.5	53.1	59.9	66.4	72.5	78.4	84.3
	25.8	36.8	45.5	53.1	59.9	66.4	72.5	78.4	84.3	90.0
BIN										
1	1.08	0.98	0.89	0.84	0.79	0.76	0.59	0.00	0.00	0.00
2	1.11	1.16	1.02	0.98	1.06	0.83	0.71	0.00	0.00	0.00
3	1.10	1.12	1.01	1.01	0.95	0.79	0.71	0.00	0.00	0.00
4	1.08	1.07	0.98	0.96	0.95	0.82	1.04	0.00	0.00	0.00
5	1.04	1.00	0.96	0.92	0.88	0.79	0.79	0.00	0.00	0.00
6	1.02	0.94	0.89	0.91	0.81	0.84	0.48	0.00	0.00	0.00
7	1.02	0.90	0.90	0.84	0.70	0.79	0.68	0.00	0.00	0.00
8	0.98	0.87	0.84	0.79	0.73	0.90	0.57	0.00	0.00	0.00
9	1.04	0.87	0.82	0.79	0.78	0.78	0.54	0.00	0.00	0.00
10	1.09	1.29	1.17	1.11	1.04	1.08	0.00	0.00	0.00	0.00
11	1.06	1.16	1.13	1.09	1.14	0.91	0.71	0.00	0.00	0.00
12	1.05	1.09	1.09	1.12	1.14	0.96	1.46	0.00	0.00	0.00
13	1.04	0.99	0.92	0.97	1.01	0.67	1.08	0.00	0.00	0.00
14	1.02	0.95	0.92	0.91	0.79	0.71	0.77	0.00	0.00	0.00
15	0.96	0.85	0.92	0.92	0.73	0.76	0.55	0.00	0.00	0.00
16	0.95	0.85	0.82	0.81	0.71	0.80	0.81	0.00	0.00	0.00
17	0.89	0.93	0.86	0.81	0.78	0.46	0.52	0.00	0.00	0.00
18	1.07	1.28	1.31	1.38	1.27	1.11	1.18	0.00	0.00	0.00
19	1.03	1.17	1.19	1.24	1.30	1.06	1.18	0.00	0.00	0.00
20	1.04	1.06	1.10	1.17	1.15	1.15	1.04	0.00	0.00	0.00
21	1.02	1.03	0.92	0.88	0.85	0.86	0.76	0.00	0.00	0.00
22	0.98	0.88	0.96	0.89	0.87	1.01	0.47	0.00	0.00	0.00
23	0.92	0.89	0.90	0.82	0.80	0.92	0.91	0.00	0.00	0.00
24	0.93	0.86	0.85	0.80	0.78	0.88	1.28	0.00	0.00	0.00
25	0.99	0.92	0.90	0.94	0.93	0.66	0.97	0.00	0.00	0.00
26	1.06	1.20	1.32	1.44	1.49	1.37	1.40	0.00	0.00	0.00
27	1.03	1.22	1.22	1.26	1.37	1.25	1.49	0.00	0.00	0.00
28	1.05	1.05	1.05	1.20	1.18	1.34	0.90	0.00	0.00	0.00
29	0.99	1.03	1.01	0.96	0.97	0.95	0.77	0.00	0.00	0.00
30	0.94	0.87	0.95	0.86	0.85	0.94	0.86	0.00	0.00	0.00
31	0.88	0.90	0.96	0.87	0.88	0.83	1.44	0.00	0.00	0.00
32	0.90	0.89	0.85	0.88	0.94	1.02	1.91	0.00	0.00	0.00
33	0.90	0.94	1.01	1.06	1.04	1.06	1.78	0.00	0.00	0.00
34	1.06	1.23	1.27	1.39	1.58	1.69	1.58	0.00	0.00	0.00
35	1.01	1.19	1.30	1.36	1.50	1.56	1.44	0.00	0.00	0.00
36	1.04	1.07	1.12	1.21	1.32	1.30	1.19	0.00	0.00	0.00
37	0.99	1.05	1.04	1.05	1.07	0.97	0.91	0.00	0.00	0.00
38	0.94	0.85	0.90	0.91	0.99	0.90	0.77	0.00	0.00	0.00
39	0.91	0.97	1.03	1.02	1.09	1.22	0.95	0.00	0.00	0.00
40	0.94	1.02	1.03	1.05	1.14	1.50	1.71	0.00	0.00	0.00
41	0.94	1.04	1.09	1.24	1.22	1.84	2.34	0.00	0.00	0.00
42	1.07	1.25	1.32	1.36	1.61	1.63	2.69	0.00	0.00	0.00
43	0.98	1.18	1.35	1.45	1.59	1.62	1.89	0.00	0.00	0.00
44	1.01	1.01	1.18	1.31	1.45	1.63	1.51	0.00	0.00	0.00
45	0.96	0.00	0.00	0.00	0.00	0.00	0.00	0.00	0.00	0.00
46	0.97	0.87	0.97	0.84	0.00	0.00	0.00	0.00	0.00	0.00
47	0.91	1.08	1.10	1.17	1.24	1.57	1.41	0.00	0.00	0.00
48	0.97	1.15	1.20	1.32	1.34	2.06	1.23	0.00	0.00	0.00
49	1.07	1.17	1.22	1.38	1.51	1.59	3.28	0.00	0.00	0.00

TABLE 2.2 RELATIVE DISPERSIONS FOR CLEAR LAND

	SOLAR ZENITH ANGLE RANGE (DEG.)									
	0.0	25.8	36.8	45.5	53.1	59.9	66.4	72.5	78.4	84.3
	25.8	36.8	45.5	53.1	59.9	66.4	72.5	78.4	84.3	90.0
BIN										
1	0.27	0.35	0.40	0.42	0.50	0.45	0.51	-9.99	-9.99	-9.99
2	0.23	0.28	0.36	0.37	0.47	0.27	0.40	-9.99	-9.99	-9.99
3	0.24	0.30	0.36	0.37	0.48	0.31	0.31	-9.99	-9.99	-9.99
4	0.25	0.32	0.39	0.39	0.34	0.25	0.50	-9.99	-9.99	-9.99
5	0.26	0.32	0.39	0.39	0.33	0.40	0.57	-9.99	-9.99	-9.99
6	0.27	0.33	0.41	0.39	0.37	0.45	0.19	-9.99	-9.99	-9.99
7	0.29	0.36	0.44	0.43	0.33	0.25	0.49	-9.99	-9.99	-9.99
8	0.29	0.35	0.44	0.43	0.49	0.44	0.29	-9.99	-9.99	-9.99
9	0.30	0.34	0.46	0.47	0.56	0.29	0.46	-9.99	-9.99	-9.99
10	0.24	0.26	0.30	0.32	0.24	0.30	-9.99	-9.99	-9.99	-9.99
11	0.24	0.28	0.33	0.36	0.48	0.21	0.16	-9.99	-9.99	-9.99
12	0.25	0.29	0.37	0.33	0.30	0.24	0.28	-9.99	-9.99	-9.99
13	0.26	0.35	0.39	0.37	0.38	0.24	0.16	-9.99	-9.99	-9.99
14	0.28	0.35	0.41	0.42	0.32	0.40	0.36	-9.99	-9.99	-9.99
15	0.31	0.34	0.44	0.41	0.39	0.50	0.39	-9.99	-9.99	-9.99
16	0.32	0.38	0.43	0.45	0.27	0.58	0.47	-9.99	-9.99	-9.99
17	0.32	0.36	0.47	0.47	0.43	0.11	0.23	-9.99	-9.99	-9.99
18	0.26	0.27	0.29	0.27	0.26	0.28	0.27	-9.99	-9.99	-9.99
19	0.25	0.26	0.31	0.30	0.33	0.22	0.47	-9.99	-9.99	-9.99
20	0.27	0.29	0.36	0.34	0.27	0.28	0.49	-9.99	-9.99	-9.99
21	0.28	0.35	0.38	0.36	0.35	0.43	0.45	-9.99	-9.99	-9.99
22	0.28	0.34	0.42	0.38	0.46	0.47	0.12	-9.99	-9.99	-9.99
23	0.31	0.37	0.45	0.44	0.38	0.43	0.85	-9.99	-9.99	-9.99
24	0.34	0.39	0.43	0.42	0.32	0.59	0.68	-9.99	-9.99	-9.99
25	0.34	0.37	0.44	0.40	0.68	0.16	0.71	-9.99	-9.99	-9.99
26	0.26	0.26	0.28	0.25	0.21	0.20	0.23	-9.99	-9.99	-9.99
27	0.26	0.27	0.30	0.29	0.27	0.20	0.31	-9.99	-9.99	-9.99
28	0.26	0.27	0.34	0.32	0.24	0.36	0.17	-9.99	-9.99	-9.99
29	0.27	0.32	0.37	0.36	0.36	0.41	0.32	-9.99	-9.99	-9.99
30	0.29	0.37	0.42	0.38	0.39	0.52	0.55	-9.99	-9.99	-9.99
31	0.31	0.32	0.45	0.42	0.31	0.30	0.55	-9.99	-9.99	-9.99
32	0.30	0.38	0.43	0.42	0.62	0.73	0.71	-9.99	-9.99	-9.99
33	0.32	0.37	0.41	0.38	0.43	0.46	0.45	-9.99	-9.99	-9.99
34	0.24	0.23	0.26	0.25	0.21	0.13	0.08	-9.99	-9.99	-9.99
35	0.24	0.24	0.29	0.26	0.23	0.24	0.27	-9.99	-9.99	-9.99
36	0.25	0.22	0.33	0.28	0.26	0.17	0.36	-9.99	-9.99	-9.99
37	0.26	0.27	0.36	0.39	0.33	0.34	0.32	-9.99	-9.99	-9.99
38	0.26	0.21	0.38	0.33	0.46	0.41	0.18	-9.99	-9.99	-9.99
39	0.27	0.30	0.39	0.35	0.40	0.38	0.27	-9.99	-9.99	-9.99
40	0.29	0.32	0.37	0.35	0.35	0.47	0.67	-9.99	-9.99	-9.99
41	0.31	0.30	0.35	0.36	0.25	0.48	0.48	-9.99	-9.99	-9.99
42	0.20	0.21	0.25	0.22	0.21	0.15	0.02	-9.99	-9.99	-9.99
43	0.21	0.22	0.26	0.25	0.18	0.18	0.20	-9.99	-9.99	-9.99
44	0.23	0.08	0.22	0.23	0.21	0.10	0.17	-9.99	-9.99	-9.99
45	0.24	-9.99	-9.99	-9.99	-9.99	-9.99	-9.99	-9.99	-9.99	-9.99
46	0.22	0.13	0.31	0.15	-9.99	-9.99	-9.99	-9.99	-9.99	-9.99
47	0.23	0.27	0.33	0.29	0.28	0.38	0.26	-9.99	-9.99	-9.99
48	0.25	0.29	0.32	0.38	0.23	0.47	0.00	-9.99	-9.99	-9.99
49	0.30	0.29	0.30	0.28	0.29	0.34	0.21	-9.99	-9.99	-9.99

TABLE 2.3 BIN POPULATIONS FOR CLEAR LAND

	SOLAR ZENITH ANGLE RANGE (DEG.)									
	0.0	25.8	36.8	45.5	53.1	59.9	66.4	72.5	78.4	84.3
	25.8	36.8	45.5	53.1	59.9	66.4	72.5	78.4	84.3	90.0
BIN										
1	4020	2106	1534	867	230	63	26	0	0	0
2	449	277	229	143	52	12	5	0	0	0
3	1183	585	379	246	73	18	7	0	0	0
4	1532	699	576	331	110	20	17	0	0	0
5	1330	588	484	329	105	30	8	0	0	0
6	1259	665	514	362	124	23	7	0	0	0
7	1193	688	496	329	94	15	11	0	0	0
8	801	518	332	138	50	15	7	0	0	0
9	299	163	151	122	29	3	5	0	0	0
10	294	200	134	84	18	8	0	0	0	0
11	563	253	242	133	37	11	7	0	0	0
12	784	297	226	135	59	23	4	0	0	0
13	768	335	245	128	53	13	5	0	0	0
14	592	301	214	128	63	10	2	0	0	0
15	447	235	239	148	54	16	5	0	0	0
16	346	283	221	141	41	16	2	0	0	0
17	182	152	127	54	11	2	7	0	0	0
18	536	308	236	153	31	12	3	0	0	0
19	1191	598	436	263	78	22	5	0	0	0
20	1645	522	410	278	78	23	11	0	0	0
21	1382	776	578	316	113	49	11	0	0	0
22	676	518	371	302	105	27	9	0	0	0
23	707	415	316	239	90	29	4	0	0	0
24	610	521	363	220	64	19	7	0	0	0
25	278	236	177	83	35	7	5	0	0	0
26	450	233	171	130	28	10	2	0	0	0
27	1009	440	349	209	71	15	7	0	0	0
28	1239	381	252	193	61	17	7	0	0	0
29	843	566	438	244	109	37	21	0	0	0
30	356	265	259	180	73	19	12	0	0	0
31	486	323	221	185	60	17	6	0	0	0
32	430	340	251	129	49	18	2	0	0	0
33	150	138	117	96	23	10	4	0	0	0
34	670	692	486	265	50	17	3	0	0	0
35	2093	929	714	482	155	57	24	0	0	0
36	1538	496	312	219	87	24	9	0	0	0
37	839	515	530	346	159	44	21	0	0	0
38	685	188	222	156	109	32	13	0	0	0
39	991	637	472	312	118	46	9	0	0	0
40	732	604	480	300	107	46	7	0	0	0
41	307	198	222	124	41	18	8	0	0	0
42	188	388	278	139	22	10	2	0	0	0
43	797	425	342	234	88	50	20	0	0	0
44	447	16	47	59	24	7	6	0	0	0
45	321	0	0	0	0	0	0	0	0	0
46	341	60	37	5	0	0	0	0	0	0
47	362	317	294	167	70	22	14	0	0	0
48	240	251	203	118	38	26	1	0	0	0
49	77	90	122	59	21	13	3	0	0	0

TABLE 3.1 ANISOTROPIC FACTORS FOR CLEAR SNOW

	SOLAR ZENITH ANGLE RANGE (DEG.)									
	0.0	25.8	36.8	45.5	53.1	59.9	66.4	72.5	78.4	84.3
	25.8	36.8	45.5	53.1	59.9	66.4	72.5	78.4	84.3	90.0
BIN										
1	0.00	0.00	0.89	0.92	0.95	0.92	0.88	0.85	0.78	0.66
2	0.00	0.00	0.77	0.94	0.97	0.94	0.91	0.85	0.77	0.67
3	0.00	0.00	1.02	0.93	0.95	0.94	0.92	0.84	0.79	0.71
4	0.00	0.00	1.30	1.03	0.98	0.95	0.91	0.85	0.77	0.66
5	0.00	0.00	0.95	0.95	0.99	0.94	0.90	0.85	0.76	0.65
6	0.00	0.00	1.01	1.01	0.99	0.95	0.91	0.85	0.78	0.67
7	0.00	0.00	0.89	0.96	0.99	0.95	0.91	0.88	0.79	0.71
8	0.00	0.00	1.14	0.91	0.97	0.95	0.92	0.91	0.84	0.74
9	0.00	0.00	0.89	1.02	1.00	0.95	0.93	0.91	0.82	0.73
10	0.00	0.00	0.90	0.92	0.99	0.97	0.94	0.90	0.82	0.72
11	0.00	0.00	0.98	1.01	1.00	0.96	0.94	0.88	0.83	0.73
12	0.00	0.00	0.70	1.05	0.99	0.96	0.92	0.87	0.78	0.72
13	0.00	0.00	1.09	0.94	0.95	0.93	0.91	0.87	0.79	0.73
14	0.00	0.00	0.67	0.95	0.97	0.94	0.93	0.87	0.81	0.74
15	0.00	0.00	0.00	1.06	1.01	0.97	0.95	0.91	0.83	0.75
16	0.00	0.00	0.84	1.00	0.99	1.01	0.97	0.96	0.93	0.83
17	0.00	0.00	0.73	1.01	1.04	0.96	0.96	0.93	0.90	0.79
18	0.00	0.00	1.16	0.93	1.00	0.98	0.96	0.94	0.88	0.83
19	0.00	0.00	1.24	1.01	1.00	0.98	0.97	0.93	0.90	0.85
20	0.00	0.00	1.27	1.09	1.00	0.96	0.96	0.93	0.84	0.75
21	0.00	0.00	0.98	0.92	0.91	0.93	0.93	0.88	0.86	0.78
22	0.00	0.00	0.55	1.03	0.97	0.94	0.94	0.89	0.84	0.79
23	0.00	0.00	1.21	1.07	1.05	1.02	1.01	1.00	0.95	0.95
24	0.00	0.00	1.08	0.97	1.05	1.07	1.08	1.10	1.07	1.02
25	0.00	0.00	0.98	1.11	1.09	1.09	1.08	1.11	1.17	1.06
26	0.00	0.00	1.19	0.97	1.03	1.02	1.02	1.01	0.99	0.94
27	0.00	0.00	0.85	1.03	1.00	1.00	1.02	0.99	0.97	0.93
28	0.00	0.00	1.03	1.01	1.01	0.99	1.01	0.98	0.93	0.85
29	0.00	0.00	1.05	0.93	0.92	0.95	0.92	0.92	0.89	0.88
30	0.00	0.00	1.05	0.87	0.94	0.96	0.95	0.92	0.88	0.85
31	0.00	0.00	1.19	1.04	1.06	1.06	1.07	1.07	1.07	1.14
32	0.00	0.00	1.14	1.09	1.11	1.12	1.18	1.22	1.31	1.45
33	0.00	0.00	1.15	1.17	1.19	1.21	1.23	1.32	1.40	1.64
34	0.00	0.00	1.07	0.91	0.99	1.06	1.11	1.15	1.21	1.19
35	0.00	0.00	0.94	0.98	0.98	1.03	1.08	1.11	1.14	1.23
36	0.00	0.00	0.75	1.06	1.00	1.01	1.04	1.06	1.08	1.08
37	0.00	0.00	0.76	0.84	0.89	0.96	0.95	0.95	0.97	0.94
38	0.00	0.00	0.00	1.06	0.95	0.99	0.95	0.97	0.96	1.07
39	0.00	0.00	1.38	1.11	1.09	1.13	1.17	1.27	1.46	1.71
40	0.00	0.00	1.12	1.04	1.20	1.29	1.37	1.62	1.91	2.59
41	0.00	0.00	1.05	1.10	1.30	1.45	1.68	2.00	2.94	2.94
42	0.00	0.00	0.96	0.82	0.97	1.05	1.16	1.25	1.41	1.66
43	0.00	0.00	1.47	0.96	0.95	1.03	1.13	1.20	1.36	1.64
44	0.00	0.00	0.00	1.14	0.99	1.01	1.13	1.16	1.24	1.42
45	0.00	0.00	0.00	0.00	0.00	0.00	0.00	0.00	0.00	0.00
46	0.00	0.00	0.00	0.00	0.00	0.00	0.00	0.00	0.00	0.00
47	0.00	0.00	1.26	1.11	1.07	1.19	1.19	1.49	1.79	2.30
48	0.00	0.00	1.24	1.05	1.28	1.36	1.57	1.92	2.99	4.00
49	0.00	0.00	0.89	1.32	1.39	1.68	2.18	3.10	4.67	5.34

TABLE 3.2 RELATIVE DISPERSIONS FOR CLEAR SNOW

	SOLAR ZENITH ANGLE RANGE (DEG.)									
	0.0	25.8	36.8	45.5	53.1	59.9	66.4	72.5	78.4	84.3
	25.8	36.8	45.5	53.1	59.9	66.4	72.5	78.4	84.3	90.0
BIN										
1	-9.99	-9.99	0.41	0.31	0.16	0.14	0.15	0.13	0.15	0.22
2	-9.99	-9.99	0.13	0.29	0.14	0.13	0.11	0.16	0.16	0.22
3	-9.99	-9.99	0.35	0.30	0.15	0.13	0.10	0.17	0.14	0.20
4	-9.99	-9.99	0.01	0.22	0.10	0.09	0.12	0.14	0.18	0.22
5	-9.99	-9.99	0.27	0.29	0.10	0.10	0.12	0.14	0.18	0.23
6	-9.99	-9.99	0.32	0.25	0.10	0.10	0.12	0.16	0.18	0.23
7	-9.99	-9.99	0.31	0.29	0.10	0.11	0.14	0.15	0.18	0.21
8	-9.99	-9.99	0.36	0.33	0.16	0.15	0.15	0.12	0.15	0.17
9	-9.99	-9.99	0.37	0.24	0.11	0.14	0.11	0.11	0.14	0.19
10	-9.99	-9.99	0.12	0.25	0.10	0.10	0.11	0.11	0.15	0.19
11	-9.99	-9.99	0.00	0.21	0.07	0.12	0.10	0.15	0.14	0.16
12	-9.99	-9.99	0.00	0.20	0.08	0.07	0.15	0.15	0.19	0.18
13	-9.99	-9.99	0.46	0.29	0.15	0.12	0.23	0.12	0.17	0.20
14	-9.99	-9.99	0.40	0.27	0.13	0.12	0.09	0.15	0.14	0.22
15	-9.99	-9.99	-9.99	0.18	0.11	0.09	0.12	0.15	0.20	0.21
16	-9.99	-9.99	0.35	0.28	0.15	0.10	0.14	0.13	0.13	0.16
17	-9.99	-9.99	0.00	0.26	0.07	0.19	0.17	0.21	0.15	0.10
18	-9.99	-9.99	0.17	0.30	0.14	0.13	0.14	0.13	0.13	0.16
19	-9.99	-9.99	0.11	0.22	0.09	0.11	0.08	0.13	0.13	0.18
20	-9.99	-9.99	0.62	0.12	0.09	0.11	0.11	0.11	0.17	0.19
21	-9.99	-9.99	0.51	0.30	0.20	0.12	0.12	0.15	0.13	0.21
22	-9.99	-9.99	0.04	0.20	0.15	0.15	0.13	0.18	0.17	0.16
23	-9.99	-9.99	0.01	0.20	0.06	0.09	0.12	0.14	0.15	0.20
24	-9.99	-9.99	0.17	0.33	0.16	0.14	0.12	0.13	0.17	0.17
25	-9.99	-9.99	0.42	0.19	0.12	0.14	0.14	0.18	0.15	0.17
26	-9.99	-9.99	0.24	0.27	0.09	0.10	0.10	0.12	0.14	0.16
27	-9.99	-9.99	0.25	0.23	0.13	0.09	0.10	0.12	0.14	0.16
28	-9.99	-9.99	0.00	0.20	0.08	0.10	0.10	0.11	0.12	0.20
29	-9.99	-9.99	0.42	0.30	0.16	0.10	0.17	0.14	0.16	0.18
30	-9.99	-9.99	0.30	0.35	0.17	0.13	0.15	0.17	0.15	0.23
31	-9.99	-9.99	0.00	0.22	0.11	0.12	0.12	0.14	0.19	0.21
32	-9.99	-9.99	0.03	0.23	0.15	0.17	0.11	0.15	0.16	0.21
33	-9.99	-9.99	0.25	0.21	0.13	0.10	0.19	0.19	0.18	0.31
34	-9.99	-9.99	0.25	0.31	0.15	0.09	0.11	0.10	0.13	0.23
35	-9.99	-9.99	0.00	0.23	0.15	0.09	0.11	0.12	0.14	0.17
36	-9.99	-9.99	0.00	0.15	0.09	0.09	0.13	0.13	0.15	0.22
37	-9.99	-9.99	0.32	0.34	0.19	0.12	0.15	0.13	0.14	0.17
38	-9.99	-9.99	-9.99	0.15	0.14	0.10	0.16	0.14	0.17	0.14
39	-9.99	-9.99	0.31	0.19	0.14	0.14	0.18	0.21	0.22	0.31
40	-9.99	-9.99	0.33	0.31	0.13	0.15	0.20	0.26	0.27	0.35
41	-9.99	-9.99	0.26	0.31	0.14	0.18	0.20	0.26	0.35	0.29
42	-9.99	-9.99	0.21	0.33	0.12	0.12	0.09	0.10	0.10	0.16
43	-9.99	-9.99	0.00	0.20	0.15	0.11	0.11	0.13	0.14	0.27
44	-9.99	-9.99	-9.99	0.07	0.04	0.11	0.12	0.12	0.13	0.23
45	-9.99	-9.99	-9.99	-9.99	-9.99	-9.99	-9.99	-9.99	-9.99	-9.99
46	-9.99	-9.99	-9.99	-9.99	-9.99	-9.99	-9.99	-9.99	-9.99	-9.99
47	-9.99	-9.99	0.00	0.10	0.16	0.16	0.17	0.28	0.22	0.32
48	-9.99	-9.99	0.00	0.28	0.12	0.18	0.23	0.31	0.31	0.35
49	-9.99	-9.99	0.30	0.10	0.17	0.22	0.17	0.33	0.34	0.40

TABLE 3.3 BIN POPULATIONS FOR CLEAR SNOW

	SOLAR ZENITH ANGLE RANGE (DEG.)									
	0.0	25.8	36.8	45.5	53.1	59.9	66.4	72.5	78.4	84.3
	25.8	36.8	45.5	53.1	59.9	66.4	72.5	78.4	84.3	90.0
BIN										
1	0	0	28	170	768	1073	1073	895	592	383
2	0	0	4	31	154	224	234	156	115	45
3	0	0	9	46	187	242	239	190	175	108
4	0	0	2	78	338	487	524	350	248	104
5	0	0	8	81	363	517	476	386	271	124
6	0	0	8	79	383	523	502	372	241	123
7	0	0	6	71	304	467	482	336	208	108
8	0	0	2	39	179	199	252	159	124	72
9	0	0	5	23	133	178	201	146	104	43
10	0	0	4	13	62	67	42	60	59	17
11	0	0	1	25	126	186	202	141	122	38
12	0	0	1	37	176	268	261	149	124	53
13	0	0	5	36	122	178	190	115	107	67
14	0	0	4	19	122	197	233	176	135	53
15	0	0	0	21	147	248	217	156	125	44
16	0	0	5	30	123	187	175	148	118	53
17	0	0	1	15	58	84	72	58	38	20
18	0	0	5	21	153	202	208	160	137	78
19	0	0	6	44	204	351	360	227	176	78
20	0	0	2	43	174	300	305	257	165	87
21	0	0	7	86	273	383	424	323	303	130
22	0	0	3	69	222	302	299	219	184	68
23	0	0	2	46	209	357	363	260	135	117
24	0	0	3	62	205	297	258	203	163	68
25	0	0	8	35	156	196	205	151	109	52
26	0	0	5	22	150	159	143	115	76	40
27	0	0	3	37	120	252	232	191	125	94
28	0	0	1	18	113	160	166	137	66	18
29	0	0	9	55	218	257	251	219	233	105
30	0	0	2	45	150	168	164	126	95	51
31	0	0	1	40	110	198	229	151	64	86
32	0	0	2	38	134	188	137	135	99	73
33	0	0	4	23	102	122	123	105	79	38
34	0	0	9	55	231	316	346	229	175	63
35	0	0	1	63	354	442	457	364	282	139
36	0	0	1	40	153	197	233	175	66	33
37	0	0	7	66	248	273	246	233	251	138
38	0	0	0	19	115	140	144	102	77	33
39	0	0	7	55	263	328	306	271	182	92
40	0	0	8	56	271	394	415	329	254	136
41	0	0	12	31	151	226	273	148	118	63
42	0	0	8	24	111	159	108	111	89	30
43	0	0	1	37	189	265	285	196	134	59
44	0	0	0	5	44	52	87	55	14	7
45	0	0	0	0	0	0	0	0	0	0
46	0	0	0	0	0	0	0	0	0	0
47	0	0	1	26	104	163	154	115	76	28
48	0	0	1	35	142	220	256	211	106	90
49	0	0	2	11	100	92	66	62	61	31

TABLE 4.1 ANISOTROPIC FACTORS FOR CLEAR ICE

	SOLAR ZENITH ANGLE RANGE (DEG.)									
	0.0	25.8	36.8	45.5	53.1	59.9	66.4	72.5	78.4	84.3
	25.8	36.8	45.5	53.1	59.9	66.4	72.5	78.4	84.3	90.0
BIN										
1	0.00	0.00	0.00	1.01	0.87	0.90	0.79	0.74	0.69	0.66
2	0.00	0.00	0.00	0.83	1.00	0.88	0.81	0.82	0.75	0.63
3	0.00	0.00	0.00	1.05	1.05	0.92	0.85	0.75	0.73	0.70
4	0.00	0.00	0.00	1.08	0.92	0.86	0.79	0.76	0.74	0.66
5	0.00	0.00	0.00	1.06	0.90	0.86	0.82	0.76	0.74	0.65
6	0.00	0.00	0.00	0.90	0.93	0.84	0.79	0.71	0.71	0.71
7	0.00	0.00	0.00	1.01	0.83	0.90	0.82	0.71	0.75	0.65
8	0.00	0.00	0.00	1.07	0.87	0.93	0.84	0.75	0.79	0.67
9	0.00	0.00	0.00	1.07	0.98	0.88	0.88	0.82	0.80	0.70
10	0.00	0.00	0.00	0.68	0.75	0.88	0.93	0.75	0.73	0.79
11	0.00	0.00	0.00	0.93	1.09	0.95	0.88	0.87	0.77	0.80
12	0.00	0.00	0.00	1.02	1.01	0.85	0.88	0.70	0.77	0.77
13	0.00	0.00	0.00	1.04	1.16	0.89	0.80	0.82	0.66	0.66
14	0.00	0.00	0.00	0.69	0.93	0.90	0.88	0.82	0.77	0.74
15	0.00	0.00	0.00	1.08	0.93	0.85	0.86	0.77	0.69	0.54
16	0.00	0.00	0.00	1.10	0.82	0.97	0.92	0.91	0.85	0.86
17	0.00	0.00	0.00	1.13	1.11	0.95	0.89	0.97	0.81	0.92
18	0.00	0.00	0.00	1.12	0.88	0.88	1.05	0.98	0.95	0.93
19	0.00	0.00	0.00	1.16	0.98	0.97	0.90	0.89	0.95	0.93
20	0.00	0.00	0.00	1.00	0.98	0.91	0.83	0.83	0.77	0.69
21	0.00	0.00	0.00	0.73	0.92	1.01	0.90	0.90	0.78	0.67
22	0.00	0.00	0.00	0.83	0.85	0.93	0.93	0.88	0.76	0.75
23	0.00	0.00	0.00	0.92	1.05	0.95	1.04	0.83	0.92	0.92
24	0.00	0.00	0.00	1.14	0.93	1.02	1.12	1.05	1.14	1.04
25	0.00	0.00	0.00	1.48	1.17	1.11	1.11	1.31	1.18	1.13
26	0.00	0.00	0.00	1.14	1.09	1.06	1.09	1.05	0.94	1.05
27	0.00	0.00	0.00	1.21	1.19	1.02	1.04	1.03	1.02	0.99
28	0.00	0.00	0.00	0.94	0.99	0.98	0.85	0.94	0.89	0.84
29	0.00	0.00	0.00	0.97	0.91	0.97	0.97	0.94	0.83	0.75
30	0.00	0.00	0.00	1.04	0.98	1.03	0.95	0.93	0.87	0.79
31	0.00	0.00	0.00	0.64	1.04	1.00	1.21	1.22	1.16	1.22
32	0.00	0.00	0.00	1.26	1.18	1.21	1.29	1.34	1.53	1.38
33	0.00	0.00	0.00	1.41	1.45	1.36	1.48	1.54	1.86	1.71
34	0.00	0.00	0.00	1.05	1.05	1.11	1.21	1.08	1.32	1.44
35	0.00	0.00	0.00	0.90	1.10	1.08	1.08	1.16	1.19	1.32
36	0.00	0.00	0.00	0.96	1.10	1.05	1.02	1.05	1.07	1.09
37	0.00	0.00	0.00	0.96	0.97	0.92	0.98	0.99	0.92	0.91
38	0.00	0.00	0.00	0.92	0.91	1.05	0.99	1.01	0.98	1.00
39	0.00	0.00	0.00	1.16	1.15	1.25	1.27	1.50	1.59	1.96
40	0.00	0.00	0.00	1.16	1.24	1.57	1.65	2.01	2.22	2.37
41	0.00	0.00	0.00	1.38	1.43	1.75	1.95	2.57	2.97	3.59
42	0.00	0.00	0.00	0.94	1.10	1.16	1.18	1.44	1.51	1.99
43	0.00	0.00	0.00	0.89	1.08	1.04	1.17	1.27	1.36	1.54
44	0.00	0.00	0.00	1.13	0.85	1.06	1.14	1.21	1.33	1.59
45	0.00	0.00	0.00	0.00	0.00	0.00	0.00	0.00	0.00	0.00
46	0.00	0.00	0.00	0.00	0.00	0.00	0.00	0.00	0.00	0.00
47	0.00	0.00	0.00	0.98	1.29	1.48	1.87	1.89	2.08	2.46
48	0.00	0.00	0.00	0.95	1.43	1.70	2.19	2.99	3.42	3.93
49	0.00	0.00	0.00	1.45	1.39	1.97	2.33	3.92	5.48	5.21

TABLE 4.2 RELATIVE DISPERSIONS FOR CLEAR ICE

	SOLAR ZENITH ANGLE RANGE (DEG.)									
	0.0	25.8	36.8	45.5	53.1	59.9	66.4	72.5	78.4	84.3
	25.8	36.8	45.5	53.1	59.9	66.4	72.5	78.4	84.3	90.0
BIN										
1	-9.99	-9.99	-9.99	0.27	0.34	0.24	0.24	0.30	0.24	0.26
2	-9.99	-9.99	-9.99	0.46	0.34	0.33	0.27	0.27	0.19	0.29
3	-9.99	-9.99	-9.99	0.18	0.24	0.21	0.22	0.36	0.30	0.22
4	-9.99	-9.99	-9.99	0.25	0.37	0.26	0.24	0.29	0.27	0.25
5	-9.99	-9.99	-9.99	0.23	0.37	0.36	0.20	0.31	0.23	0.20
6	-9.99	-9.99	-9.99	0.30	0.36	0.33	0.22	0.30	0.32	0.25
7	-9.99	-9.99	-9.99	0.12	0.36	0.30	0.23	0.27	0.26	0.25
8	-9.99	-9.99	-9.99	0.07	0.34	0.22	0.20	0.28	0.22	0.22
9	-9.99	-9.99	-9.99	0.10	0.29	0.30	0.21	0.30	0.29	0.15
10	-9.99	-9.99	-9.99	0.66	0.46	0.29	0.12	0.37	0.27	0.14
11	-9.99	-9.99	-9.99	0.33	0.22	0.27	0.21	0.25	0.25	0.22
12	-9.99	-9.99	-9.99	0.03	0.34	0.27	0.19	0.34	0.19	0.20
13	-9.99	-9.99	-9.99	0.13	0.16	0.29	0.18	0.21	0.26	0.18
14	-9.99	-9.99	-9.99	0.45	0.30	0.26	0.12	0.29	0.15	0.09
15	-9.99	-9.99	-9.99	0.05	0.36	0.41	0.24	0.38	0.42	0.28
16	-9.99	-9.99	-9.99	0.08	0.42	0.26	0.18	0.28	0.16	0.20
17	-9.99	-9.99	-9.99	0.00	0.13	0.28	0.22	0.14	0.36	0.11
18	-9.99	-9.99	-9.99	0.14	0.41	0.32	0.11	0.24	0.15	0.19
19	-9.99	-9.99	-9.99	0.08	0.32	0.29	0.24	0.27	0.15	0.24
20	-9.99	-9.99	-9.99	0.20	0.25	0.30	0.21	0.21	0.27	0.38
21	-9.99	-9.99	-9.99	0.54	0.35	0.11	0.13	0.16	0.16	0.16
22	-9.99	-9.99	-9.99	0.28	0.28	0.19	0.09	0.18	0.21	0.12
23	-9.99	-9.99	-9.99	0.33	0.24	0.24	0.15	0.33	0.16	0.29
24	-9.99	-9.99	-9.99	0.16	0.33	0.27	0.21	0.26	0.18	0.18
25	-9.99	-9.99	-9.99	0.20	0.17	0.20	0.17	0.20	0.22	0.24
26	-9.99	-9.99	-9.99	0.08	0.18	0.26	0.13	0.17	0.23	0.15
27	-9.99	-9.99	-9.99	0.10	0.12	0.24	0.17	0.17	0.14	0.18
28	-9.99	-9.99	-9.99	0.30	0.27	0.17	0.25	0.18	0.24	0.12
29	-9.99	-9.99	-9.99	0.29	0.33	0.17	0.07	0.13	0.17	0.17
30	-9.99	-9.99	-9.99	0.10	0.22	0.12	0.10	0.17	0.17	0.23
31	-9.99	-9.99	-9.99	0.55	0.31	0.22	0.17	0.15	0.20	0.28
32	-9.99	-9.99	-9.99	0.04	0.20	0.18	0.23	0.29	0.22	0.18
33	-9.99	-9.99	-9.99	0.04	0.09	0.19	0.16	0.27	0.25	0.24
34	-9.99	-9.99	-9.99	0.17	0.31	0.25	0.09	0.27	0.15	0.25
35	-9.99	-9.99	-9.99	0.23	0.28	0.18	0.15	0.18	0.17	0.15
36	-9.99	-9.99	-9.99	0.34	0.23	0.22	0.09	0.15	0.14	0.28
37	-9.99	-9.99	-9.99	0.21	0.17	0.20	0.12	0.12	0.13	0.15
38	-9.99	-9.99	-9.99	0.14	0.31	0.14	0.11	0.17	0.13	0.17
39	-9.99	-9.99	-9.99	0.15	0.26	0.28	0.18	0.29	0.23	0.26
40	-9.99	-9.99	-9.99	0.24	0.24	0.20	0.25	0.34	0.30	0.28
41	-9.99	-9.99	-9.99	0.02	0.17	0.22	0.27	0.38	0.36	0.31
42	-9.99	-9.99	-9.99	0.29	0.15	0.14	0.15	0.14	0.09	0.24
43	-9.99	-9.99	-9.99	0.29	0.19	0.15	0.11	0.18	0.15	0.13
44	-9.99	-9.99	-9.99	0.05	0.27	0.12	0.06	0.19	0.14	0.14
45	-9.99	-9.99	-9.99	-9.99	-9.99	-9.99	-9.99	-9.99	-9.99	-9.99
46	-9.99	-9.99	-9.99	-9.99	-9.99	-9.99	-9.99	-9.99	-9.99	-9.99
47	-9.99	-9.99	-9.99	0.32	0.18	0.22	0.15	0.35	0.24	0.24
48	-9.99	-9.99	-9.99	0.39	0.23	0.21	0.24	0.34	0.29	0.38
49	-9.99	-9.99	-9.99	0.10	0.10	0.21	0.26	0.35	0.28	0.20

TABLE 4.3 BIN POPULATIONS FOR CLEAR ICE

	SOLAR ZENITH ANGLE RANGE (DEG.)									
	0.0	25.8	36.8	45.5	53.1	59.9	66.4	72.5	78.4	84.3
	25.8	36.8	45.5	53.1	59.9	66.4	72.5	78.4	84.3	90.0
BIN										
1	0	0	0	36	112	179	224	173	152	102
2	0	0	0	6	19	26	27	25	30	8
3	0	0	0	12	24	41	66	33	32	41
4	0	0	0	9	39	66	98	56	65	15
5	0	0	0	8	43	68	86	41	60	23
6	0	0	0	7	41	81	69	49	46	23
7	0	0	0	9	33	65	69	46	40	19
8	0	0	0	8	26	54	54	35	36	36
9	0	0	0	6	13	19	23	17	19	9
10	0	0	0	2	9	20	13	14	10	4
11	0	0	0	8	12	29	35	15	15	8
12	0	0	0	2	21	33	55	30	26	11
13	0	0	0	8	17	37	35	25	28	12
14	0	0	0	8	21	36	33	35	18	5
15	0	0	0	2	11	34	21	19	14	10
16	0	0	0	4	14	34	24	21	31	25
17	0	0	0	1	7	14	24	5	8	6
18	0	0	0	8	17	25	25	22	32	23
19	0	0	0	4	12	26	45	35	32	29
20	0	0	0	2	25	30	29	23	35	12
21	0	0	0	20	48	58	148	122	65	28
22	0	0	0	8	29	64	50	67	45	24
23	0	0	0	10	28	52	30	42	30	22
24	0	0	0	9	21	65	36	39	45	17
25	0	0	0	6	11	42	36	24	38	22
26	0	0	0	7	10	20	27	17	13	15
27	0	0	0	3	20	36	34	23	33	23
28	0	0	0	6	13	25	10	15	20	8
29	0	0	0	24	38	66	65	81	69	25
30	0	0	0	4	19	41	34	43	48	21
31	0	0	0	9	27	31	20	25	26	10
32	0	0	0	6	28	42	31	36	37	18
33	0	0	0	2	7	20	16	16	12	13
34	0	0	0	9	17	43	44	20	41	24
35	0	0	0	17	39	81	81	45	65	37
36	0	0	0	8	15	22	14	10	21	23
37	0	0	0	15	33	66	78	116	77	29
38	0	0	0	7	13	28	42	51	26	14
39	0	0	0	16	41	49	37	40	43	23
40	0	0	0	13	50	81	89	61	84	40
41	0	0	0	2	18	29	36	19	21	22
42	0	0	0	4	10	24	34	7	15	8
43	0	0	0	2	34	30	32	37	30	10
44	0	0	0	2	11	13	4	14	13	7
45	0	0	0	0	0	0	0	0	0	0
46	0	0	0	0	0	0	0	0	0	0
47	0	0	0	2	10	19	22	5	20	8
48	0	0	0	4	22	52	29	44	50	32
49	0	0	0	3	6	11	21	10	16	17

TABLE 5.1 ANISOTROPIC FACTORS FOR LOW CLOUD

	SOLAR ZENITH ANGLE RANGE (DEG.)									
	0.0	25.8	36.8	45.5	53.1	59.9	66.4	72.5	78.4	84.3
	25.8	36.8	45.5	53.1	59.9	66.4	72.5	78.4	84.3	90.0
BIN										
1	1.21	1.10	0.99	0.91	0.85	0.81	0.74	0.64	0.53	0.57
2	1.27	1.08	1.03	1.01	0.91	0.94	0.92	0.79	0.60	0.60
3	1.01	1.19	1.11	1.04	0.95	0.92	0.89	0.74	0.55	0.75
4	1.05	1.11	1.11	1.11	0.93	0.89	0.77	0.68	0.61	0.62
5	1.02	1.22	1.17	0.95	0.86	0.83	0.70	0.67	0.64	0.62
6	1.09	1.08	0.91	0.98	0.88	0.78	0.73	0.70	0.65	0.51
7	1.27	1.13	0.95	0.96	0.79	0.84	0.78	0.74	0.63	0.65
8	1.30	1.25	0.85	0.92	0.84	0.95	0.70	0.74	0.60	0.67
9	1.45	1.01	0.87	0.93	0.95	0.96	0.83	0.71	0.60	0.69
10	1.04	1.45	1.07	1.07	0.75	1.01	1.02	0.52	0.49	0.46
11	0.99	1.17	1.17	1.04	0.95	1.02	0.99	0.80	0.67	0.71
12	0.99	1.08	1.20	1.13	1.12	0.86	0.91	0.83	0.73	0.62
13	0.98	1.08	1.16	1.01	0.85	0.73	0.72	0.84	0.54	0.60
14	0.98	0.92	1.04	0.89	0.93	0.80	0.64	0.65	0.67	0.51
15	0.99	1.01	1.02	1.09	0.89	0.95	0.81	0.91	0.78	0.77
16	1.16	1.28	0.90	1.01	0.88	0.85	0.87	0.88	0.67	0.79
17	1.09	1.30	0.99	1.04	0.95	1.18	0.92	0.84	0.79	0.85
18	1.18	1.30	1.21	1.12	1.11	1.02	1.07	1.00	0.67	0.95
19	1.05	1.34	1.16	1.01	1.13	0.98	0.93	0.92	0.83	0.71
20	0.95	0.87	1.15	1.00	1.09	0.87	0.91	0.83	0.73	0.68
21	0.84	1.06	0.92	0.91	0.91	0.89	0.76	0.70	0.74	0.64
22	0.87	0.59	0.97	0.94	0.90	0.88	0.78	0.70	0.81	0.64
23	0.95	1.16	1.03	1.21	1.00	0.95	0.96	1.02	0.95	0.92
24	1.04	1.03	1.11	1.07	1.08	1.16	1.11	1.09	1.24	0.98
25	1.08	1.25	1.07	1.15	1.13	1.27	1.33	1.24	1.16	0.94
26	1.04	1.30	1.11	1.14	0.99	1.16	1.18	1.05	0.84	1.10
27	0.96	1.22	1.16	1.02	1.12	1.01	1.01	1.01	1.03	1.05
28	0.88	0.81	0.97	1.06	1.04	1.04	0.93	0.79	0.90	0.84
29	0.86	0.70	0.74	0.76	0.85	0.79	0.84	0.88	0.80	0.81
30	0.79	0.60	0.71	0.91	0.89	0.92	0.88	0.89	0.80	0.76
31	0.98	1.11	1.14	0.97	1.33	1.12	1.15	1.11	1.42	1.19
32	0.96	0.98	1.31	1.15	1.27	1.25	1.47	1.55	1.88	1.54
33	0.94	1.43	1.29	1.36	1.37	1.63	1.50	1.80	2.02	1.38
34	1.03	1.27	1.22	1.18	1.09	1.29	1.44	1.33	1.38	1.40
35	0.94	0.91	1.10	1.05	1.06	1.16	1.17	1.19	1.26	1.25
36	0.83	0.61	0.63	0.89	0.97	0.99	1.08	1.13	1.12	1.29
37	0.88	0.57	0.55	0.64	0.66	0.71	0.74	0.76	0.84	0.80
38	0.88	0.56	0.47	0.58	0.70	0.73	0.82	0.86	0.84	0.88
39	0.95	0.85	0.99	1.25	1.39	1.46	1.69	1.88	1.50	1.93
40	0.99	1.21	1.27	1.37	1.61	1.80	2.14	2.69	2.84	3.45
41	1.05	1.49	1.53	1.56	1.65	2.31	2.63	2.76	3.88	3.68
42	1.11	1.02	1.21	1.08	1.02	1.44	1.50	1.45	1.27	1.83
43	1.07	0.90	0.88	1.04	1.14	1.22	1.26	1.35	1.41	1.78
44	0.91	0.67	0.71	0.62	0.90	0.98	1.07	1.21	1.35	1.34
45	0.92	0.00	0.00	0.00	0.00	0.00	0.00	0.00	0.00	0.00
46	0.98	0.62	0.48	0.00	0.00	0.00	0.00	0.00	0.00	0.00
47	1.03	0.94	1.00	1.11	1.29	1.71	2.10	2.25	2.71	3.37
48	1.12	1.06	1.46	1.51	1.76	2.18	2.70	3.14	4.59	4.76
49	1.34	1.30	1.50	1.50	2.01	2.54	3.14	4.18	5.81	5.98

TABLE 5.2 RELATIVE DISPERSIONS FOR LOW CLOUD

BIN	SOLAR ZENITH ANGLE RANGE (DEG.)									
	0.0	25.8	36.8	45.5	53.1	59.9	66.4	72.5	78.4	84.3
	25.8	36.8	45.5	53.1	59.9	66.4	72.5	78.4	84.3	90.0
1	0.61	0.59	0.41	0.33	0.30	0.34	0.35	0.30	0.41	0.38
2	0.77	0.61	0.34	0.35	0.31	0.33	0.33	0.27	0.30	0.33
3	0.78	0.59	0.34	0.25	0.26	0.25	0.27	0.22	0.36	0.21
4	0.78	0.67	0.37	0.28	0.30	0.34	0.28	0.29	0.36	0.36
5	0.75	0.58	0.31	0.28	0.32	0.35	0.28	0.27	0.32	0.41
6	0.73	0.66	0.41	0.29	0.30	0.36	0.27	0.31	0.31	0.45
7	0.64	0.60	0.42	0.38	0.35	0.35	0.29	0.33	0.42	0.40
8	0.56	0.46	0.40	0.31	0.24	0.29	0.35	0.30	0.32	0.44
9	0.67	0.53	0.44	0.32	0.28	0.31	0.43	0.34	0.32	0.35
10	0.74	0.50	0.39	0.23	0.20	0.25	0.26	0.00	0.30	0.00
11	0.82	0.62	0.29	0.35	0.26	0.28	0.27	0.28	0.26	0.32
12	0.77	0.65	0.34	0.21	0.26	0.31	0.20	0.25	0.30	0.33
13	0.76	0.63	0.32	0.19	0.32	0.25	0.27	0.28	0.33	0.51
14	0.81	0.70	0.26	0.37	0.39	0.22	0.33	0.23	0.21	0.44
15	0.70	0.64	0.40	0.30	0.24	0.22	0.23	0.44	0.26	0.26
16	0.67	0.40	0.35	0.30	0.26	0.32	0.25	0.18	0.25	0.33
17	0.72	0.42	0.32	0.27	0.30	0.28	0.31	0.26	0.17	0.17
18	0.80	0.53	0.37	0.36	0.23	0.22	0.22	0.16	0.52	0.16
19	0.76	0.54	0.31	0.34	0.21	0.29	0.19	0.27	0.23	0.32
20	0.77	0.75	0.33	0.31	0.24	0.28	0.21	0.24	0.30	0.34
21	0.81	0.64	0.44	0.27	0.27	0.27	0.20	0.29	0.21	0.30
22	0.80	0.80	0.43	0.28	0.29	0.32	0.26	0.26	0.18	0.31
23	0.78	0.59	0.35	0.31	0.32	0.23	0.22	0.27	0.23	0.37
24	0.77	0.58	0.30	0.24	0.24	0.28	0.18	0.22	0.24	0.33
25	0.75	0.44	0.25	0.18	0.23	0.18	0.19	0.14	0.16	0.57
26	0.76	0.52	0.32	0.20	0.19	0.18	0.20	0.12	0.07	0.29
27	0.69	0.53	0.29	0.27	0.22	0.24	0.16	0.23	0.10	0.18
28	0.68	0.69	0.50	0.22	0.24	0.22	0.24	0.27	0.17	0.20
29	0.69	0.77	0.60	0.39	0.36	0.33	0.25	0.23	0.26	0.28
30	0.67	0.78	0.54	0.28	0.33	0.36	0.30	0.28	0.26	0.26
31	0.76	0.61	0.36	0.29	0.24	0.27	0.25	0.33	0.31	0.35
32	0.75	0.61	0.23	0.24	0.19	0.30	0.21	0.19	0.22	0.25
33	0.79	0.44	0.29	0.19	0.22	0.20	0.16	0.21	0.30	0.39
34	0.59	0.50	0.26	0.21	0.21	0.19	0.17	0.18	0.17	0.17
35	0.55	0.62	0.30	0.17	0.20	0.22	0.17	0.10	0.18	0.19
36	0.47	0.53	0.55	0.40	0.29	0.30	0.21	0.21	0.19	0.23
37	0.55	0.54	0.61	0.54	0.45	0.39	0.34	0.32	0.20	0.36
38	0.53	0.63	0.63	0.51	0.51	0.35	0.37	0.25	0.31	0.24
39	0.53	0.61	0.46	0.24	0.17	0.24	0.18	0.26	0.30	0.28
40	0.58	0.55	0.33	0.19	0.15	0.21	0.22	0.32	0.33	0.28
41	0.59	0.36	0.24	0.15	0.22	0.19	0.16	0.22	0.39	0.46
42	0.44	0.47	0.29	0.18	0.26	0.14	0.13	0.18	0.32	0.20
43	0.40	0.44	0.35	0.18	0.15	0.13	0.14	0.12	0.20	0.20
44	0.27	0.23	0.38	0.35	0.21	0.19	0.23	0.19	0.15	0.19
45	0.33	-9.99	-9.99	-9.99	-9.99	-9.99	-9.99	-9.99	-9.99	-9.99
46	0.39	0.41	0.24	-9.99	-9.99	-9.99	-9.99	-9.99	-9.99	-9.99
47	0.37	0.50	0.40	0.41	0.30	0.22	0.23	0.28	0.15	0.16
48	0.42	0.51	0.25	0.23	0.11	0.24	0.25	0.23	0.27	0.34
49	0.34	0.41	0.31	0.07	0.24	0.15	0.26	0.19	0.05	0.31

TABLE 5.3 BIN POPULATIONS FOR LOW CLOUD

	SOLAR ZENITH ANGLE RANGE (DEG.)									
	0.0	25.8	36.8	45.5	53.1	59.9	66.4	72.5	78.4	84.3
	25.8	36.8	45.5	53.1	59.9	66.4	72.5	78.4	84.3	90.0
BIN										
1	1215	252	190	187	210	200	189	129	85	80
2	137	57	30	27	27	34	38	20	9	16
3	337	97	53	41	50	29	33	16	9	11
4	460	91	77	37	53	39	50	37	40	22
5	421	90	70	44	52	54	57	30	45	19
6	345	95	74	40	48	40	53	26	37	24
7	343	108	76	38	44	51	36	28	34	19
8	275	53	40	46	38	21	21	18	14	9
9	112	34	27	15	20	21	28	13	11	18
10	75	30	15	11	7	11	7	1	4	1
11	194	52	34	21	22	17	21	12	10	8
12	227	52	40	17	25	14	8	12	19	10
13	195	42	34	16	26	25	27	11	11	8
14	188	37	27	18	17	13	19	9	18	14
15	177	38	30	15	27	18	24	3	19	21
16	112	44	32	30	23	20	20	13	9	9
17	54	17	16	12	8	6	13	8	4	2
18	206	46	38	24	41	30	29	15	6	15
19	473	65	62	41	29	41	31	23	23	26
20	634	105	51	26	36	28	28	24	33	21
21	493	155	84	68	66	47	45	30	28	28
22	330	103	79	41	63	46	39	23	12	38
23	214	75	47	33	22	36	44	23	25	11
24	204	75	38	27	33	36	29	15	18	13
25	68	45	29	27	30	18	16	11	8	10
26	221	68	19	21	15	22	23	10	3	5
27	532	74	51	22	35	32	27	24	16	7
28	655	126	42	23	20	25	23	16	33	12
29	415	178	83	52	51	34	35	32	18	21
30	251	84	59	29	35	53	32	29	23	18
31	184	59	37	32	17	21	21	25	18	14
32	163	36	45	16	23	18	23	16	13	13
33	50	24	18	19	14	21	13	9	7	9
34	494	165	66	48	39	44	39	25	16	11
35	1314	170	118	62	74	51	71	46	32	34
36	1006	331	95	34	39	61	40	39	29	17
37	608	343	145	113	95	82	72	58	15	16
38	405	142	92	56	49	62	50	36	41	14
39	419	139	48	49	38	22	28	40	24	20
40	281	94	72	39	39	39	40	31	39	18
41	96	37	31	29	36	31	24	8	9	16
42	166	88	34	19	22	11	8	7	2	8
43	426	110	57	27	42	23	26	29	21	9
44	208	19	31	8	12	26	17	10	19	11
45	189	0	0	0	0	0	0	0	0	0
46	218	59	13	0	0	0	0	0	0	0
47	203	80	52	27	21	11	19	17	9	6
48	107	44	34	20	14	32	19	18	24	10
49	29	15	11	10	9	8	15	8	4	5

TABLE 6.1 ANISOTROPIC FACTORS FOR MIDDLE CLOUD

	SOLAR ZENITH ANGLE RANGE (DEG.)									
	0.0	25.8	36.8	45.5	53.1	59.9	66.4	72.5	78.4	84.3
	25.8	36.8	45.5	53.1	59.9	66.4	72.5	78.4	84.3	90.0
BIN										
1	1.10	1.04	0.97	0.90	0.86	0.84	0.77	0.74	0.66	0.60
2	1.19	1.09	1.07	0.98	0.96	0.92	0.83	0.76	0.69	0.64
3	1.15	1.10	1.01	0.97	0.93	0.91	0.81	0.76	0.68	0.63
4	1.16	1.03	1.01	0.97	0.96	0.89	0.81	0.76	0.68	0.61
5	1.13	1.03	0.98	0.94	0.89	0.87	0.81	0.75	0.67	0.63
6	1.12	1.01	0.95	0.94	0.89	0.84	0.80	0.75	0.67	0.63
7	1.11	1.00	0.94	0.94	0.90	0.89	0.84	0.79	0.70	0.64
8	1.09	0.96	0.95	0.90	0.86	0.88	0.84	0.81	0.74	0.68
9	1.14	1.04	0.91	0.92	0.88	0.91	0.83	0.80	0.71	0.69
10	1.15	1.17	1.10	1.03	0.97	0.92	0.89	0.84	0.78	0.70
11	1.20	1.12	1.06	1.05	0.99	0.96	0.92	0.83	0.73	0.71
12	1.06	1.06	1.02	1.09	1.05	0.95	0.88	0.79	0.74	0.64
13	1.12	1.07	1.01	0.94	0.90	0.89	0.83	0.77	0.69	0.69
14	1.05	1.00	0.97	0.97	0.89	0.85	0.87	0.78	0.68	0.68
15	1.03	0.97	0.96	0.95	0.95	0.93	0.88	0.81	0.74	0.72
16	1.14	1.02	1.00	0.94	0.93	0.92	0.90	0.87	0.84	0.82
17	1.06	1.00	0.99	0.95	0.96	0.92	0.92	0.92	0.87	0.81
18	1.12	1.15	1.16	1.09	1.03	1.01	0.97	0.94	0.91	0.78
19	1.07	1.11	1.07	1.10	1.04	0.98	0.94	0.91	0.86	0.78
20	1.02	1.07	1.06	1.07	1.06	0.96	0.89	0.84	0.79	0.72
21	1.01	1.04	0.96	0.87	0.92	0.88	0.86	0.80	0.76	0.71
22	0.96	0.97	0.96	0.94	0.89	0.89	0.87	0.83	0.79	0.71
23	1.13	1.04	1.01	1.01	1.05	1.01	0.98	0.96	0.93	0.91
24	1.07	1.04	1.05	1.05	1.10	1.08	1.11	1.08	1.12	1.09
25	1.03	1.10	1.08	1.08	1.07	1.16	1.11	1.17	1.16	1.15
26	0.97	1.13	1.15	1.14	1.10	1.04	1.00	1.03	1.01	0.99
27	0.93	1.09	1.06	1.08	1.04	1.01	1.00	0.99	0.99	1.01
28	0.87	1.01	1.01	1.02	0.99	0.98	0.98	0.95	0.89	0.87
29	0.84	0.89	0.91	0.90	0.88	0.88	0.89	0.85	0.81	0.79
30	0.88	0.92	0.94	0.90	0.89	0.92	0.91	0.91	0.88	0.80
31	1.00	0.98	1.05	1.06	1.21	1.15	1.16	1.17	1.17	1.16
32	1.03	1.07	1.09	1.16	1.24	1.28	1.31	1.42	1.52	1.53
33	1.08	1.15	1.14	1.26	1.30	1.38	1.44	1.49	1.62	1.73
34	0.80	1.05	1.07	1.07	1.07	1.10	1.18	1.19	1.26	1.28
35	0.79	0.99	1.04	1.02	1.05	1.09	1.12	1.13	1.20	1.26
36	0.71	0.76	0.93	0.93	0.97	1.03	1.07	1.09	1.09	1.15
37	0.69	0.76	0.83	0.83	0.83	0.87	0.90	0.89	0.89	0.88
38	0.81	0.77	0.84	0.88	0.87	0.90	0.96	0.98	0.97	0.99
39	0.90	0.97	1.06	1.14	1.24	1.34	1.50	1.63	1.76	1.74
40	0.98	1.10	1.16	1.29	1.45	1.63	1.91	2.04	2.53	2.85
41	0.92	1.14	1.28	1.41	1.51	1.80	1.98	2.58	3.31	3.50
42	0.76	0.88	0.99	0.98	1.07	1.09	1.22	1.38	1.52	1.71
43	0.81	0.90	0.98	0.98	1.01	1.07	1.16	1.27	1.40	1.57
44	0.74	0.76	0.89	0.91	0.97	1.03	1.15	1.26	1.31	1.40
45	0.71	0.00	0.00	0.00	0.00	0.00	0.00	0.00	0.00	0.00
46	0.77	0.67	0.83	1.10	0.00	0.00	0.00	0.00	0.00	0.00
47	0.83	0.88	1.02	1.12	1.25	1.49	1.66	1.92	2.27	2.65
48	0.95	1.09	1.23	1.40	1.67	1.90	2.37	2.90	3.71	4.53
49	0.91	1.21	1.33	1.44	1.70	2.23	2.61	3.78	5.32	7.19

TABLE 6.2 RELATIVE DISPERSIONS FOR MIDDLE CLOUD

	SOLAR ZENITH ANGLE RANGE (DEG.)									
	0.0	25.8	36.8	45.5	53.1	59.9	66.4	72.5	78.4	84.3
	25.8	36.8	45.5	53.1	59.9	66.4	72.5	78.4	84.3	90.0
BIN										
1	0.29	0.24	0.22	0.25	0.22	0.19	0.22	0.21	0.20	0.26
2	0.33	0.25	0.22	0.23	0.18	0.17	0.21	0.22	0.20	0.22
3	0.29	0.23	0.19	0.21	0.21	0.19	0.22	0.22	0.20	0.27
4	0.27	0.24	0.20	0.26	0.20	0.20	0.21	0.22	0.20	0.28
5	0.28	0.25	0.21	0.24	0.21	0.18	0.22	0.21	0.23	0.26
6	0.31	0.26	0.21	0.24	0.22	0.20	0.23	0.22	0.22	0.26
7	0.31	0.26	0.21	0.23	0.21	0.19	0.19	0.20	0.20	0.24
8	0.28	0.27	0.25	0.23	0.21	0.19	0.19	0.21	0.19	0.26
9	0.29	0.23	0.22	0.24	0.21	0.20	0.20	0.20	0.21	0.22
10	0.25	0.22	0.19	0.21	0.18	0.17	0.19	0.18	0.17	0.21
11	0.27	0.20	0.17	0.20	0.18	0.15	0.17	0.20	0.19	0.24
12	0.29	0.27	0.19	0.23	0.17	0.13	0.19	0.22	0.22	0.25
13	0.32	0.24	0.19	0.25	0.20	0.15	0.19	0.18	0.22	0.24
14	0.32	0.23	0.18	0.23	0.23	0.19	0.20	0.21	0.22	0.21
15	0.36	0.24	0.18	0.22	0.20	0.16	0.19	0.22	0.20	0.21
16	0.29	0.24	0.19	0.21	0.21	0.20	0.21	0.21	0.19	0.20
17	0.27	0.26	0.18	0.21	0.17	0.17	0.19	0.23	0.22	0.23
18	0.31	0.22	0.18	0.20	0.16	0.17	0.17	0.17	0.14	0.18
19	0.33	0.21	0.20	0.18	0.19	0.15	0.18	0.18	0.16	0.24
20	0.31	0.23	0.20	0.16	0.19	0.16	0.21	0.19	0.17	0.21
21	0.35	0.22	0.21	0.23	0.19	0.18	0.17	0.17	0.18	0.17
22	0.32	0.27	0.20	0.22	0.22	0.17	0.19	0.20	0.18	0.22
23	0.28	0.23	0.20	0.22	0.19	0.15	0.22	0.22	0.21	0.20
24	0.25	0.21	0.20	0.20	0.16	0.18	0.20	0.23	0.18	0.18
25	0.21	0.18	0.17	0.20	0.16	0.15	0.23	0.21	0.22	0.22
26	0.35	0.19	0.16	0.17	0.13	0.16	0.17	0.15	0.14	0.17
27	0.35	0.20	0.14	0.17	0.19	0.15	0.17	0.15	0.14	0.19
28	0.35	0.24	0.17	0.20	0.21	0.17	0.16	0.17	0.17	0.20
29	0.36	0.29	0.19	0.21	0.18	0.16	0.15	0.18	0.15	0.22
30	0.34	0.25	0.20	0.19	0.17	0.16	0.18	0.18	0.17	0.20
31	0.29	0.23	0.16	0.20	0.16	0.15	0.22	0.24	0.22	0.19
32	0.28	0.20	0.18	0.17	0.16	0.14	0.22	0.24	0.26	0.23
33	0.20	0.24	0.15	0.15	0.18	0.18	0.23	0.24	0.28	0.26
34	0.38	0.22	0.14	0.17	0.13	0.14	0.18	0.15	0.16	0.16
35	0.37	0.23	0.14	0.17	0.14	0.14	0.14	0.15	0.15	0.20
36	0.39	0.36	0.21	0.20	0.18	0.18	0.16	0.17	0.18	0.19
37	0.39	0.36	0.22	0.21	0.18	0.16	0.13	0.17	0.15	0.21
38	0.28	0.32	0.24	0.22	0.19	0.17	0.14	0.19	0.16	0.24
39	0.27	0.19	0.17	0.17	0.15	0.20	0.24	0.26	0.24	0.25
40	0.25	0.17	0.15	0.15	0.20	0.19	0.27	0.32	0.34	0.38
41	0.30	0.17	0.11	0.15	0.22	0.20	0.30	0.32	0.40	0.41
42	0.35	0.22	0.14	0.16	0.12	0.14	0.13	0.15	0.12	0.16
43	0.26	0.21	0.15	0.17	0.17	0.15	0.13	0.12	0.13	0.21
44	0.26	0.18	0.18	0.14	0.22	0.15	0.15	0.12	0.13	0.20
45	0.27	-9.99	-9.99	-9.99	-9.99	-9.99	-9.99	-9.99	-9.99	-9.99
46	0.26	0.26	0.21	0.06	-9.99	-9.99	-9.99	-9.99	-9.99	-9.99
47	0.25	0.25	0.17	0.18	0.17	0.18	0.23	0.25	0.23	0.26
48	0.23	0.17	0.13	0.15	0.17	0.18	0.21	0.30	0.30	0.28
49	0.22	0.15	0.08	0.19	0.15	0.20	0.34	0.31	0.31	0.46

TABLE 6.3 BIN POPULATIONS FOR MIDDLE CLOUD

	SOLAR ZENITH ANGLE RANGE (DEG.)									
	0.0	25.8	36.8	45.5	53.1	59.9	66.4	72.5	78.4	84.3
	25.8	36.8	45.5	53.1	59.9	66.4	72.5	78.4	84.3	90.0
BIN										
1	574	545	611	444	507	739	921	986	961	363
2	63	80	95	70	78	94	142	173	153	48
3	176	156	156	110	121	169	212	228	162	89
4	222	217	198	143	154	220	309	379	314	112
5	216	199	204	149	158	218	332	377	305	146
6	156	250	176	173	146	236	316	363	345	122
7	152	218	201	150	151	202	282	349	306	109
8	112	135	106	90	122	135	204	172	158	72
9	36	75	72	45	49	61	116	134	149	50
10	48	66	55	26	29	38	50	54	52	26
11	87	80	78	74	56	88	129	143	110	46
12	116	108	92	66	75	93	125	167	131	59
13	95	89	128	62	65	111	169	144	128	70
14	97	91	90	62	78	138	144	157	127	75
15	68	90	75	55	66	121	139	201	148	71
16	62	98	94	74	78	113	142	144	133	53
17	20	59	38	31	39	39	55	65	67	26
18	93	86	90	73	99	122	174	155	145	49
19	240	199	139	122	117	156	199	242	170	79
20	276	183	144	101	88	119	173	251	224	81
21	279	259	306	224	173	309	390	328	337	136
22	167	181	196	134	135	257	320	274	304	137
23	95	146	127	110	124	135	226	264	213	104
24	81	146	130	109	99	155	213	261	201	74
25	32	71	90	54	72	95	94	114	129	63
26	116	75	77	58	57	77	94	127	101	35
27	282	145	136	87	89	111	168	228	161	50
28	332	208	129	78	66	93	169	148	149	59
29	246	302	271	200	156	192	248	277	253	109
30	110	120	165	93	95	168	221	224	221	105
31	83	105	103	93	64	99	143	161	138	55
32	79	120	88	71	75	90	139	146	128	68
33	29	34	37	39	40	42	89	85	96	27
34	349	255	199	147	109	162	172	226	152	72
35	859	381	324	220	205	332	377	449	344	166
36	867	430	218	131	69	142	197	304	268	136
37	625	466	389	351	254	262	322	346	304	170
38	251	183	125	130	124	143	186	246	268	171
39	204	251	227	165	123	183	265	293	246	107
40	118	161	203	182	164	221	314	345	382	168
41	52	74	64	76	63	112	142	115	140	51
42	114	162	86	67	51	88	74	79	55	24
43	244	231	184	148	98	182	200	224	185	66
44	130	9	17	26	24	33	70	117	103	76
45	162	0	0	0	0	0	0	0	0	0
46	143	57	24	3	0	0	0	0	0	0
47	121	175	118	92	65	93	114	145	97	45
48	59	72	82	69	81	122	154	173	178	74
49	15	35	33	27	20	41	52	68	76	24

TABLE 7.1 ANISOTROPIC FACTORS FOR HI WTR CLD

	SOLAR ZENITH ANGLE RANGE (DEG.)									
	0.0	25.8	36.8	45.5	53.1	59.9	66.4	72.5	78.4	84.3
	25.8	36.8	45.5	53.1	59.9	66.4	72.5	78.4	84.3	90.0
BIN										
1	1.07	1.00	0.97	0.94	0.93	0.85	0.84	0.78	0.71	0.61
2	1.07	0.96	0.96	0.95	0.94	0.94	0.86	0.79	0.73	0.64
3	1.06	1.00	0.92	0.95	0.91	0.92	0.87	0.79	0.73	0.65
4	1.02	1.01	0.94	0.93	0.94	0.88	0.85	0.77	0.75	0.68
5	1.06	1.05	0.97	0.89	0.94	0.87	0.84	0.81	0.75	0.64
6	1.02	1.00	0.89	0.91	0.94	0.89	0.83	0.82	0.75	0.65
7	1.08	1.03	0.94	0.96	0.94	0.94	0.87	0.81	0.79	0.69
8	1.02	1.06	0.98	0.96	0.94	0.96	0.90	0.84	0.76	0.71
9	1.01	1.03	0.97	0.97	1.01	0.98	0.89	0.82	0.79	0.70
10	1.00	1.02	1.03	0.99	0.92	0.95	0.90	0.84	0.77	0.66
11	1.05	1.09	0.93	1.00	0.97	0.99	0.93	0.86	0.81	0.71
12	1.02	1.06	0.92	0.95	0.97	0.92	0.88	0.84	0.78	0.71
13	1.04	0.96	0.95	1.00	0.92	0.91	0.86	0.80	0.75	0.75
14	0.99	1.00	0.97	0.96	0.94	0.88	0.86	0.85	0.80	0.70
15	1.06	1.01	1.00	1.01	0.99	0.93	0.91	0.89	0.85	0.74
16	1.13	0.95	1.02	1.00	1.03	0.98	0.96	0.92	0.90	0.79
17	0.99	0.97	1.04	1.05	1.00	1.10	1.03	0.98	0.92	0.84
18	1.01	1.00	1.06	1.02	1.07	0.98	0.98	0.92	0.86	0.80
19	1.07	1.01	0.98	1.01	0.95	0.95	0.93	0.88	0.87	0.81
20	1.00	0.95	1.07	0.98	0.95	0.92	0.94	0.87	0.80	0.81
21	1.01	1.02	1.02	0.95	0.92	0.92	0.89	0.85	0.77	0.76
22	0.94	1.08	0.95	0.96	0.97	0.90	0.90	0.86	0.80	0.72
23	1.03	1.07	1.04	1.02	1.00	1.05	1.01	1.04	0.97	0.95
24	1.06	1.03	1.08	1.05	1.11	1.12	1.04	1.06	1.06	1.07
25	1.02	1.07	1.09	1.14	1.10	1.13	1.04	1.16	1.13	1.14
26	1.04	0.94	1.07	1.06	0.98	0.98	1.01	0.97	0.96	0.92
27	1.03	1.03	1.02	1.02	0.97	1.04	0.98	0.97	0.96	0.93
28	0.95	0.94	0.99	0.99	0.96	0.96	0.96	0.96	0.90	0.87
29	0.97	0.97	0.96	0.94	0.91	0.91	0.92	0.87	0.81	0.79
30	0.97	0.99	0.96	0.99	0.91	0.98	0.96	0.90	0.86	0.88
31	1.03	1.09	1.12	1.07	1.11	1.15	1.15	1.22	1.20	1.21
32	1.00	1.07	1.14	1.14	1.18	1.23	1.23	1.30	1.41	1.44
33	0.97	1.09	1.13	1.28	1.28	1.29	1.46	1.39	1.58	1.56
34	0.95	0.98	1.05	0.97	1.07	1.03	1.09	1.15	1.18	1.19
35	0.95	0.98	0.96	0.99	0.97	1.00	1.03	1.09	1.12	1.19
36	0.87	0.84	1.02	0.98	0.98	1.00	1.06	1.06	1.07	1.15
37	0.86	0.80	0.90	0.92	0.90	0.90	0.89	0.92	0.88	0.91
38	0.90	0.97	0.93	0.97	0.91	0.94	0.97	0.97	0.96	1.01
39	1.00	1.03	1.07	1.14	1.19	1.30	1.44	1.62	1.69	1.79
40	0.99	1.09	1.20	1.28	1.36	1.52	1.60	1.83	2.19	2.58
41	0.95	1.06	1.24	1.35	1.45	1.62	1.63	2.24	2.75	3.36
42	0.85	0.87	0.98	0.97	0.99	1.01	1.17	1.26	1.53	1.68
43	0.82	0.86	0.89	0.93	0.98	1.02	1.04	1.17	1.26	1.44
44	0.90	0.00	0.00	0.97	1.03	1.04	1.14	1.11	1.21	1.40
45	0.74	0.00	0.00	0.00	0.00	0.00	0.00	0.00	0.00	0.00
46	0.82	0.80	0.96	0.83	0.00	0.00	0.00	0.00	0.00	0.00
47	0.90	0.99	1.08	1.17	1.19	1.38	1.65	1.81	2.21	2.31
48	1.00	1.00	1.18	1.36	1.57	1.66	1.98	2.36	3.39	4.66
49	0.88	1.20	1.19	1.42	1.82	1.59	1.98	3.04	4.60	5.87

TABLE 7.2 RELATIVE DISPERSIONS FOR HI WTR CLD

	SOLAR ZENITH ANGLE RANGE (DEG.)									
	0.0	25.8	36.8	45.5	53.1	59.9	66.4	72.5	78.4	84.3
	25.8	36.8	45.5	53.1	59.9	66.4	72.5	78.4	84.3	90.0
BIN										
1	0.19	0.14	0.17	0.16	0.12	0.15	0.11	0.11	0.15	0.24
2	0.21	0.23	0.11	0.17	0.13	0.11	0.09	0.11	0.18	0.21
3	0.18	0.15	0.13	0.15	0.11	0.11	0.10	0.11	0.14	0.25
4	0.19	0.17	0.12	0.15	0.13	0.12	0.08	0.11	0.16	0.23
5	0.18	0.14	0.16	0.12	0.15	0.18	0.08	0.11	0.15	0.24
6	0.20	0.18	0.19	0.17	0.14	0.15	0.11	0.09	0.16	0.25
7	0.17	0.19	0.16	0.15	0.13	0.10	0.12	0.14	0.15	0.19
8	0.20	0.13	0.15	0.16	0.08	0.10	0.09	0.14	0.14	0.19
9	0.23	0.12	0.13	0.09	0.10	0.13	0.12	0.13	0.12	0.16
10	0.17	0.11	0.20	0.18	0.09	0.11	0.12	0.04	0.11	0.17
11	0.18	0.15	0.13	0.11	0.15	0.05	0.06	0.13	0.15	0.16
12	0.21	0.13	0.19	0.14	0.11	0.12	0.06	0.11	0.15	0.19
13	0.16	0.17	0.16	0.17	0.16	0.12	0.10	0.10	0.14	0.30
14	0.18	0.12	0.11	0.12	0.17	0.17	0.16	0.13	0.13	0.27
15	0.20	0.14	0.12	0.12	0.13	0.14	0.09	0.09	0.15	0.20
16	0.14	0.13	0.16	0.13	0.09	0.10	0.07	0.14	0.13	0.24
17	0.19	0.20	0.11	0.06	0.12	0.00	0.05	0.07	0.12	0.19
18	0.18	0.11	0.15	0.16	0.11	0.15	0.07	0.12	0.14	0.18
19	0.16	0.14	0.15	0.11	0.14	0.15	0.06	0.14	0.13	0.16
20	0.19	0.17	0.15	0.15	0.12	0.09	0.09	0.14	0.14	0.18
21	0.18	0.13	0.12	0.15	0.12	0.11	0.11	0.10	0.14	0.24
22	0.23	0.10	0.18	0.19	0.12	0.16	0.12	0.14	0.15	0.23
23	0.14	0.12	0.15	0.14	0.13	0.13	0.05	0.10	0.20	0.19
24	0.16	0.14	0.11	0.10	0.08	0.08	0.07	0.14	0.18	0.24
25	0.09	0.16	0.13	0.05	0.09	0.10	0.14	0.10	0.14	0.19
26	0.17	0.13	0.13	0.11	0.11	0.11	0.07	0.07	0.13	0.19
27	0.19	0.13	0.10	0.11	0.10	0.10	0.07	0.10	0.13	0.18
28	0.19	0.14	0.16	0.17	0.18	0.14	0.11	0.12	0.12	0.21
29	0.19	0.17	0.13	0.15	0.14	0.13	0.11	0.10	0.14	0.18
30	0.15	0.13	0.16	0.12	0.14	0.13	0.10	0.12	0.13	0.16
31	0.12	0.07	0.12	0.11	0.13	0.10	0.07	0.15	0.17	0.23
32	0.15	0.08	0.12	0.09	0.12	0.14	0.12	0.13	0.17	0.29
33	0.20	0.13	0.13	0.11	0.17	0.08	0.14	0.22	0.22	0.23
34	0.20	0.13	0.05	0.10	0.14	0.10	0.06	0.13	0.16	0.16
35	0.18	0.11	0.12	0.12	0.13	0.12	0.10	0.12	0.13	0.18
36	0.23	0.21	0.10	0.13	0.12	0.15	0.12	0.14	0.14	0.20
37	0.21	0.20	0.15	0.14	0.12	0.13	0.13	0.09	0.11	0.19
38	0.17	0.16	0.17	0.07	0.13	0.13	0.10	0.11	0.14	0.18
39	0.14	0.11	0.14	0.12	0.15	0.13	0.17	0.17	0.22	0.29
40	0.16	0.11	0.11	0.13	0.12	0.19	0.13	0.18	0.34	0.34
41	0.08	0.09	0.16	0.17	0.15	0.14	0.20	0.29	0.29	0.42
42	0.15	0.15	0.09	0.10	0.10	0.10	0.07	0.11	0.15	0.13
43	0.17	0.18	0.11	0.13	0.14	0.11	0.11	0.15	0.12	0.19
44	0.11	-9.99	-9.99	0.01	0.10	0.15	0.13	0.10	0.17	0.18
45	0.20	-9.99	-9.99	-9.99	-9.99	-9.99	-9.99	-9.99	-9.99	-9.99
46	0.21	0.12	0.00	0.00	-9.99	-9.99	-9.99	-9.99	-9.99	-9.99
47	0.16	0.12	0.11	0.10	0.12	0.08	0.18	0.21	0.19	0.29
48	0.15	0.10	0.10	0.14	0.18	0.10	0.16	0.28	0.37	0.43
49	0.14	0.00	0.06	0.05	0.11	0.02	0.16	0.29	0.21	0.41

TABLE 7.3 BIN POPULATIONS FOR HI WTR CLD

	SOLAR ZENITH ANGLE RANGE (DEG.)									
	0.0	25.8	36.8	45.5	53.1	59.9	66.4	72.5	78.4	84.3
	25.8	36.8	45.5	53.1	59.9	66.4	72.5	78.4	84.3	90.0
BIN										
1	186	75	116	146	146	92	113	252	315	207
2	18	10	17	22	20	17	21	43	46	30
3	59	21	27	23	24	18	33	46	71	48
4	88	29	43	52	41	47	41	74	105	65
5	80	19	32	26	46	30	40	74	115	75
6	80	24	32	37	37	32	37	69	108	62
7	66	19	34	47	52	38	41	79	111	73
8	65	24	35	41	35	15	26	42	74	51
9	13	8	16	13	14	9	10	31	29	25
10	17	2	7	13	11	8	11	13	14	12
11	33	15	11	15	24	8	14	29	49	25
12	41	17	18	22	22	14	15	31	44	26
13	43	19	24	22	30	22	20	56	44	29
14	27	17	25	26	30	19	27	57	45	25
15	21	15	5	21	21	15	24	37	50	35
16	14	11	13	16	18	12	14	28	36	29
17	11	7	17	8	10	2	2	6	19	7
18	24	9	17	27	29	13	16	41	50	42
19	57	28	33	29	30	30	39	59	77	36
20	77	26	21	40	40	20	17	29	56	51
21	89	43	55	85	71	48	83	143	146	90
22	48	17	35	30	54	18	41	98	89	64
23	39	15	26	41	37	22	35	34	54	31
24	26	9	15	23	26	19	23	48	70	56
25	7	14	16	7	19	8	21	30	52	22
26	27	2	10	9	13	12	15	23	38	24
27	61	20	17	29	31	10	24	35	64	52
28	76	25	17	25	32	19	25	35	36	42
29	76	40	50	67	74	56	40	125	102	66
30	19	10	33	37	53	30	54	80	93	87
31	31	10	16	22	27	13	19	32	53	31
32	25	10	17	27	21	14	17	37	68	28
33	8	7	12	9	6	5	7	22	34	24
34	74	29	16	18	24	28	38	59	61	29
35	157	38	71	83	92	55	64	117	115	86
36	100	63	38	23	29	29	33	47	80	49
37	93	54	99	108	104	111	82	141	164	124
38	36	9	11	23	72	43	72	85	108	102
39	78	35	49	80	60	43	33	56	81	48
40	61	34	37	31	55	34	34	63	105	85
41	15	5	12	11	17	10	27	25	44	33
42	20	27	9	13	12	22	8	21	14	12
43	57	29	43	37	32	52	52	49	78	48
44	11	0	0	2	4	15	17	20	38	29
45	9	0	0	0	0	0	0	0	0	0
46	27	11	1	1	0	0	0	0	0	0
47	28	20	28	48	24	18	27	39	29	27
48	13	9	19	20	19	12	16	45	45	49
49	2	1	4	3	8	2	12	19	16	12

TABLE 8.1 ANISOTROPIC FACTORS FOR HI ICE CLD

	SOLAR ZENITH ANGLE RANGE (DEG.)									
	0.0	25.8	36.8	45.5	53.1	59.9	66.4	72.5	78.4	84.3
	25.8	36.8	45.5	53.1	59.9	66.4	72.5	78.4	84.3	90.0
BIN										
1	1.04	1.01	1.00	0.94	0.91	0.88	0.86	0.79	0.73	0.67
2	1.07	1.01	1.03	0.96	0.87	0.90	0.88	0.84	0.77	0.71
3	1.06	1.00	0.98	0.94	0.92	0.91	0.87	0.81	0.75	0.72
4	1.05	1.04	0.96	0.95	0.93	0.92	0.85	0.82	0.76	0.69
5	1.04	1.04	0.95	0.93	0.91	0.92	0.87	0.82	0.76	0.69
6	1.06	1.09	0.98	0.97	0.92	0.92	0.87	0.82	0.76	0.69
7	1.05	1.00	0.99	0.98	0.94	0.96	0.89	0.85	0.81	0.71
8	1.06	1.02	1.00	0.99	0.97	0.96	0.90	0.85	0.80	0.73
9	1.03	0.95	1.04	1.01	1.01	0.96	0.92	0.85	0.81	0.71
10	1.03	0.99	1.01	0.95	0.90	0.95	0.90	0.87	0.83	0.76
11	1.04	1.04	0.97	1.00	0.97	0.92	0.89	0.85	0.82	0.76
12	1.06	1.04	0.95	1.01	0.94	0.93	0.90	0.87	0.81	0.74
13	1.05	1.01	0.96	0.93	0.92	0.93	0.85	0.82	0.75	0.71
14	1.03	1.02	0.98	0.98	1.00	0.95	0.90	0.83	0.77	0.69
15	1.04	1.09	0.99	0.99	0.97	0.95	0.93	0.90	0.87	0.80
16	1.07	1.04	1.02	1.01	0.96	1.00	0.96	0.93	0.86	0.80
17	1.00	1.11	1.02	1.04	1.02	1.01	0.98	0.93	0.90	0.86
18	1.04	0.99	1.07	0.98	1.00	1.04	0.91	0.91	0.90	0.82
19	1.03	1.02	1.02	1.00	0.99	0.97	0.93	0.90	0.86	0.82
20	1.01	0.96	1.03	0.98	0.93	0.88	0.90	0.89	0.86	0.80
21	0.98	1.01	0.94	0.95	0.93	0.90	0.91	0.87	0.79	0.76
22	1.00	0.99	0.96	0.96	0.99	0.96	0.94	0.89	0.82	0.78
23	1.07	1.04	1.08	1.04	1.05	1.03	1.04	1.01	0.97	0.91
24	1.04	1.07	1.10	1.08	1.07	1.06	1.05	1.07	1.04	1.05
25	1.02	1.10	1.04	1.08	1.17	1.13	1.12	1.13	1.10	1.10
26	0.98	0.99	1.03	1.04	1.04	1.04	1.01	0.99	1.00	0.96
27	0.97	0.96	0.97	0.99	0.98	1.00	0.97	0.96	0.95	0.96
28	0.95	0.92	0.98	0.93	0.93	0.92	0.94	0.94	0.93	0.89
29	0.94	0.92	0.94	0.96	0.93	0.94	0.93	0.92	0.87	0.86
30	0.97	0.98	0.94	0.97	1.00	0.97	0.97	0.96	0.91	0.89
31	1.02	1.06	1.10	1.09	1.10	1.08	1.15	1.10	1.08	1.12
32	1.05	1.08	1.13	1.16	1.20	1.23	1.23	1.31	1.32	1.36
33	1.03	1.10	1.15	1.20	1.25	1.31	1.34	1.31	1.43	1.46
34	0.92	0.93	0.95	1.00	1.00	1.04	1.05	1.13	1.19	1.23
35	0.89	0.92	0.96	0.98	1.00	1.01	1.05	1.06	1.12	1.28
36	0.87	0.88	0.92	0.94	0.94	0.91	1.00	1.03	1.11	1.19
37	0.88	0.88	0.94	0.93	0.94	0.94	0.96	0.96	0.94	0.97
38	0.94	0.89	0.95	1.01	1.01	0.98	1.02	1.05	1.03	1.06
39	0.95	1.02	1.04	1.16	1.20	1.24	1.36	1.44	1.55	1.59
40	0.98	1.05	1.15	1.20	1.33	1.49	1.58	1.76	2.00	2.39
41	0.94	1.11	1.15	1.29	1.40	1.58	1.71	2.00	2.84	3.08
42	0.84	0.86	0.91	0.92	0.98	1.02	1.10	1.23	1.42	1.59
43	0.83	0.88	0.90	0.94	0.98	0.96	1.08	1.17	1.33	1.57
44	0.81	0.90	0.94	0.91	0.92	0.97	1.05	1.12	1.30	1.58
45	0.82	0.00	0.00	0.00	0.00	0.00	0.00	0.00	0.00	0.00
46	0.85	0.85	1.01	0.99	0.00	0.00	0.00	0.00	0.00	0.00
47	0.90	0.95	1.05	1.14	1.25	1.29	1.42	1.75	2.04	2.32
48	0.94	1.03	1.16	1.21	1.41	1.73	1.87	2.42	2.99	3.84
49	0.86	1.08	1.09	1.27	1.50	1.86	2.32	2.95	4.42	4.74

TABLE 8.2 RELATIVE DISPERSIONS FOR HI ICE CLD

	SOLAR ZENITH ANGLE RANGE (DEG.)									
	0.0	25.8	36.8	45.5	53.1	59.9	66.4	72.5	78.4	84.3
	25.8	36.8	45.5	53.1	59.9	66.4	72.5	78.4	84.3	90.0
BIN										
1	0.20	0.19	0.14	0.16	0.12	0.13	0.13	0.15	0.17	0.24
2	0.18	0.18	0.13	0.18	0.15	0.11	0.13	0.11	0.16	0.21
3	0.18	0.18	0.15	0.14	0.13	0.13	0.14	0.11	0.15	0.22
4	0.18	0.18	0.18	0.13	0.14	0.11	0.15	0.16	0.15	0.21
5	0.19	0.17	0.16	0.15	0.17	0.12	0.11	0.16	0.16	0.22
6	0.19	0.14	0.14	0.13	0.15	0.13	0.12	0.16	0.17	0.23
7	0.19	0.19	0.13	0.13	0.15	0.10	0.11	0.17	0.15	0.24
8	0.18	0.21	0.15	0.12	0.10	0.12	0.16	0.16	0.15	0.22
9	0.18	0.18	0.10	0.15	0.13	0.12	0.12	0.17	0.17	0.21
10	0.19	0.17	0.14	0.12	0.12	0.12	0.13	0.12	0.10	0.19
11	0.18	0.18	0.12	0.09	0.14	0.13	0.12	0.11	0.14	0.22
12	0.19	0.19	0.17	0.11	0.17	0.12	0.09	0.13	0.15	0.21
13	0.18	0.17	0.15	0.15	0.12	0.09	0.13	0.15	0.15	0.19
14	0.20	0.18	0.17	0.15	0.16	0.11	0.09	0.15	0.16	0.19
15	0.19	0.14	0.13	0.15	0.12	0.11	0.09	0.15	0.14	0.23
16	0.19	0.17	0.12	0.13	0.13	0.13	0.13	0.15	0.17	0.21
17	0.18	0.18	0.10	0.12	0.14	0.13	0.14	0.15	0.13	0.20
18	0.19	0.18	0.10	0.14	0.11	0.08	0.12	0.12	0.11	0.19
19	0.20	0.19	0.11	0.11	0.11	0.10	0.11	0.11	0.13	0.20
20	0.18	0.21	0.13	0.13	0.16	0.12	0.10	0.12	0.16	0.20
21	0.19	0.18	0.14	0.13	0.14	0.13	0.11	0.12	0.14	0.18
22	0.19	0.16	0.16	0.16	0.12	0.12	0.09	0.13	0.17	0.19
23	0.16	0.18	0.12	0.13	0.15	0.10	0.09	0.16	0.15	0.17
24	0.17	0.15	0.10	0.11	0.10	0.13	0.14	0.14	0.14	0.19
25	0.18	0.16	0.16	0.14	0.07	0.10	0.10	0.12	0.12	0.23
26	0.19	0.14	0.10	0.09	0.12	0.08	0.07	0.09	0.09	0.16
27	0.19	0.16	0.14	0.12	0.15	0.09	0.09	0.13	0.13	0.19
28	0.20	0.20	0.13	0.12	0.15	0.13	0.10	0.11	0.14	0.19
29	0.20	0.20	0.17	0.13	0.13	0.12	0.09	0.11	0.13	0.18
30	0.18	0.19	0.16	0.19	0.12	0.10	0.12	0.12	0.15	0.19
31	0.15	0.15	0.11	0.14	0.11	0.13	0.07	0.14	0.17	0.18
32	0.16	0.16	0.10	0.13	0.09	0.10	0.11	0.13	0.17	0.20
33	0.17	0.16	0.10	0.10	0.08	0.12	0.11	0.16	0.17	0.28
34	0.20	0.14	0.10	0.09	0.11	0.13	0.12	0.10	0.13	0.17
35	0.19	0.18	0.10	0.10	0.11	0.10	0.08	0.13	0.14	0.20
36	0.21	0.21	0.15	0.13	0.14	0.13	0.12	0.11	0.14	0.22
37	0.21	0.19	0.15	0.15	0.14	0.13	0.11	0.10	0.12	0.17
38	0.16	0.22	0.18	0.14	0.11	0.12	0.10	0.11	0.14	0.19
39	0.17	0.14	0.13	0.10	0.13	0.11	0.14	0.15	0.22	0.27
40	0.17	0.14	0.12	0.11	0.13	0.15	0.15	0.23	0.32	0.40
41	0.20	0.14	0.14	0.07	0.09	0.12	0.16	0.24	0.41	0.34
42	0.18	0.16	0.09	0.08	0.13	0.13	0.09	0.10	0.14	0.18
43	0.17	0.15	0.13	0.08	0.10	0.10	0.10	0.11	0.14	0.18
44	0.19	0.04	0.02	0.16	0.12	0.10	0.09	0.11	0.13	0.20
45	0.18	-9.99	-9.99	-9.99	-9.99	-9.99	-9.99	-9.99	-9.99	-9.99
46	0.17	0.18	0.10	0.00	-9.99	-9.99	-9.99	-9.99	-9.99	-9.99
47	0.18	0.13	0.12	0.11	0.13	0.14	0.14	0.16	0.20	0.29
48	0.14	0.11	0.09	0.13	0.15	0.12	0.15	0.27	0.37	0.42
49	0.22	0.19	0.11	0.10	0.07	0.08	0.18	0.26	0.31	0.35

TABLE 8.3 BIN POPULATIONS FOR HI ICE CLD

	SOLAR ZENITH ANGLE RANGE (DEG.)									
	0.0	25.8	36.8	45.5	53.1	59.9	66.4	72.5	78.4	84.3
	25.8	36.8	45.5	53.1	59.9	66.4	72.5	78.4	84.3	90.0
BIN										
1	1241	267	194	162	181	196	285	450	870	863
2	147	39	25	27	25	47	43	55	120	130
3	376	91	59	51	51	50	76	130	224	240
4	492	96	69	54	67	64	80	179	269	266
5	506	97	73	62	74	68	100	188	303	281
6	446	100	56	61	66	87	84	183	309	283
7	423	106	63	50	52	61	58	143	258	240
8	279	67	43	37	40	42	54	108	193	213
9	102	26	21	16	18	27	37	62	103	92
10	106	31	22	18	16	16	25	22	54	69
11	215	46	26	29	35	31	42	76	131	132
12	299	59	21	37	22	28	33	107	155	118
13	253	64	39	23	23	30	42	73	143	126
14	207	63	33	36	40	27	38	95	177	126
15	215	30	25	29	36	34	30	62	139	119
16	139	45	22	29	29	37	52	73	135	154
17	63	22	16	10	15	11	19	31	66	63
18	209	52	27	27	24	34	44	76	137	167
19	487	93	57	56	48	47	55	118	192	198
20	681	123	54	68	52	46	67	91	163	192
21	485	201	91	136	110	118	140	245	404	346
22	406	108	89	71	74	80	69	178	298	280
23	242	73	34	49	49	59	52	101	168	169
24	231	80	64	50	39	58	68	109	215	184
25	92	36	25	29	24	26	46	70	149	144
26	217	45	26	31	19	27	37	47	110	112
27	461	80	49	40	41	30	47	91	163	139
28	590	135	55	44	49	39	64	64	74	123
29	405	202	120	145	93	80	123	186	290	292
30	217	89	62	76	64	63	109	157	265	189
31	206	70	38	47	49	29	27	63	95	113
32	168	36	32	31	30	26	35	78	151	123
33	59	29	22	18	14	29	20	56	119	98
34	482	194	75	52	56	62	64	117	213	157
35	1184	212	138	132	110	77	124	175	323	351
36	923	259	93	91	79	96	124	143	179	178
37	591	279	225	217	233	204	215	290	421	384
38	324	90	76	67	105	96	156	153	372	266
39	444	177	96	107	82	52	97	128	187	214
40	274	115	91	62	65	68	96	194	324	273
41	96	48	39	26	37	28	50	95	145	187
42	138	127	30	26	18	32	34	68	98	91
43	414	95	76	76	72	70	76	90	173	173
44	170	3	4	26	25	30	45	68	85	75
45	138	0	0	0	0	0	0	0	0	0
46	183	49	11	1	0	0	0	0	0	0
47	198	92	53	49	50	48	50	79	112	71
48	134	36	19	44	22	28	41	87	203	163
49	30	21	17	12	7	10	19	48	91	119

Appendix A

(Copy of article publ. in Journal of Geophysical Research, June 1984)

REFLECTANCE CHARACTERISTICS OF UNIFORM EARTH AND CLOUD SURFACES DERIVED FROM NIMBUS-7 ERB

by

V. Ray Taylor and Larry L. Stowe

NOAA / National Earth Satellite Service
Washington, D. C. 20233

April 4, 1983

ABSTRACT

Data from the scanning channels of the Nimbus-7 Earth Radiation Budget (ERB) experiment are combined with other data on Earth surface conditions and cloudiness. Patterns of bi-directional reflectance are constructed from these data for uniform Earth and cloud surfaces. Examples are shown that illustrate the bi-directional properties of surfaces and how these properties vary with solar zenith angle (SZA). Dependence of albedo on SZA is also shown. Conclusions may be summarized as follows: (1) Water surfaces exhibit limb brightening at all SZAs; (2) Cloud and land surfaces change from limb darkening to brightening as SZA increases; (3) The land surface exhibits higher backward reflection for SZAs less than about 50°; (4) All of the surfaces in this study become more specular as SZA increases; (5) Snow is the most nearly isotropic of these surfaces; (6) Snow albedo shows very little variation with SZA and even shows a slight decrease over a limited range; (7) Albedo generally increases with increasing SZA for other than snow surfaces; (8) Angular patterns for high water and ice clouds are quite similar, but ice clouds are more nearly isotropic; (9) The angular patterns developed in this study are in qualitative agreement with those from other investigations.

1. Introduction

An accurate measurement of the Earth's radiation budget may be possible because of the availability of large quantities of high quality satellite radiation data. Satellite borne, scanning, narrow field-of-view instruments routinely measure the radiation from Earth and cloud surfaces. These measurements are usually confined to certain local times and specific directions of view, depending on orbital and instrumental limitations. If one knew the angular dependence of reflected and emitted radiation from an identifiable surface, the total outgoing flux at the top of the atmosphere in all directions could be inferred from a single observation [Raschke et al., 1973]. As a result, it has been increasingly important to understand the angular dependence of reflected and emitted radiation from Earth and cloud surfaces, including the effects of the intervening atmosphere. Development of angular models to describe this dependence is one of the objectives of the Earth Radiation Budget experiment (ERB) on the Nimbus-7 satellite.

A limitation of early reflectance models was the lack of sufficient quantities of data that were representative of a wide range of viewing angles and illumination conditions. More recently and especially for models based on satellite data, it has been difficult to associate radiance measurements with specific surface types. Models such as those developed by Arking [1965] and Ruff et al. [1968] used radiation thresholding in order to identify predominantly cloudy and clear scenes. Other models for more specific surface types were made by aiming balloon or aircraft borne instruments at certain surfaces or by separately associating scanned measurements with visual or photographic observations. For an example of such models see Salomonson and Marlatt [1968], Bartram [1968] and Brennen and Bandeen [1970]. Davis and Cox [1981] have developed models for several different surface types based on data gathered from high altitude aircraft. These should be very useful in spanning the gap between local and limited studies and the spaceview global observations that are possible from satellites.

The advantage of using satellite data such as those from the Nimbus-7 ERB is that a large data base can be accumulated that covers the entire Earth for an extended period of time. Most naturally and commonly occurring surface types can be viewed under a wide range of viewing, illumination and seasonal conditions. The ERB instrument and its scanning characteristics were specifically designed to yield data of the quantity and quality necessary to develop a comprehensive set of angular reflectance and emission models. Some preliminary results have been described in Stowe et al. [1980a] and Stowe and Taylor [1981].

Thus far our study has been restricted to eight uniform surface types (land, water, snow, ice; low, middle, high water and high ice clouds). The amount of data used in this study (61 days) is only a fraction of the total data base (388 days) that may ultimately be available. However, when compared with preliminary results based on smaller samples, it seems that a further increase in sample size will not appreciably change the appearance of the models. In the 61 day composite, land, snow and ice surfaces are sampled sparsely in a few solar zenith angle (SZA) ranges. These may be filled in somewhat by the addition of more data. However, the combination of Nimbus orbit characteristics and geographical distribution of these surface types will always cause some sampling limitations. It will ultimately be possible, with additional data, to analyze more specifically defined uniform or mixed type surfaces. For example, various partly cloudy scenes may be examined or land may be separated into desert, tundra, grasslands, etc. This will be done by

more fully utilizing the topographical and geographical information on the ERB Sub-Target Radiance (STR) tapes [Stowe et al., 1980b].

A brief explanation of the ERB instrument and the STR data base is given next. Samples of reflectance patterns and a discussion of analysis proceedures follow. Included is a comparison of characteristics based upon illumination and viewing conditions as well as surface type. Also shown and discussed is the changing relationship between surface albedo and illumination angle for different surfaces. Albedo is an important climatological parameter and its dependence on solar zenith angle is needed for the computation of a daily average radiation budget [Raschke et al., 1973].

Our main purpose is to describe the results of our study and to suggest possibilities for the use of a new, large and comprehensive data base. We have not included an exhaustive comparison with theory or with previously developed models based on other types of data. However, references to these are included to clarify the interpretation of our results.

2. The Data Base

The ERB experiment is equipped with a bi-axial scanning set of four telescopes [Jacobowitz et al., 1978]. A pair of detectors shares each telescope and senses broad band visible (0.2 - 4.5 μm) and infrared (4 - 50 μm) radiation separately. The scan rate is variable and results in a field-of-view that ranges from (90 km.)^2 at nadir to about (250 km.)^2 at the horizon. By utilizing one of five pre-programmed scanning modes, the instrument is capable of sampling approximately 80% of the Earth's viewable disc in just under four minutes. During this time interval about 1700 observations of reflected and emitted radiation are recorded on magnetic tape and subsequently transmitted to a NASA ground station. Data for each day are formatted onto a Master Archive Tape.

Further processing is done at the National Earth Satellite Service (NESS) on an IBM 360-195. Each radiance pair is located in one of 18630 regions of approximately (160 km.)^2 into which the entire Earth surface has been divided. Radiance data within each of these 'Sub-Target Areas' (STAs) is identified with (1) SZA and azimuth angle relative to north; (2) satellite zenith angle and azimuth angle of the satellite measured clockwise from the sun direction (see Fig. 1). (3) amounts and types of surfaces in the STA; (4) the fraction (9ths) of the FOV that lies in the STA; and (5) telescope number (one of four).

Surface type is determined by processing information from other sources. Cloudiness associated with each STA is determined for a time within 10 minutes of the ERB observation by analysis of data from the Nimbus-7 Temperature-Humidity Infrared Radiometer (THIR). THIR 11 μm equivalent black-body temperatures are located in each STA. Resolution is 7 km. at nadir, yielding up to 600 observations per STA. Temperatures are compared with climatological values [Crutcher and Meserve, 1970 and Jenne et al., 1974] at altitude boundaries typically separating the surface and low, middle and high clouds [International Cloud Atlas, 1956]. The fraction of clear area and of each cloud type is then computed for each STA viewed by THIR. A distinction is made between high water and high ice clouds based on the mean cloud temperature. If that temperature is below 240° K, the cloud is assumed

to be composed predominantly of ice crystals [Mason, 1962]. Accuracy of the cloud estimates has been evaluated by Stowe [1982]. It was concluded that, except for land areas at night (frequently misidentified as cloud), the cloud amounts are accurate to 10 - 20%. Low cloud amount was the most difficult to estimate accurately. A simultaneous measure of reflected radiation, which could have confirmed the presence of low cloud, was unfortunately absent from the THIR instrument.

Climatological information specifying fractions of terrain and vegetation types is given for each ERB target area (3 x 3 array of STAs). These data are taken from a geographical atlas [James, 1951].

For each STA the fraction of land, water, snow and ice is given for a time within 24 hours of the ERB observations. This information is determined by the U. S. Air Force in support of their 3-D nephanalysis program [Fye, 1978]. This was the only available data set with snow/ice information in digitized form at the time of this study. These snow and ice amounts agree favorably with analyses done at the National Meteorological Center (NMC), particularly in those SZA ranges for which we derive reflectance patterns. Snow and ice are restricted respectively to land and water surfaces.

The final sorted and merged compilation of the above information is termed the ERB Sub-Target Radiance tape (STR). About 9 days of STR data can be stored on one 6250 bpi tape.

3. Construction and Analysis of Reflectance Patterns

Patterns of bi-directional reflectance were derived by combining appropriate STR data from 61 days of the period Nov. 17, 1978 to Sept. 12, 1979. These STR tapes were the first processed and were well distributed over the first year of ERB measurements. This provided the largest possible range of SZA. Data were sorted into one of eight uniform types only if 8/9 or more of the FOV was contained in an STA covered by more than 95% of that surface type. They were further divided into ten equal ranges in the cosine of the SZA.

In the STR data base, each radiance pair is identified with one of 389 discrete angular intervals (bins). Each bin measures about 15° in relative azimuth and 6° in satellite zenith angle (θ and ϕ, repectively in Fig. 1). To reduce the need for interpolation to fill unsampled bins within each SZA range, the original 389 bins were condensed into an 85 bin array. The azimuth dimension of most bins in this array is 30° with somewhat higher resolution (21° and 18°) near and at the principal plane. The zenith angle interval is 12° for all bins except the central bin which is 15° in radius (360° azimuth) and the outer ring of bins which covers a 15° interval. Initial studies with limited data showed no evidence of asymmetry about the 0 - 180° plane. Therefore, to increase the population of sparsely sampled bins, the array halves on either side of the principal plane were combined, yielding 49 unique bins.

For all of the polar diagrams discussed in sec. 4, less than 3% of the bins were unsampled and required interpolation. Such occurrences were almost always near azimuths 90° and 270° and were more frequent at larger SZAs. They are due to a

design limitation of the ERB instrument scanning pattern. Otherwise, the total populations were relatively well distributed among the individual bins. Even some very small total populations (for example, fig. 4b) yielded coherent and reasonable, though noisier, patterns.

For display purposes it was found that smoother appearing contours resulted from a transformation back to the original 389 bin array. This was accomplished by using second order Lagrangian interpolation.

Prior to averaging within the angular bins, each visible radiance is normalized to a vertically incident sun (divided by cosine of the SZA) at mean Earth-Sun distance. In addition to averaging, the standard deviation and relative dispersion of the radiance are computed for each bin. The relative dispersion is computed by dividing each standard deviation by the bin average. It is expressed as a percentage and is a measure of variability of radiance within each bin.

The variability in each angular bin is most probably the result of the following effects: (1) errors of scene identification; (2) mixing of scene types due to 8/9 FOV matching and 95% scene uniformity criteria; (3) natural variability of surfaces such as variations in optical depth of clouds or changes in land surfaces due to precipitation and seasonal vegetation cycles. With the exception of the low cloud surface, we do not believe these effects seriously compromise the quality of our results. The reflectance patterns, in general, are realistic in shape and vary smoothly with changes in viewing and solar illumination conditions. Resultant albedos are also within expected limits and vary smoothly with changing SZA.

Angular patterns, some of which are described in sec. 4, were constructed for each surface type and SZA range. Each pattern has been displayed as a polar diagram with the radial coordinate representing the satellite zenith angle and the azimuthal coordinate representing the relative azimuth between the satellite and the sun. The sun lies along the 0° azimuth line at a distance from the center corresponding to the SZA. The values in the vicinity of 0° azimuth represent 'backscatter' as compared with 'forward scatter' near 180° azimuth. The angular bin average radiances are converted to anisotropic reflectance factors, $f(\theta,\phi)$, following the approach of Rashcke et al. [1973]. These factors are defined as:

$$f(\theta',\phi') = \pi R(\theta',\phi') \Big/ \int_0^{2\pi}\int_0^{\pi/2} R(\theta,\phi)\cos\theta\sin\theta\, d\theta\, d\phi \qquad (1)$$

where, $R(\theta',\phi')$ is the average of radiances in an angular bin centered at θ' and ϕ'. The numerator is the radiant exitance for an isotropic surface. The denominator is the actual radiant exitance computed from a numerical integration (trapazoidal rule) of bin averages.

The anisotropic factors are plotted and contoured by objective analysis routines available in the NESS computer system. The contour labeled 1.0 represents the angles at which the isotropic assumption gives the correct radiant exitance. Any departure from 1.0 represents the fractional error that would be made if the radiance at that location were used to estimate total outgoing flux by applying the isotropic assumption. For example, a radiance on the 1.5 isopleth would overestimate total outgoing flux by 50% if isotropy were assumed. Areas are clear or stippled (lined or crosshatched) when the anisotropic factor is greater (less) than one. To conserve space, each pattern shown will consist of a pair of matched

'half' patterns from two SZA ranges. At the bottom left and right of each angular diagram the integrated flux (integral) and effective isotropic radiance (integral/pi) are shown. Also given are the population of radiance observations and the SZA range in which the data were selected. The albedo is defined as the ratio of the outgoing flux over the upwelling hemisphere (integral) to a solar constant of 1376 watts/m [Hickey et al., 1980].

4. Individual Reflectance Patterns

Only selected individual patterns will be shown to illustrate the more important characteristics of each surface type. The entire set will be published later as part of an atlas. Figures 2a and 2b show relative reflectance patterns over water for SZA ranges 0 - 26°and 26 - 37°, respectively. In fig. 2a, the reflectance increases as the water surface is viewed at larger zenith angles (limb brightening). This is observed for all SZA ranges and is the result of atmospheric scattering over the relatively dark ocean background. The bright area near the lower center of the diagram is a result of specular reflection (sun glint) from the water.

Each anisotropic value is a mean within an angular bin and is composed of individual observations both larger and smaller than the mean value. Relative dispersions for water are large and themselves highly variable between bins at all SZAs. Values typically range between 30 and 90%. These are larger than for other surfaces because of the low reflectance values of water. Misclassification of cloudiness or other bright surfaces will have a larger effect on the relative dispersions of surfaces with low albedo. The large variability for water is not thought to be due to insufficient populations or to sampling deficiencies, since the patterns vary in a consistent manner as the SZA changes. Also, the variability did not change appreciably for smaller subsets of the 61-day data set.

In fig. 2b as the sun moves toward the horizon, the glint area correspondingly shifts. Note the tendency for other areas to become darker, compensating for the brightening of the glint area, since the anisotropic factors are normalized quantities. As SZA increases, the horizon area near azimuths 90° and 270° becomes sparsely sampled as previously discussed. Thus, even with ample total populations, occasional interpolation in those regions is necessary. This causes some of the irregularities that are observed. Irregularities at other azimuths and some of the small scale 'waviness' of the contours are artifacts of the objective analysis proceedures.

Figs. 3a and 3b show the patterns over water for SZA ranges 37 - 46°and 46 - 53°, respectively. The maximum anisotropic factors continue to increase and to move opposite the sun. The maximum value of radiance increases from over 2 times the effective isotropic value in fig. 3a to nearly 3 times that value in fig. 3b. It will also be noticed that the area of maximum values seems to be merging with a maximum that forms near the horizon. The maximum values are located closer to the horizon than would be expected for simple specular reflection from a flat surface. This is caused by waves on the ocean surface as shown by the theoretical calculations of Plass et al. [1975 and 1976]. Similar changes also are observed for water at the remaining, larger SZA ranges.

Uniform water surfaces occur less frequently at high values of SZA, since the Nimbus-7 satellite views this condition only in relatively high-latitude regions. For these ranges, some irregularity due to decreased population occurs. Two ranges covering SZAs of 60 - 66° and 84 -90° are shown in figs. 4a and 4b. At these low sun angles, the specular reflection at the horizon becomes very intense, reaching values greater than 7. In this region, of course, individual observations could represent values that are much greater than this.

Figs. 5a and 5b are samples of reflectance patterns over land for SZA between 0 - 26° and 60 - 66°. The pattern in Fig. 5a is relatively flat and most values are near 1.0 (isotropic). This is typical for all other Earth surfaces in this study at these low SZAs. For SZAs from 0 - 60° it was seen that water scattered and reflected most of the available energy in the forward direction. Land, on the other hand, at those same SZAs is predominantly a 'backscatterer'. This has also been demonstrated by others, e.g. in the laboratory by Coulson et al. [1966]. As the SZA increases, land gradually becomes more strongly forward scattering, and at SZA of 60 - 66° yields the pattern seen in Fig. 5b. ERB is unable to observe clear land areas at SZAs greater than about 70°. This is because such land areas are necessarily at high latitudes due to the noon sun-synchronous orbit. Land in these regions is predominantly covered either by snow or cloudiness. We presume the trend to strong forward scattering would continue as the sun moved to the horizon, consistent with laboratory measurements.

The relative dispersions for land are in the range of 20 - 45%. Land, when considered as a single type, may be quite non-uniform. The resultant patterns and the relative dispersions will depend largely on the particular mix of land types that may have been sampled in any given SZA range. We await the availability of a larger data sample to analyze more specific land types.

Broad uniform snow surfaces are confined to higher latitudes and do not exist where the SZA is small. Hence we have no patterns for snow at SZAs less than 45°. Snow areas in mountainous regions at low latitudes are not extensive nor uniform enough to fit the definitions used in this study. Fig. 6a shows how nearly isotropic uniform snow surfaces are at SZAs up to 66°. At greater SZAs snow becomes strongly forward scattering as shown in Fig. 6b. This pattern qualitatively resembles those for all other uniform surfaces at large SZAs. The relative dispersions for snow are only 10 - 20%, among the lowest of the Earth and cloud surfaces we have studied. Uniform snow surfaces are observed mostly from the Antarctic and Greenland icecaps. In such regions adjacent fields-of-view are unlikely to contain any surface type but snow, and mislocations or misidentification of surfaces will add little, if any, variability.

Patterns for sea ice are very similar to snow at all available SZAs and as a result are not shown. Although similar in pattern, albedos for sea ice are consistently lower. This will be described in the following section.

Reflectance patterns for the four uniform cloud types (low, middle, high water, and high ice) are similar to each other and show similar variations with changing SZA. Figs. 7a and 7b for middle cloud at 0 - 26° and 84 - 90°, respectively, will be used to illustrate a few characteristics of cloud patterns in general. Whereas water (disregarding sunglint) shows limb brightening at low SZAs, clouds show limb darkening (Fig. 7a). That is, they appear significantly brighter when viewed from overhead than when viewed near the horizon. This effect is also clearly shown in the theoretical model calculations of Davies [1980]. As the SZA increases, the limb

darkening gradually diminishes. Clouds become quite isotropic in the middle SZA ranges and at large SZAs (Fig. 7b) become limb brightened with enhanced reflection in the specular region. As cloud altitude increases, the bi-directional reflectance patterns become gradually more isotropic and tend to resemble snow patterns. Higher clouds contain increasing amounts of ice particles and in this regard physically resemble snow. The relative dispersions are much higher than for snow, however, due to inhomogeneities in the cloud as well as increased possibilities for misidentifications and FOV-STA mismatches. Values of relative dispersion for middle clouds typically range between 15 and 35% and are somewhat lower for high clouds, between 10 and 20%.

5. A Comparison of Albedos

The observed variation of albedo as a function of the cosine of SZA for the eight uniform surfaces is shown in figs. 8 and 9. The first of these shows plots of the albedo for the four cloudless Earth surfaces. Also shown are ocean, snow and cloud-land curves that were used in conjunction with Nimbus-3 ERB data for calculation of the Earth's radiation budget [Raschke et al., 1973]. These Nimbus-3 normalized models were arbitrarily scaled to provide the best fit to the ERB albedo curves. The curves from Nimbus-3 are not based upon a very extensive set of observations and are presented here only to compare the ERB curves with what has been used previously in satellite radiation budget experiments. In general the two sets of curves are similar.

Variations in the observed albedo for land are probably caused by the tendency for land types of different albedos to be stratified by latitude and thus also by SZA range. We know, for example, that the North African desert region, being a vast, uniform, generally cloud-free area, must dominate the lower and middle SZAs. At somewhat larger SZAs heavily vegetated regions may be predominant. The land albedo appears to increase very slowly, whereas ocean values rise more rapidly with increasing SZA. Land and water albedos appear nearly equal at SZA between 66° and 73°. At larger SZAs, ocean surfaces may actually reflect more energy than land surfaces. These albedos are based upon measurements above the top of the atmosphere. Thus for water the observed albedo at vertical incidence is near 9% rather than 2 - 3%, the latter having been measured experimentally just above water surfaces [Kondratyev, 1972].

Theoretical calculations by Warren [1982] indicate that some decrease in snow albedo may be expected for SZAs greater than about 70°. This decrease is due to increased atmospheric attenuation of the incoming solar beam. A slight decrease is seen in the ERB snow curve over a larger range of SZA and no decrease is indicated by the Nimbus-3 curve. Overall the changes with SZA are very small and this is in agreement with the theoretical calculations cited.

The ice albedo curve parallels that for snow very closely, but values are lower by 10 - 20%. This may be due to the effects of small unresolved open water areas, some surface melting, and perhaps shadowing associated with a generally rougher texture. These conditions are consistent with relative dispersions that are larger for ice than snow.

Fig. 9 shows the albedo-SZA relationship for the four cloud surfaces we have defined. A normalized 'cloud-land' curve from the previously mentioned Nimbus-3 work is included in the diagram for comparison. It has been arbitrarily scaled to an albedo of 45% for an overhead sun to lie approximately midway between the cloud curves. Because of the way clouds are defined, higher clouds are colder and probably have greater optical thickness. They are clearly observed to be more reflective than lower, warmer clouds. Also, the albedo for high clouds may be greater because less atmosphere lies between the cloud tops and the detector, thereby reducing the attenuation by water vapor in the near infrared.

An increase in albedo with SZA is seen for all four cloud types. Such an increase is also predicted by the calculations of Plass and Kattawar [1968]. Except for low clouds at small SZA, the observed increase in albedo is smaller than indicated by the Nimbus-3 model.

The albedos determined for low clouds at small SZAs are unrealistically low. For example, Liou and Wittman [1979] show albedos of not less than 25% for low clouds at small SZA. This discrepancy is partly caused by the THIR cloud detection algorithm, which is least sensitive to low clouds. Since these occur most frequently over oceans, any error in low cloud detection will significantly lower the albedo. At larger SZAs beyond 45°, however, the low cloud albedos are reasonable. We know of no reason why the accuracy of the infrared detection scheme for low clouds should vary with SZA.

6. Conclusions and Future Studies

Conclusions may be summarized as follows: (1) Water surfaces exhibit limb brightening at all SZAs; (2) Cloud and land surfaces change from limb darkening to brightening as SZA increases; (3) The land surface exhibits higher backward reflection for SZAs less than about 50°; (4) All of the surfaces in this study become more specular as SZA increases; (5) Snow is the most nearly isotropic of these surfaces; (6) Snow albedo shows very little variation with SZA and even shows a slight decrease over a limited range; (7) Albedo generally increases with increasing SZA for other than snow surfaces; (8) Angular patterns for high water and ice clouds are quite similar, but ice clouds are more nearly isotropic; (9) The angular patterns developed in this study are in qualitative agreement with those from other investigations.

The ERB-7 Sub-Target Radiance Tape is to date the most comprehensive set of information available for the study of reflection and emission properties of the Earth/atmosphere system. This data set will be used to continue the study of the emission properties of these same surfaces [Stowe and Taylor, 1981]. A complete atlas of reflectance and emittance patterns for all eight surfaces mentioned in this study will be prepared. Eventually, the radiation properties of broken cloud fields and specific Earth surface types will be derived from this data base.

The complete set of as many as 388 days of ERB Sub-Target Radiance tapes is now projected to be available in 1983. These will probably be archived at NASA / National Space Science Data Center, Greenbelt, Md.

REFERENCES

1. Arking, A.: The Angular Distribution of Scattered Radiation and The Earth Albedo as Observed from TIROS. Goddard Institute for Space Studies, Annual Research Report, 46-67, June, 1965.

2. Bartram, F. L.: Earth Reflectance Patterns Measured by Radiometer on High Altitude Balloon Flights. Tech. Rept. 05863-13-T, 15pp., 1968.

3. Brennan, B. and W. R. Bandeen: Anisotropic Reflectance Characteristics of Natural Earth Surfaces, Applied Optics, No. 9, pp. 405-412., 1970.

4. Coulson, K. L., E. L. Gray and G. M. B. Bouricius: Effect of Surface Reflection on Planetary Albedo, Icarus, New York, 5(2) pp. 139-148, March, 1966.

5. Crutcher, M. L. and J. M. Meserve: Selected Level Heights, Temperatures and Dew Points for the Northern Hemisphere, NAVAIR 50-1C-52, U. S. Navy, 1970.

6. Davies, R.: Fast Azimuthally Dependent Model of the Reflection of Solar Radiation by Plane-parallel Clouds, Applied Optics, Vol. 19 No. 2, 15 Jan. 1980.

7. Davis, J. M. and S. K. Cox: Regional Properties of Angular Reflectance Models. Atmos. Sci. Paper No. 338, Colorado State University, Ft. Collins, Colo., 1981.

8. Fye, F. K.: The AFGWC Automated Cloud Analysis Model, AFGWC Tech. Memo 78-002, HQ AFGWC, Offutt AFB, Nebraska, 97 pp., 1978.

9. Hickey, J. R., L. L. Stowe, H. Jacobowitz, P. Pelligrino, R. H. Maschoff, F. House and T. H. Vonder Haar: Solar Parameter Measurements from Nimbus Satellites and Other Solar Constant Experiments, Science, Vol. 208, pp. 281-283, April 1980.

10. International Cloud Atlas, Vol. 1, WMO 195, Geneva, Switzerland.

11. Jacobowitz, H., L. L. Stowe, J. R. Hickey: The Nimbus-7 Users Guide, NASA, Goddard Space Flight Center, Greenbelt, Md., pp. 33-69, 1978.

12. James, P. E.: A Geography of Man, Ginn and Co., New York, N. Y., 631 pp., 1951.

13. Jenne, R. L., H. L. Crutcher, H. Van Loon and J. J. Taljaard: A Selected Climatology of the Southern Hemisphere: Computer Methods and Data Availability, NCAR-TN/STR-92, Boulder, Colo., 91 pp., 1974.

14. Kondratyev, K. Ya, Radiation Processes in the Atmosphere, W. M. O. No. 309, 1972.

15. Liou, K. N. and G. D. Wittman: Parameterization of the Radiative Properties of Clouds, J. Atmos. Sci., 36, pp. 1261-1273, 1979.

16. Mason, B. J., Clouds, Rain and Rainmaking, Cambridge University Press, London, 1962.

17. Plass, G. N. and G. W. Kattawar: Monte Carlo Calculations of Light Scattering From Clouds, Applied Optics, Vol. 7 No. 3, pp.415-419, 1968.

18. Plass, G. N., G. W. Kattawar and J. A. Guinn, Jr.: Radiative Transfer in the Earth's Atmosphere and Ocean, Applied Optics, Vol. 14 No. 8, pp. 1924-1936, 1975.

19. Plass, G. N., G. W. Kattawar and J. A. Guinn, Jr.: Radiance Distribution Over a Ruffled Sea, Applied Optics, Vol. 15 No. 12, Dec., 1976.

20. Raschke, E., T. H. Vonder Haar, M. Pasternak and W. R. Bandeen: The Radiation Balance of the Earth-Atmosphere System from Nimbus-3 Radiation Measurements, NASA TN D-7249, Goddard Space Flight Center, Greenbelt, Md., 73 pp., 1973.

21. Ruff, I. R., R. Koffler, S. Fritz, J. S. Winston and P. K. Rao: Angular Distribution of Solar Radiation Reflected from Clouds as Determined from TIROS-IV Radiation Measurements, J. Atmos. Sci. 25, 323-332, 1968.

22. Salomonson, V. V., and W. E. Marlatt: Atmospheric Solar Reflectance over White Sand, Snow and Stratus Clouds. Atmos. Sci. Paper No. 120, Colorado State University, Ft. Collins, Colo., 41 pp., 1968.

23. Stowe, L. L., H. Jacobowitz and V. R. Taylor: Reflectance Characteristics of Earth and Cloud Surfaces as Measured by the ERB Scanning Channels on the Nimbus-7 Satellite. Proceedings, International Radiation Symposium, Aug. 11-16, Ft. Collins, Colo., pp. 430-432, 1980a.

24. Stowe, L. L., V. R. Taylor, H. Jacobowitz, I. Ruff, E. Baldwin, F. Van Cleef, M. Hill and D. Coleman: A Unique Data Base for Studying Reflectance and Emittance Characteristics of Earth and Cloud Surfaces. Proceedings, International Radiation Symposium, Ft. Collins, Colo., pp. 413-415, Aug. 11-16, 1980b.

25. Stowe, L. L. and V. R. Taylor: Emission Characteristics of Earth and Cloud Surfaces as Measured by the ERB Scanning Channels on the Nimbus-7 Satellite. Preprint, Fourth Conference on Atmospheric Radiation, Toronto, Canada, June 16-18, 1981.

26. Stowe, L. L.: Validation of Nimbus-7 Temperature-Humidity Infrared Radiometer Estimates of Cloud Type and Amount, Advances in Geophysics, Submitted for publication, 1982.

27. Warren, S. G.: Optical Properties of Snow, Reviews of Geophysics and Space Physics, Vol. 20, no. 1, pp. 67-89, Feb. 1982.

Figure Legends

Fig. 1 Geometry of a reflected (scattered) ray of visible radiation.

Fig. 2 Reflectance patterns for water at solar zenith angles (a) 0 - 26° and (b) 26 - 37°.

Fig. 3 Reflectance patterns for water at solar zenith angles (a) 37 - 46° and (b) 46 - 53°.

Fig. 4 Reflectance patterns for water at solar zenith angles (a) 60 - 66° and (b) 84 - 90°.

Fig. 5 Reflectance patterns for land at solar zenith angles (a) 0 - 26° and (b) 60 - 66°.

Fig. 6 Reflectance patterns for snow at solar zenith angles (a) 60 - 66° and (b) 84 - 90°.

Fig. 7 Reflectance patterns for middle cloud at solar zenith angles (a) 0 - 26° and (b) 84 - 90°.

Fig. 8 Albedo as a function of solar zenith angle for ERB cloud-free uniform surfaces (solid) and corresponding Nimbus-3 model curves (dashed) taken from Raschke et al. [1973].

Fig. 9 Albedo as a function of solar zenith angle for ERB uniform cloud surfaces (solid) and the Nimbus-3 cloud curve (dashed) from Raschke et al. [1973].

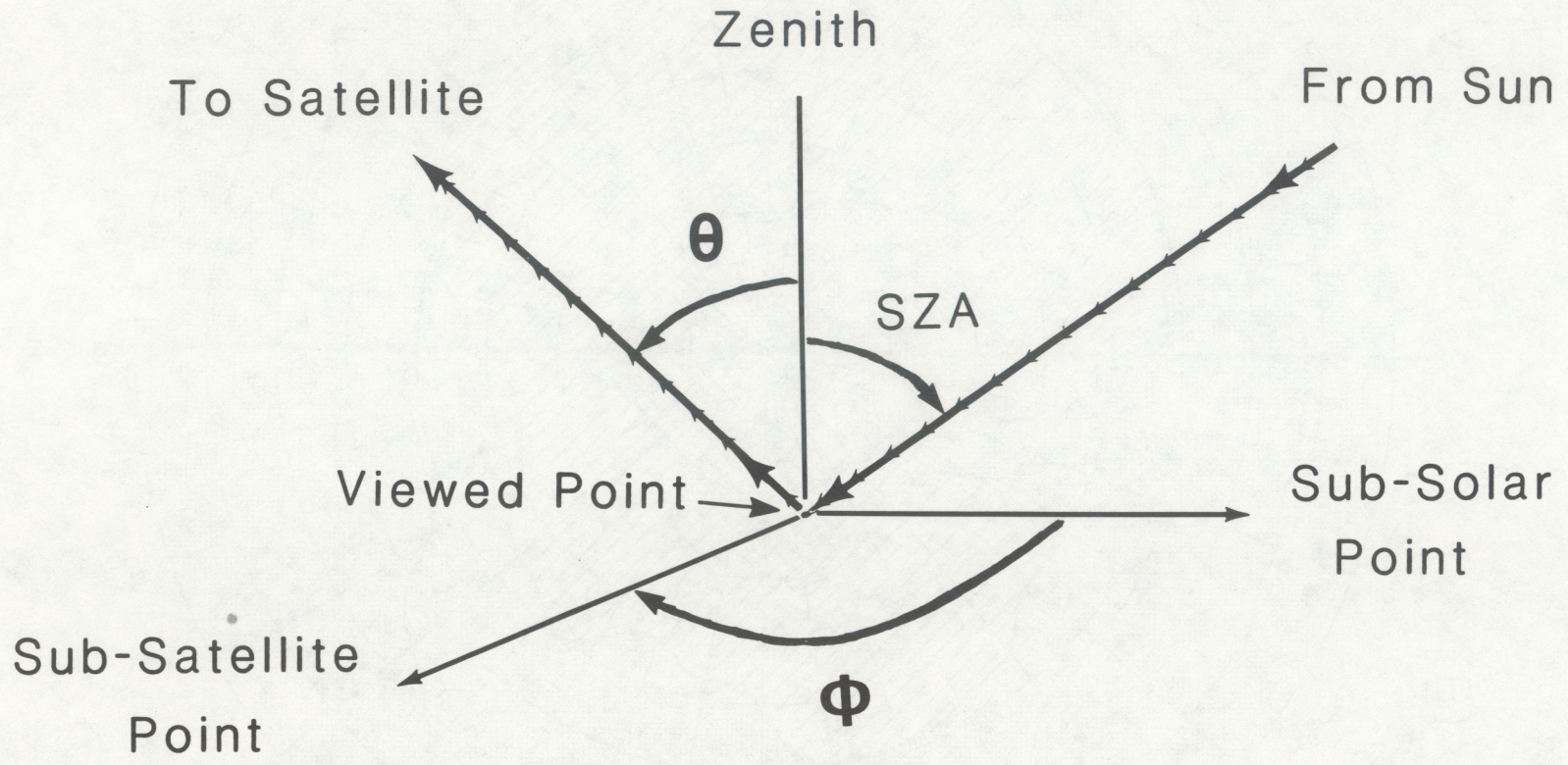
Zenith
To Satellite
From Sun
θ
SZA
Viewed Point
Sub-Solar
Point
Sub-Satellite
Point
Φ

Fig. 1

NIMBUS-7 ERB BI-DIRECTIONAL REFLECTANCE

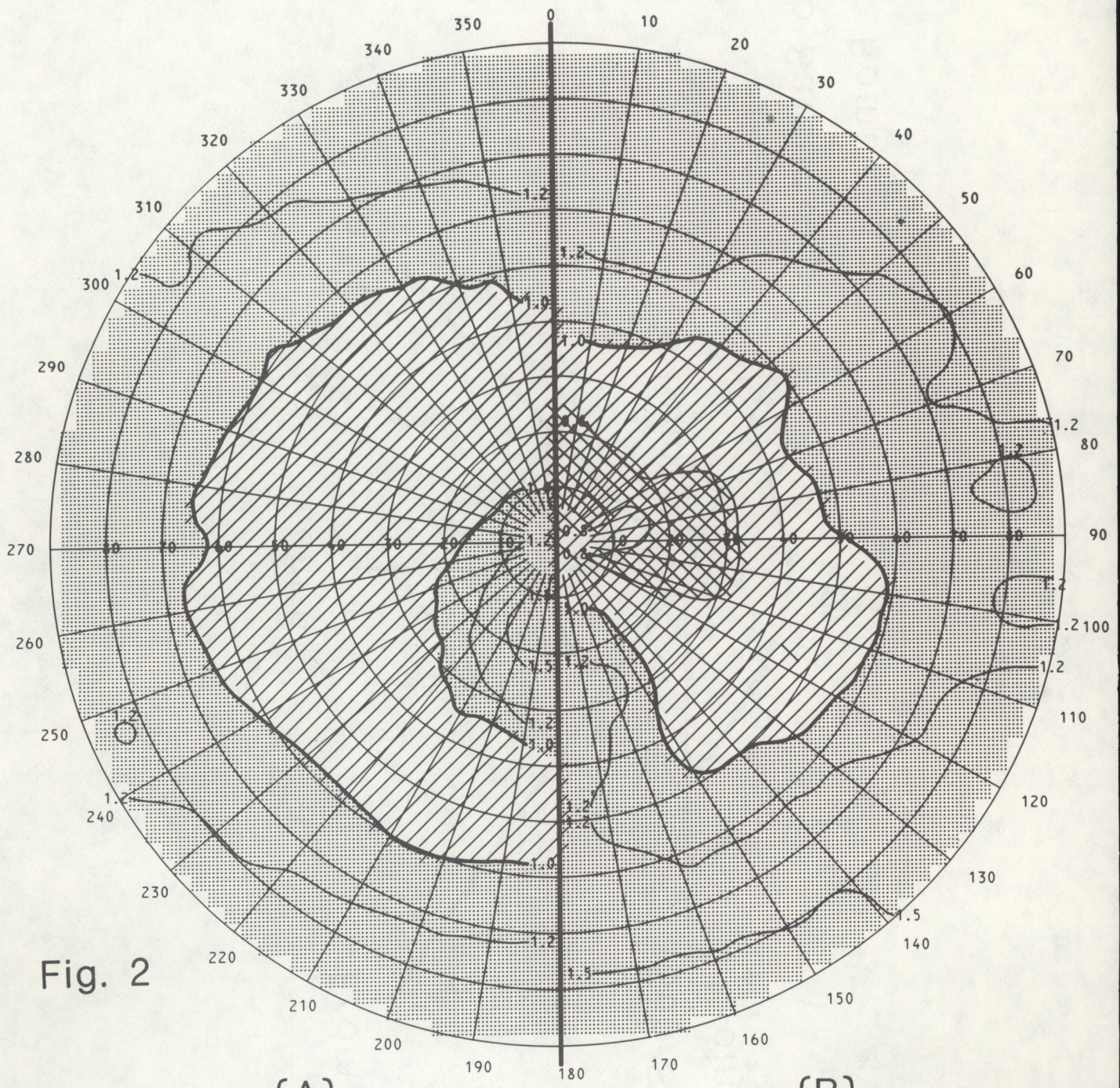

Fig. 2

(A)

ALBEDO=.09

POPULATION= 27065

SOLAR ZENITH ANG (0.0-25.8)

INTEGRAL= 119.5 INTEGRAL/PI= 38.0

(B)

ALBEDO=.10

POPULATION= 12345

SOLAR ZENITH ANG (25.8-36.9)

INTEGRAL= 139.6 INTEGRAL/PI= 44.4

WATER 61-DAY COMPOSITE 11/17/78 TO 09/12/79

NIMBUS-7 ERB BI-DIRECTIONAL REFLECTANCE

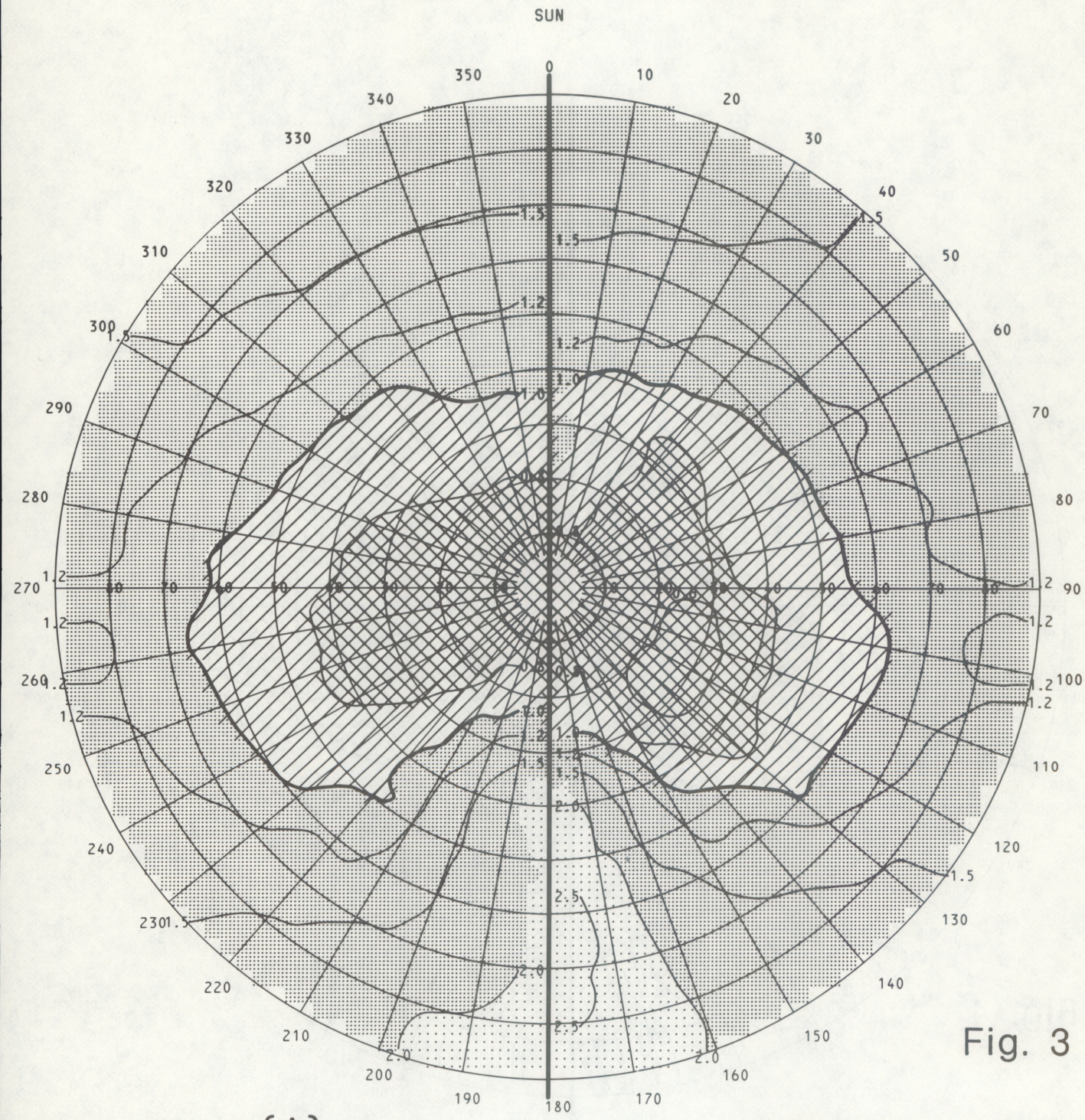

Fig. 3

(A)

ALBEDO=.11

POPULATION= 9923

SOLAR ZENITH ANG (36.9-45.6)

INTEGRAL= 153.2 INTEGRAL/PI= 48.8

(B)

ALBEDO=.13

POPULATION= 4858

SOLAR ZENITH ANG (45.6-53.1)

INTEGRAL= 175.6 INTEGRAL/PI= 55.9

WATER 61-DAY COMPOSITE 11/17/78 TO 09/12/79

NIMBUS-7 ERB BI-DIRECTIONAL REFLECTANCE

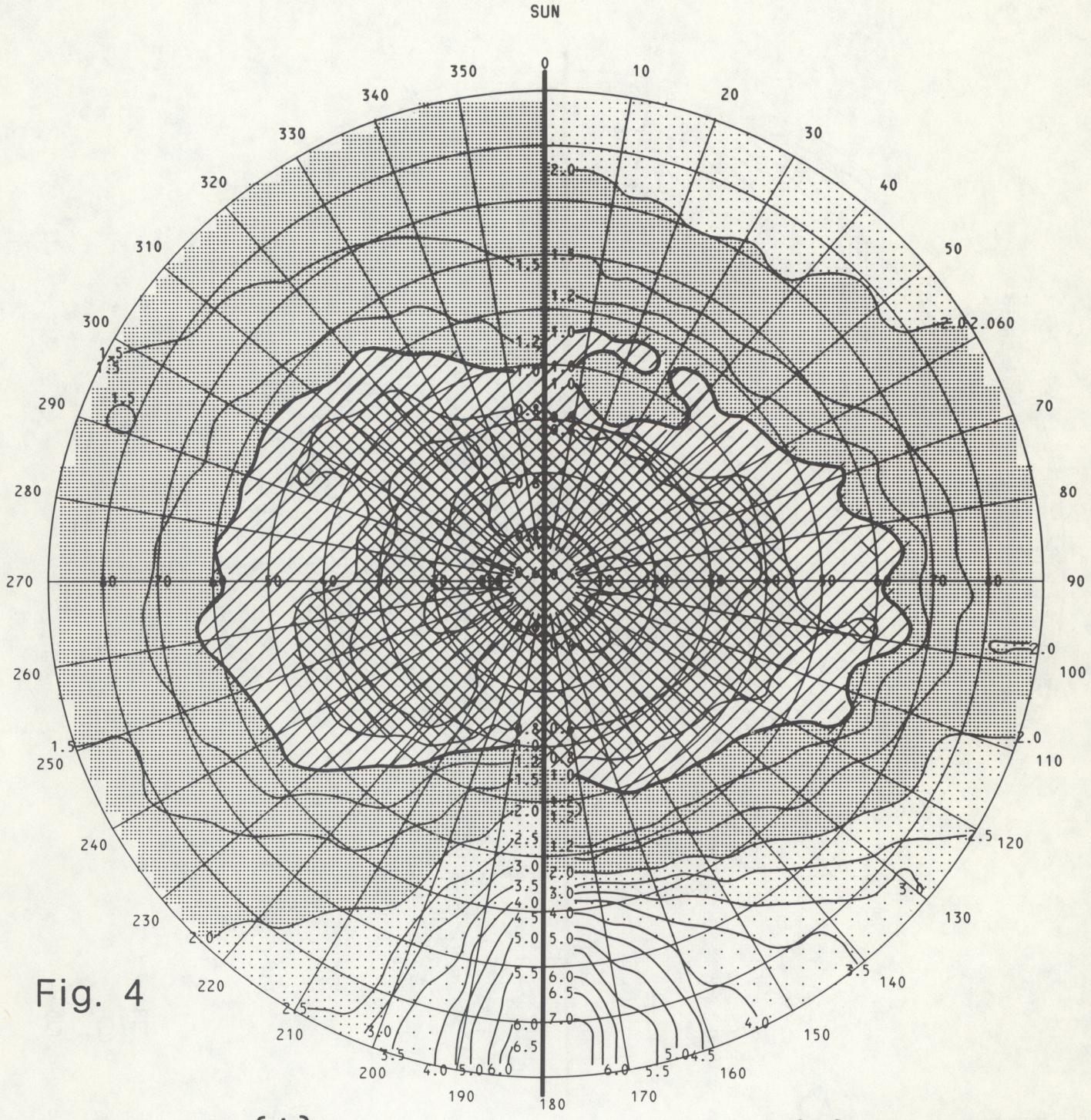

Fig. 4

(A)

ALBEDO=.18

POPULATION= 1680

SOLAR ZENITH ANG (60.0-66.4)

INTEGRAL= 252.0 INTEGRAL/PI= 80.1

(B)

ALBEDO=.43

POPULATION= 284

SOLAR ZENITH ANG (84.3-90.0)

INTEGRAL= 599.3 INTEGRAL/PI= 190.7

WATER 61-DAY COMPOSITE 11/17/78 TO 09/12/79

NIMBUS-7 ERB BI-DIRECTIONAL REFLECTANCE

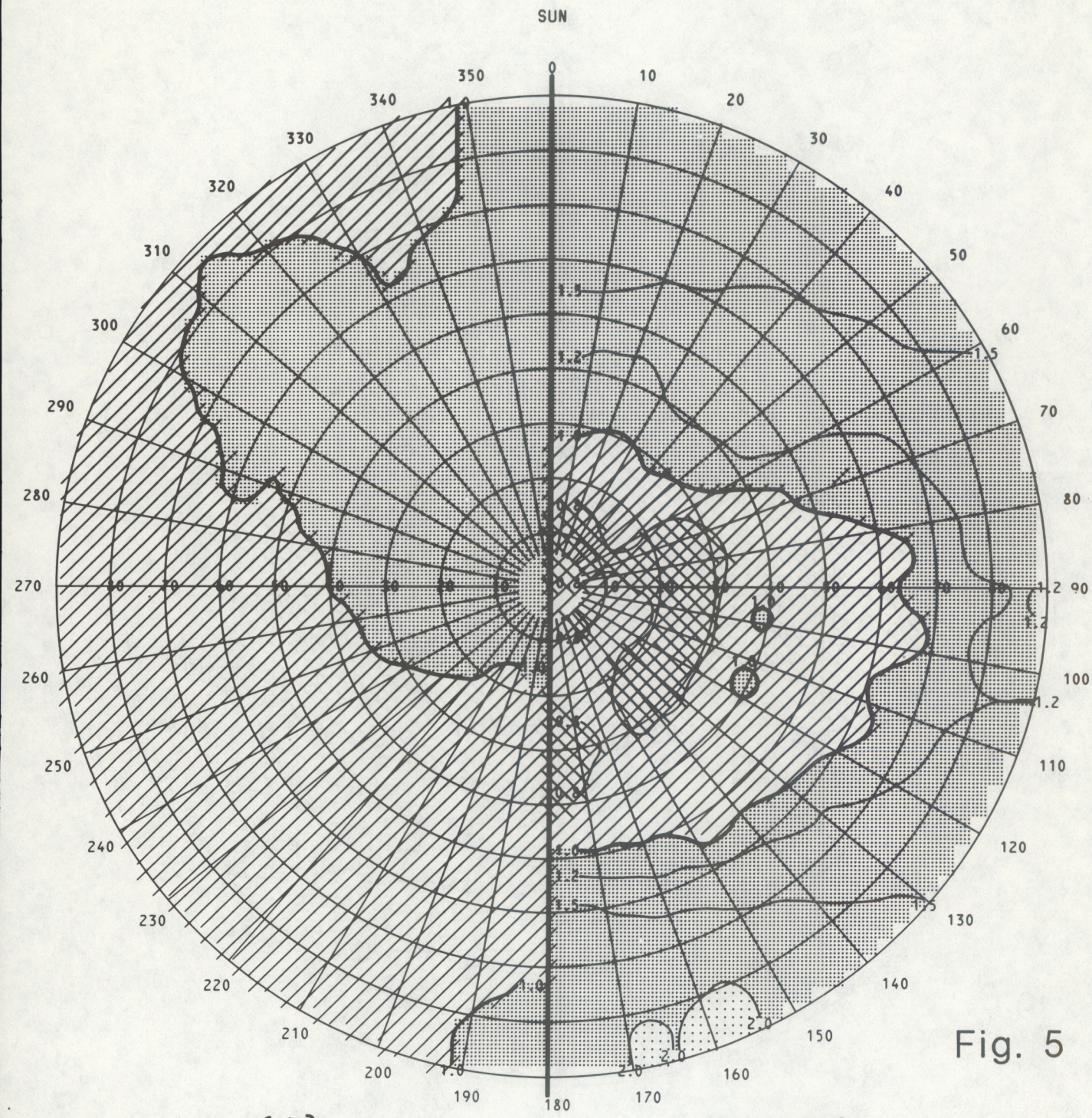

Fig. 5

(A)

ALBEDO=.22

POPULATION= 38658

SOLAR ZENITH ANG (0.0-25.8)

INTEGRAL= 298.0 INTEGRAL/PI= 94.8

(B)

ALBEDO=.26

POPULATION= 1041

SOLAR ZENITH ANG (60.0-66.4)

INTEGRAL= 358.3 INTEGRAL/PI= 114.0

LAND 61-DAY COMPOSITE 11/17/78 TO 09/12/79

NIMBUS-7 ERB BI-DIRECTIONAL REFLECTANCE

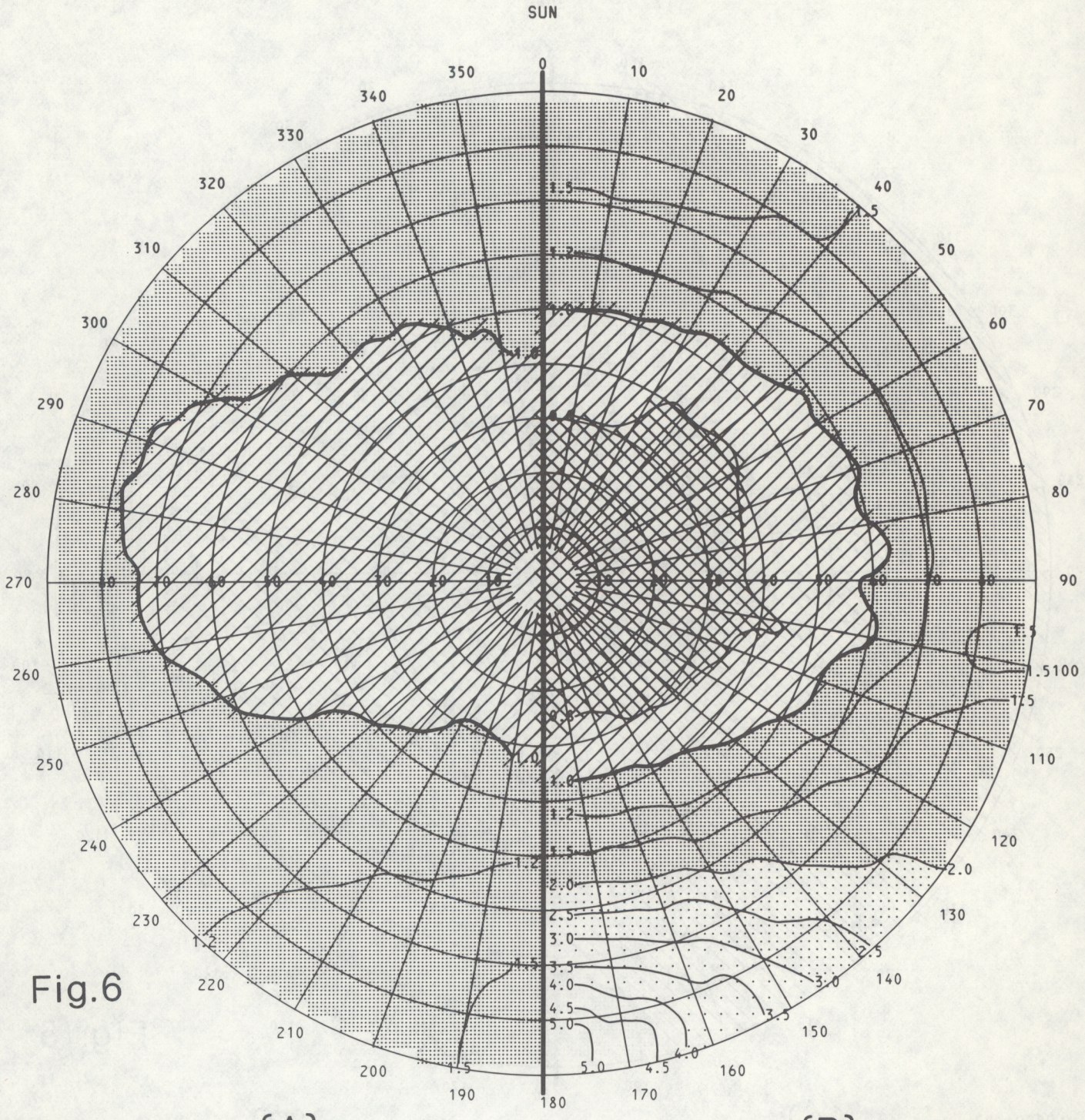

Fig.6

(A)

ALBEDO=.73

POPULATION= 12484

SOLAR ZENITH ANG (60.0-66.4)

INTEGRAL=1005.4 INTEGRAL/PI= 320.0

(B)

ALBEDO=.74

POPULATION= 3580

SOLAR ZENITH ANG (84.3-90.0)

INTEGRAL=1019.5 INTEGRAL/PI= 324.5

SNOW 61-DAY COMPOSITE 11/17/78 TO 09/12/79

NIMBUS-7 ERB BI-DIRECTIONAL REFLECTANCE

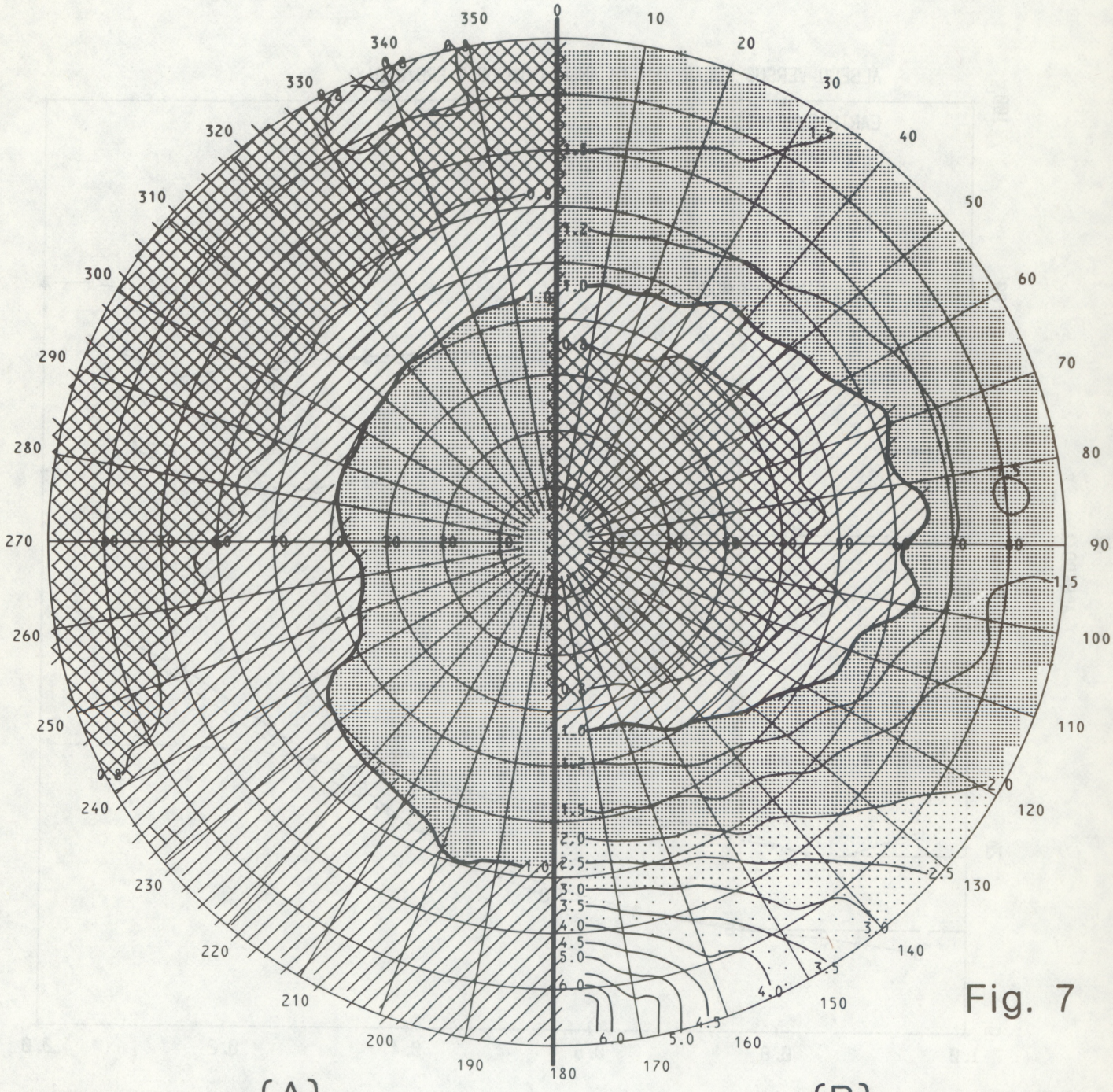

Fig. 7

(A)

ALBEDO=.36

POPULATION= 9153

SOLAR ZENITH ANG (0.0-25.8)

INTEGRAL= 491.7 INTEGRAL/PI= 156.5

(B)

ALBEDO=.66

POPULATION= 4118

SOLAR ZENITH ANG (84.3-90.0)

INTEGRAL= 907.3 INTEGRAL/PI= 288.7

MID CLD 61-DAY COMPOSITE 11/17/78 TO 09/12/79

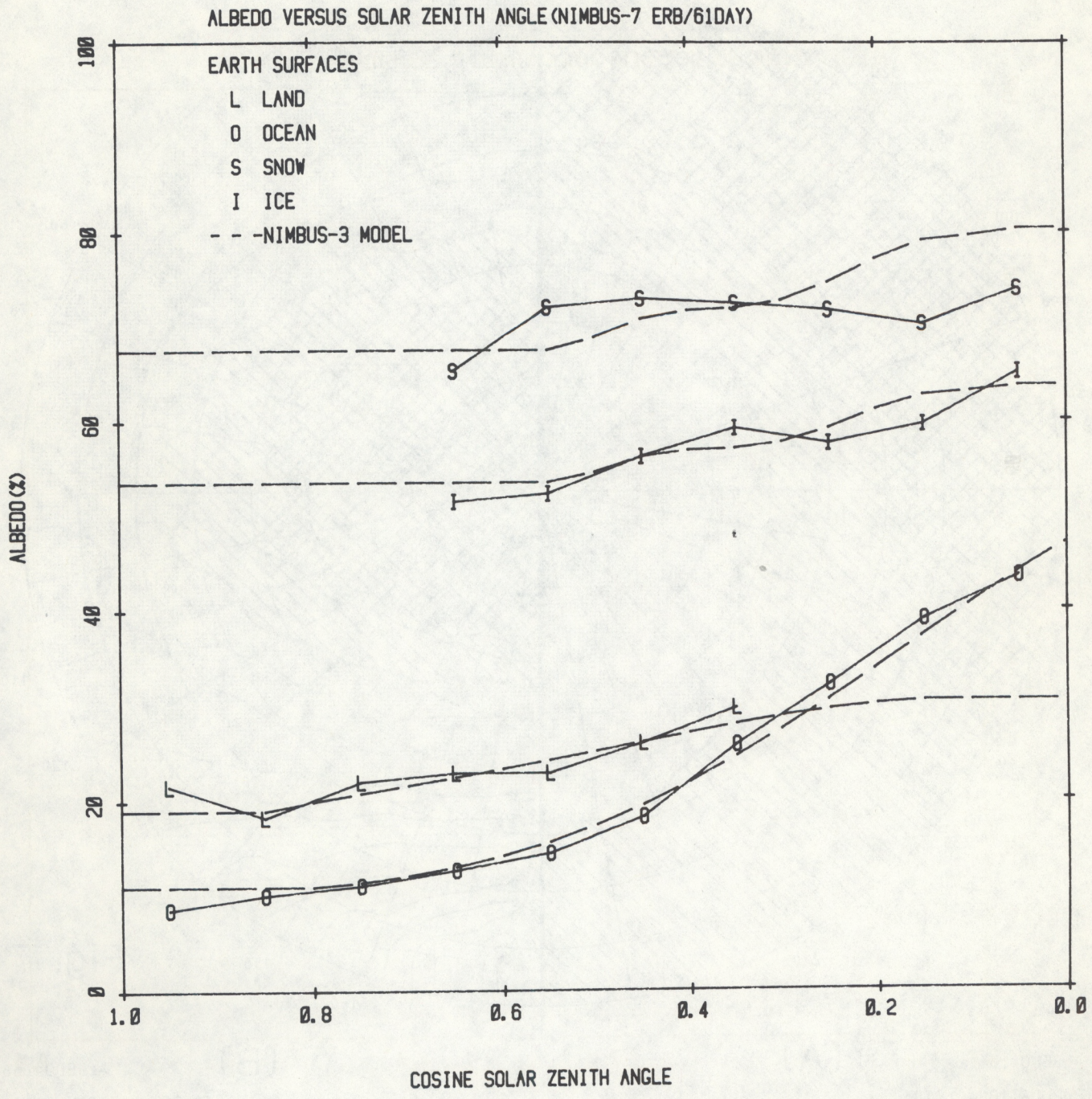
ALBEDO VERSUS SOLAR ZENITH ANGLE(NIMBUS-7 ERB/61DAY)
EARTH SURFACES
L LAND
O OCEAN
S SNOW
I ICE
- - -NIMBUS-3 MODEL
ALBEDO(%)
100
80
60
40
20
0
1.0
0.8
0.6
0.4
0.2
0.0
COSINE SOLAR ZENITH ANGLE

Fig. 8

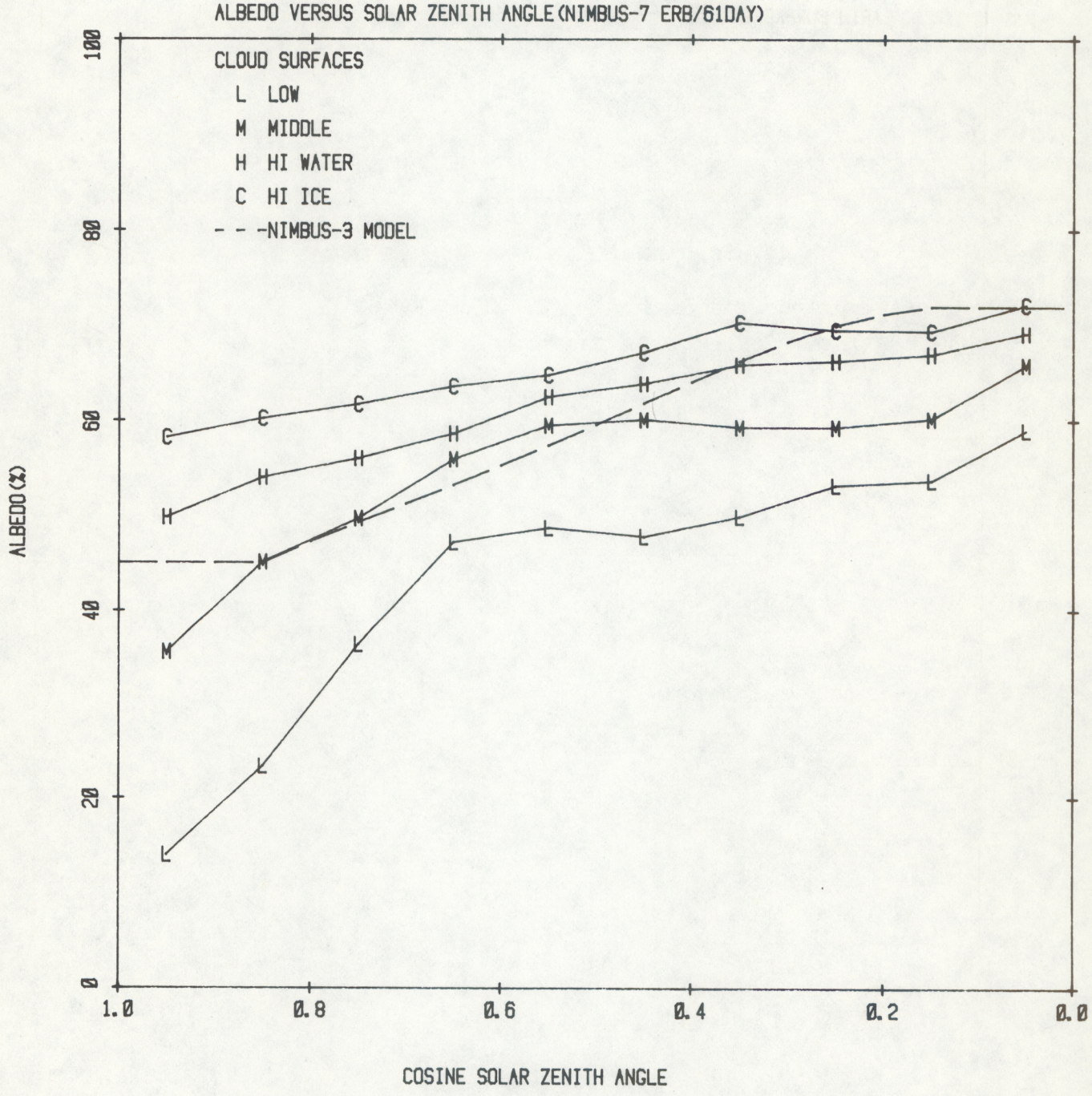
ALBEDO VERSUS SOLAR ZENITH ANGLE(NIMBUS-7 ERB/61DAY)
CLOUD SURFACES
L LOW
M MIDDLE
H HI WATER
C HI ICE
- - -NIMBUS-3 MODEL
ALBEDO(%)
100
80
60
40
20
0
1.0
0.8
0.6
0.4
0.2
0.0
COSINE SOLAR ZENITH ANGLE

Fig. 9

APPENDIX B

61-Day Reflectance Tape Description

The data which describe the 61-day Nimbus-7 ERB reflectance patterns for uniform surfaces are contained in a single file. This file is written to a 'non-labeled', 1600 bpi tape on an IBM 360-195 computer using a 'DCB' of (RECFM=FB, LRECL=1012, BLKSIZE=10120).

Each of 8 physical records (10120 bytes, each) is divided into 10 logical records (1012 bytes, each). Each physical record contains data for a single surface type. Each logical record contains data for one of 10 equal intervals (.1) of the cosine of the solar zenith angle. Each logical record is formatted as in the following table. Data for the pattern as a whole are followed by repeated information specific to each bin in the sequence.

All data except for label information (character strings) were written by the PL/1 language as 'fixed binary' with the number of fractional bits as shown. Numerical data may be interpreted in FORTRAN by reading each quantity as an integer, floating, then dividing by 2^n, where n is the number of fractional bits.

Whole Pattern Information:	Length(bytes)	No. of fract. bits
Label(characters)	16	-
Total population	4	0
Integral(watts/m^2)	4	8
Lower Sol. Zen. Ang. (deg.)	2	6
Upper " " " "	2	6
Albedo	2	10
Integral/Pi(watts/m^2-str.)	2	3
Bin Information (repeated 49 times)		
Sequential bin no.	2	0
Anisotropic factor	2	10
Visible radiance(watts/m^2-str.)	2	3
I. R. " "	2	3
Vis. stand. dev. "	2	3
I. R. " " "	2	3
Unused	2	-
Bin population	2	0
Satellite Zenith Ang.(deg.)	2	1
Relative Azimuth " "	2	1

Whole Pattern info. 32 bytes + Bin info. 980 bytes (20 x 49) = 1012 bytes/log. rec.

(Continued from inside front cover)

NESDIS 6 Spatial and Temporal Distribution of Northern Hemisphere Snow Cover. Burt J. Morse (NESDIS) and Chester F. Ropelewski, October 1983. (PB84 118348)

NESDIS 7 Fire Detection Using the NOAA--Series Satellites. Michael Matson and Stanley R. Schneider (NESDIS), Billie Aldridge and Barry Satchwell (NWS), January 1984.

NESDIS 8 Monitoring of Long Waves in the Eastern Equatorial Pacific 1981-83 Using Satellite Multi-Channel Sea Surface Temperature Charts. Richard Legeckis and William Pichel, April 1984. (PB84 190487)

NESDIS 9 The NESDIS-SEL Lear Aircraft Instruments and Data Recording System. Gilbert R. Smith, Kenneth O. Hayes, John S. Knoll, and Robert S. Koyanagi, June 1984.

NOAA CENTRAL LIBRARY
CIRC QC879.5 .U47no.10
Taylor, V. R. Atlas of reflectance patte
3 8398 0004 4383 2

NOAA SCIENTIFIC AND TECHNICAL PUBLICATIONS

The National Oceanic and Atmospheric Administration was established as part of the Depa Commerce on October 3, 1970. The mission responsibilities of NOAA are to assess the socioeconom of natural and technological changes in the environment and to monitor and predict the state of Earth, the oceans and their living resources, the atmosphere, and the space environment of the E

The major components of NOAA regularly produce various types of scientific and technical tion in the following kinds of publications:

PROFESSIONAL PAPERS—Important definitive research results, major techniques, and special investigations.

CONTRACT AND GRANT REPORTS—Reports prepared by contractors or grantees under NOAA sponsorship.

ATLAS—Presentation of analyzed data generally in the form of maps showing distribution of rainfall, chemical and physical conditions of oceans and atmosphere, distribution of fishes and marine mammals, ionospheric conditions, etc.

TECHNICAL SERVICE PUBLICATIONS—Reports containing data, observations, instructions, etc. A partial listing includes data serials; prediction and outlook periodicals; technical manuals, training papers, planning reports, and information serials; and miscellaneous technical publications.

TECHNICAL REPORTS—Journal quality with extensive details, mathematical developments, or data listings.

TECHNICAL MEMORANDUMS—Reports of preliminary, partial, or negative research or technology results, interim instructions, and the like.

Information on availability of NOAA publications can be obtained from:

PUBLICATION SERVICES BRANCH (E/AI13)
NATIONAL ENVIRONMENTAL SATELLITE, DATA, AND INFORMATION SERVICE
NATIONAL OCEANIC AND ATMOSPHERIC ADMINISTRATION
U.S. DEPARTMENT OF COMMERCE

Washington, DC 20235

NOAA--S/T 84-204